INFORMATION TO USERS

This manuscript has been reproduced from the microfilm master. UMI films the text directly from the original or copy submitted. Thus, some thesis and dissertation copies are in typewriter face, while others may be from any type of computer printer.

The quality of this reproduction is dependent upon the quality of the copy submitted. Broken or indistinct print, colored or poor quality illustrations and photographs, print bleedthrough, substandard margins, and improper alignment can adversely affect reproduction.

In the unlikely event that the author did not send UMI a complete manuscript and there are missing pages, these will be noted. Also, if unauthorized copyright material had to be removed, a note will indicate the deletion.

Oversize materials (e.g., maps, drawings, charts) are reproduced by sectioning the original, beginning at the upper left-hand corner and continuing from left to right in equal sections with small overlaps. Each original is also photographed in one exposure and is included in reduced form at the back of the book.

Photographs included in the original manuscript have been reproduced xerographically in this copy. Higher quality 6" x 9" black and white photographic prints are available for any photographs or illustrations appearing in this copy for an additional charge. Contact UMI directly to order.

U·M·I

University Microfilms International
A Bell & Howell Information Company
300 North Zeeb Road, Ann Arbor, MI 48106-1346 USA
313/761-4700 800/521-0600

Order Number 9124156

Energy consumption among static and proliferating hybridoma cell populations

Okerlund, Linda Susan, Ph.D.

The University of Arizona, 1991

U·M·I
300 N. Zeeb Rd.
Ann Arbor, MI 48106

ENERGY CONSUMPTION AMONG STATIC AND PROLIFERATING HYBRIDOMA CELL POPULATIONS

by

Linda Susan Okerlund

A Dissertation Submitted to the Faculty of the

DEPARTMENT OF BIOCHEMISTRY

In Partial Fulfillment of the Requirements

For the Degree of

DOCTOR OF PHILOSOPY

In the Graduate College

THE UNIVERSITY OF ARIZONA

1 9 9 1

THE UNIVERSITY OF ARIZONA
GRADUATE COLLEGE

As members of the Final Examination Committee, we certify that we have read the dissertation prepared by Linda S. Okerlund

entitled Energy Consumption Among Static and Proliferating Hybridoma Cell Populations

and recommend that it be accepted as fulfilling the dissertation requirement for the Degree of Doctor of Philosophy.

N. MacKenzie	15 Apr 91 4/15/91
Neil E. MacKenzie	Date
Michael F. Brown	15 April, 1991
	Date
William J. Grimes	4/15/91 4/15/91
	Date
Robert J. Gillies	4/18/91 4/18/91
	Date
Marc E. Tischler	4/18/91 4/18/91
	Date

Final approval and acceptance of this dissertation is contingent upon the candidate's submission of the final copy of the dissertation to the Graduate College.

I hereby certify that I have read this dissertation prepared under my direction and recommend that it be accepted as fulfilling the dissertation requirement.

Robert J. Gillies	4/18/91 4/18/21
Dissertation Director	Date

STATEMENT BY AUTHOR

This dissertation has been submitted in partial fulfillment of requirements for an advanced degree at The University of Arizona and is deposited in the University Library to be made available to borrowers under rules of the Library.

Brief quotations from this dissertation are allowable without special permission, provided that accurate acknowledgement of source is made. Requests for permission for extended quotation from or reproduction of this manuscript in whole or in part may be granted by the head of the major department or the Dean of the Graduate College when in his or her judgement the proposed use of the material is in the interests of scholarship. In all other instances, however, permission must be obtained from the author.

SIGNED: 

ACKNOWLEDGEMENTS

I wish to acknowledge, and most of all thank, the two people whose friendship and support has most helped me throughout the frequent ups and downs of my graduate career. I owe what remains of my sanity and self-esteem to my husband, John Rose. His amazing patience and understanding has allowed me to continue in spite of our rather long separations and infrequent visits. My mother, Arlene Okerlund, has provided the insights and advice of one who has "been through it" herself, always providing encouragement as I occasionally neared the final stages of exasperation and despair.

TABLE OF CONTENTS

LIST OF ILLUSTRATIONS

LIST OF TABLES

Abstract

To investigate the effects of proliferation on metabolism and cell product yields, proliferating and growth-limited EPO8F7 hybridoma cells have been compared as to their growth rates, energy demand, relative energy distributions, and monoclonal antibody (MAb) yield. Medium deprivation of leucine or serum was used to prevent growth. Energy consumption rates were determined in cell suspensions from rates of glucose consumption, lactate production, and oxygen utilization. In addition, the energy consumption of pathways critical to cell growth and survival were estimated from the relative decreases occurring in oxygen and glucose consumption upon pathway inhibition. The overall rate of energy consumption was significantly lower among growth-limited cultures. In addition, the distributions of oxidative and glycolytic energy among cellular synthetic pathways differed significantly between the culture conditions. Non-growing cultures also produced significantly lower antibody yields.

Cell growth was also investigated using ^{31}P nuclear magnetic resonance (NMR) spectroscopy of cells grown and maintained in bioreactor culture. Saturation transfer methods detected measurable transfer between inorganic phosphate (P_i) and the gamma resonance of ATP. This transfer rate could be correlated with cellular growth rates within the reactor. Transfer of magnetization from the gamma resonance of ATP to P_i was also detected, although the rate of this transfer did not appear to be related to the growth rate. The ratio of these transfer rates was consistently near 4. This information is

believed to suggest the importance of other reactions through which ATP may donate its terminal phosphate.

Cells in bioreactor culture were found to grow more slowly and produce lower levels of monoclonal antibody when compared to cells proliferating in suspension. Such phenomena may be a function of diffusion limitations within the reactor such that the cells cannot obtain the nutrient supply required for optimal cell growth or product formation.

I. Introduction

Despite the commercial significance of efficient monoclonal antibody production, little is known as to the hormonal and metabolic mechanisms regulating production, or how this production is effected by an increased metabolic rate, such as would occur when a cell is stimulated to divide. The production of antibodies requires cellular energy, yet it remains relatively unknown how metabolic energy is distributed within hybridoma cells, or how this distribution may differ among proliferating and non-proliferating cells.

Metabolism is the process of converting chemical energy (e.g. as stored in foodstuffs) into forms able to drive processes necessary for the growth and survival of a cell or organism. Much of the current knowledge of metabolism arises from studies of cells growing in culture. Rates of substrate (e.g. glucose, oxygen) consumption and product (e.g. lactate) formation can be used to calculate approximate rates of ATP synthesis and the energetic demands of a cell population. Direct determinations of ATP synthesis rates are somewhat more difficult to determine, and usually require the destruction of the cell sample under study.

Hollow fiber bioreactors (Knazek *et al*, 1972) provide an alternative means of growing and maintaining cells in culture. These systems, consisting of a series of encapsulated semipermeable hollow fibers, through which medium is continuously perfused, closely resemble tissue morphology. Studies of cells growing in bioreactor culture may, therefore, generate results which differ from those found among more

traditional culture methods. This warrants the study of cells in bioreactor culture for comparison with those grown using other, and perhaps more commonly used, culture methods.

Nuclear magnetic resonance (NMR) spectroscopy (Bovey, 1988) also provides an alternative means of studying cells in culture. NMR spectroscopy is a non-invasive technique, permitting one to monitor cells continuously throughout potentially long culture periods. Much of the usefulness of NMR spectroscopy in the study of biological systems stems from the visibility of phosphorus-31 and the high energy phosphorus-containing metabolites which drive metabolism.

The growth of cells in bioreactors can be combined with NMR studies, potentially yielding new information about cell systems as well the differences between cells grown using differing culture methods.

A. Cell growth and metabolism.

The growth and survival of cells, tissues, and living organisms is dependent on the production of cellular energy in the form of adenosine triphosphate (ATP) (Lehninger, 1965; Racker, 1976; Atkinson, 1977). A large portion of cellular energy is derived from the oxidation of carbohydrates such as glucose and sucrose (Eagle, 1955; Levintow and Eagle, 1961). A small amount of energy is derived from the initial breakdown of glucose to pyruvate *via* the glycolytic pathway (figure 1). Glycolysis yields two molecules of ATP per molecule of glucose. In muscle and adipose tissue, fructose enters the pathway at the level of fructose 6-phosphate, while more complex carbohydrates must first be broken down into their constituent simple sugars before metabolism.

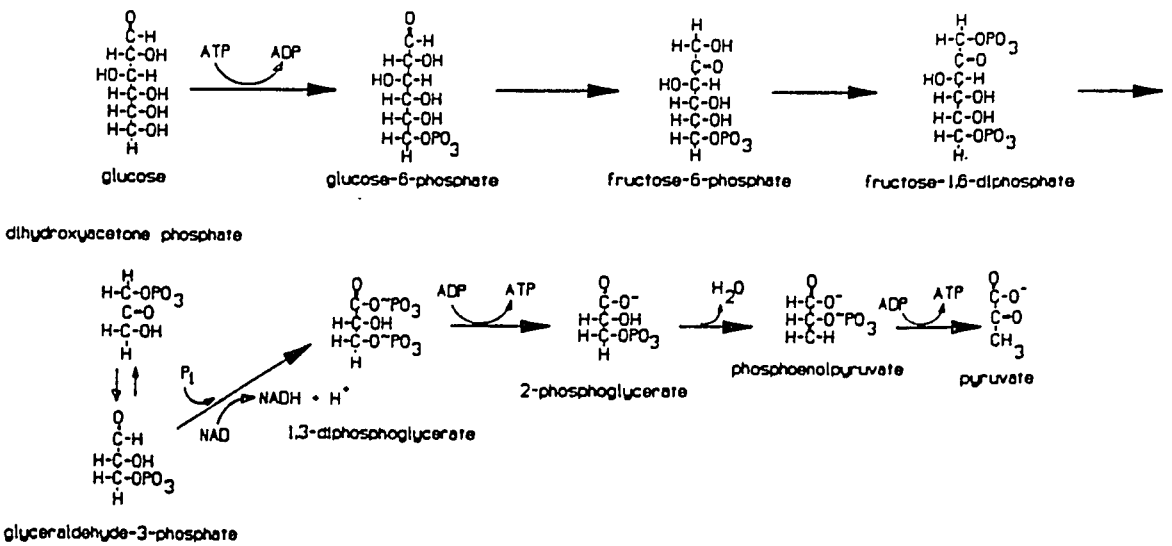

Figure 1. The glycolytic pathway. Through a series of phosphorylations, cleavage, and isomerizations, one molecule of glucose in cleaved into two molecules of pyruvate. This series of reactions yields two molecules of ATP (net) and two molecules of NADH. Under aerobic conditions the NADH is transferred to the electron transport chain, where it is used for the generation of additional ATP. ATP generated via glycolysis is a portion of the total used to drive the energy-requiring processes of the cell.

If oxygen is readily available, pyruvate will be funnelled into the tricarboxylic acid (TCA) cycle as acetyl CoA (figure 2). Through one turn of the cycle, the carbons of acetyl CoA are released as carbon dioxide. In addition, three molecules of nicotinamide adenine dinucleotide (NADH), one molecule of flavin adenine dinucleotide ($FADH_2$), and one molecule of guanosine triphosphate (GTP) are formed. NADH and $FADH_2$ donate electrons to the mitochondrial electron transport chain (Chance, 1977), yeilding three and two ATP molecules, respectively. Thus, the net equation for the oxidation of glucose is (Racker, 1976):

$$C_6H_{12}O_6(\text{glucose}) + 6O_2 + 38ADP + 38P_i \rightarrow 6CO_2 + 6H_2O + 38ATP$$

If insufficient oxygen is available for the support of mitochondrial electron transport, cells are able to generate ATP from glycolysis alone. As shown in figure 1, during glycolysis, two molecules of NAD^+ are reduced to NADH (Atkinson, 1977; Racker, 1976). When oxygen is present, this NADH is re-oxidized by the mitochondrial electron transport chain (Chance, 1977). As electrons are removed from NADH, they are transported down this transport chain. This is coupled to the pumping of protons across the inner mitochondrial membrane, to form a proton gradient. The energy stored in this gradient provides the energy for ATP synthesis as the protons are funnelled down their electrochemical gradient (Mitchell, 1979) The NAD^+ thus formed may then participate in another round of glycolysis. Without this regeneration, continued glycolysis would no longer be possible and the

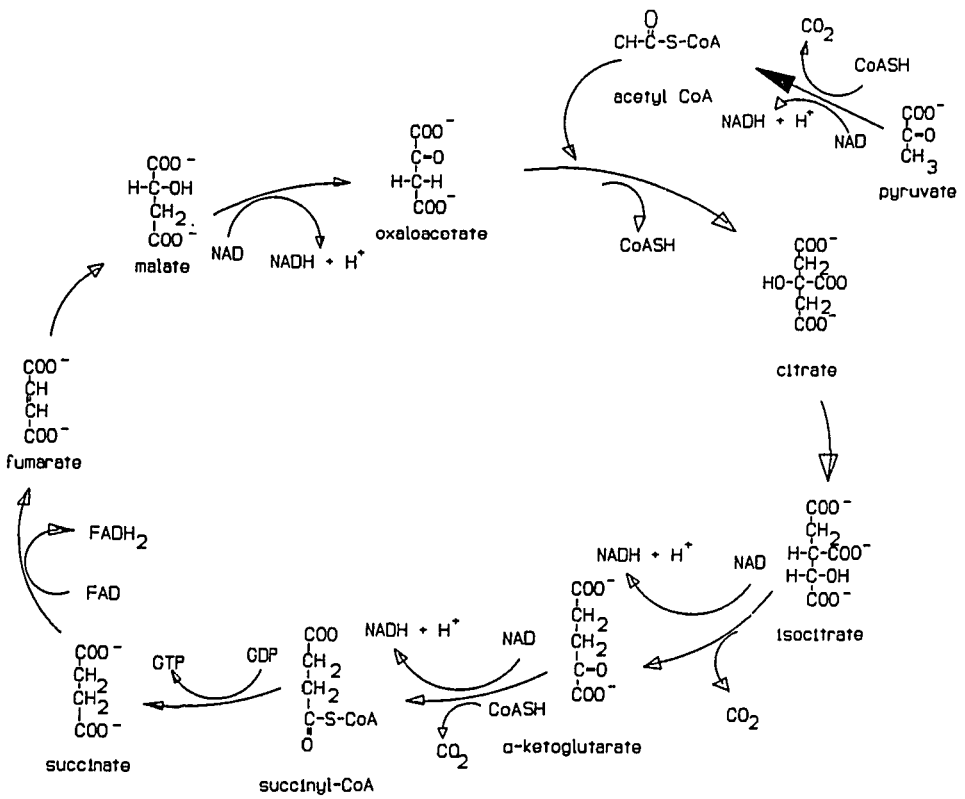

Figure 2. The tricarboxylic acid (TCA) cycle. Pyruvate generated *via* glycolysis is decarboxylated and the remaining two carbons are funnelled into the TCA cycle as acetyl coenzyme A (acetyl CoA). The enzymatic condensation of acetyl CoA and oxaloacetate generates citrate, which through a series of isomerizations and cleavage reactions generates three molecules of NADH, one molecule of $FADH_2$, and one molecule of GTP. Oxaloacetate is regenerated following each turn of the cycle. NADH and $FADH_2$ are transferred to the electron transport chain where they are used for the generation of three and two molecules of ATP, respectively. GTP is a high-energy phosphate compound equivalent to ATP in energy content and its ability to drive energy-consuming reactions.

subsequent reactions of the TCA cycle would cease. Under anaerobic conditions, NADH cannot be oxidized through the activity of the electron transport chain (Lehninger, 1965). Instead, it donates its electrons to pyruvate, thus forming either lactate or ethanol (figure 3).

Glycolysis alone produces much less energy than available from the complete oxidation of glucose under aerobic conditions (Racker, 1976). Therefore, in the absence of oxygen, the rate of glycolysis must increase dramatically in order to meet the ATP demand of the cell. This phenomenon was first documented in yeast by Louis Pasteur in 1861 (Racker, 1976), and has also been observed in mammalian cells in culture (Racker and Wu, 1959; Racker, 1976).

Energy (in the form of ATP) may also be generated from the partial oxidation of amino acids through the TCA cycle. Amino acids may be deaminated, decarboxylated, and/or isomerized to form TCA cycle intermediates (Shrivastava and Quastel, 1962; Graff *et al*, 1965; McKeehan, 1982; Zielke *et al*, 1984). Similarly, when TCA cycle intermediates are not needed to satisfy the energy demands of a cell, or are needed elsewhere in metabolism, these intermediates may be removed from the cycle and used for the synthesis of amino acids and cellular proteins (Shrivastava and Quastel, 1962).

1. Normal cells in culture. Within any organism, there exist populations of proliferating and quiescent cells (Nilausen and Green, 1965; Todaro *et al*, 1965; Pardee, 1974). Most cells within an organism are relatively quiescent, dividing only as necessary to replace cells

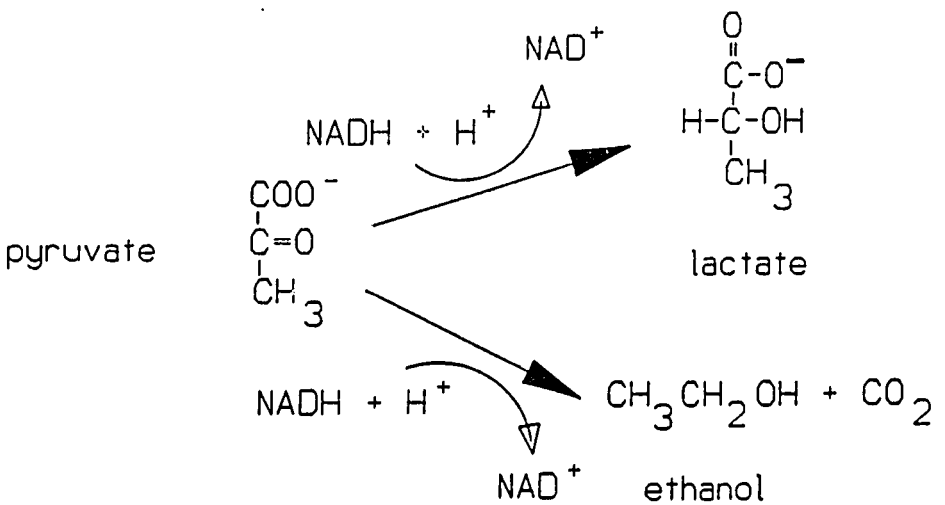

Figure 3. The anaerobic regeneration of NAD^+ from NADH. Under anaerobic conditions, when the transfer of electrons to oxygen cannot be used to regenerate the finite pool of cellular NAD^+, the electrons of NADH are instead transferred to pyruvate. Thus, energy generation and metabolism may continue. Dependent on the organism involved, the end product of this enzymatic reactions is either lactate (as in mammalian systems) or ethanol, commonly generated by yeast and other microorganisms.

which die naturally or are killed as a result of injury or trauma (Dulbecco, 1970; James, 1984).

a. Stimulation of cell growth. As early as 1916, cells could be grown and maintained in tissue plasma (Rous and Jones, 1916). Plasma and blood sera contain those factors necessary for the survival and proliferation of cells in culture (Sanford *et al*, 1948; Eagle, 1955; Ham, 1972). Many of the individual factors which support proliferation have been identified, and their mechanisms of action elucidated (Sato and Reid, 1978; Carpenter, 1979; James, 1984; Heldin and Westermark, 1984).

These "growth factors" are peptide hormones which bind to hormone-specific receptors on the cell plasma membrane (James, 1984; Sato and Reid, 1978). Hormone-receptor binding elicits specific intracellular responses which culminate in cell division (James, 1984).

A few of the growth factors isolated, and at least partially characterized to date, include epidermal growth factor (EGF, Carpenter, 1979; Carpenter and Cohen, 1975; Hopkins, 1980; Carpenter and Cohen, 1990), basic fibroblast growth factor (FGF, Gospodarowicz, 1985; Huang *et al*, 1986), platelet-derived growth factor (PDGF, Pledger *et al*, 1977; Vogel *et al*, 1978; Lipton, 1985), and "transforming" growth factors alpha (α) and beta (β) (TGFs, DeLarco and Todaro, 1978; Anzano *et al*, 1983; Marquardt *et al*, 1984; Massaque, 1983; Halper and Moses, 1987).

EGF is a potent mitogen for many cell types (Carpenter, 1979; Carpenter and Cohen, 1975; Gospodarowicz, 1985), stimulating proliferation and delaying normal cell senescence. TGF-α is similar to

EGF in structure, binds to the EGF receptor, and is able to stimulate cell proliferation. TGF-α may also render cells "anchorage independent", inducing them to assume a neoplastic or tumorigenic morphology (Massaque, 1983; Marquardt *et al*, 1984). PDGF, on the other hand, is usually referred to as a "competence factor," rendering cells "competent" to traverse the cell cycle and initiate DNA synthesis, while unable to stimulate proliferation alone (Vogel *et al*, 1978; Pledger *et al*, 1977).

b. Growth factor transduction mechanisms. At the cellular level, each of these growth factors binds to a specific cell surface receptor (James, 1984; Hashman, 1985; Bowen-Pope *et al*, 1985). These receptors are transmembrane proteins consisting of an extracellular hormone binding domain, a transmembrane region, and a cytoplasmic domain. The cytoplasmic domain possesses intrinsic protein kinase activity which is regulated by hormone binding (Bowen-Pope *et al*, 1985; Hashman, 1985; Sefton, 1985). For example, EGF binding to its receptor induces auto-phosphorylation within the receptor's cytoplasmic domain. This, in turn, activates receptor kinase activity specific for tyrosine residues (for reviews on this subject, see Carpenter, 1979; Cohen and Carpenter, 1979; Gospodarowicz, 1985). Several potential substrates for the EGF receptor kinase include specific isozymes of phospholipase C and phosphatidylinositol kinase, each believed to be involved in the mitogenic response (Berridge and Irvine, 1984; Chambard *et al*, 1987; Carpenter and Cohen, 1990). PDGF is also believed to act *via* receptor

kinase activity, although less is currently known concerning the PDGF receptor mechanism of action (Bowen-Pope *et al*, 1985).

c. Metabolic changes associated with growth. When cells are stimulated to divide, they must produce the energy required to double all cellular components. Energy, in the form of ATP, is produced in "steady state," or only as needed to satisfy the energy demands of the cell (Chance, 1959; Racker, 1976). ATP levels within the cell remain relatively constant (Racker and Wu, 1959; Atkinson, 1977) while the rate of ATP hydrolysis and turnover increases.

Immediately following mitogenic stimulation, the glycolytic rate increases (Carpenter, 1979). Ion channels and cell transport systems are also activated (Rudland *et al*, 1974; Fix and Moore, 1981; Inman and Colowick, 1987). This is followed by increases in protein synthesis (Ballard, 1982) and DNA replication (Pledger *et al*, 1977; Carpenter, 1979). Following DNA replication, duplicated chromosomes segregate to their respective daughter cells, and two identical cells are formed (Prescott, 1968). At this point, the cell may or may not go through a period of quiescence before initiating another round of cell growth (Pardee, 1974).

2. Cancer cells and transformed cell lines. Cancer is a pathological condition resulting from the "transformation" of cells such that they are no longer bound by the constraints of normal cell growth (Levintow and Eagle, 1961; Nilausen and Green, 1965; Pierce, 1979; Pardee, 1974). Normal cells divide only when stimulated by the appropriate growth factors (Prescott, 1968; Pardee, 1974; Pledger *et al*, 1977; Vogel *et al*,

1978), and may only be passaged for a finite number of divisions in culture (Swim and Parker, 1957; Miles, 1964; Hayflick, 1965; Hay and Strehler, 1967; Martin *et al*, 1970). Cancer cells may have different nutritional requirements than their normal counterparts, and in many cases, are able to synthesize many of the nutrients or growth factors needed for proliferation (Levintow and Eagle, 1963; Vuk-Pavlovic *et al*, 1986; Klein *et al*, 1987; Metcalf, 1989). Cancer cells also appear to be immune from any limitation on the number of divisions possible (Ethier and Cundiff, 1987). As such, they are referred to as "immortalized" cell lines. Such transformations are the result of a multistage process, in which the immortalization event is to be distinct from the loss of growth regulation.

a. Macroscopic differences between normal and cancer cells. Most normal cells, with the exception of circulating blood cells, demonstrate "attachment dependence" (Rous and Jones, 1916; Sanford *et al*, 1948; Swim and Parker, 1957; Ham, 1972; Jensen, 1981). *In vivo*, attachment to basal lamina or a network of cell-to-cell contact is required for the continued growth and survival of cells within a tissue (Sanford *et al*, 1948). In culture, this environment is simulated with the attachment of individual cells to a glass or plastic culture dish (Ham, 1972; Eagle, 1972; Jensen, 1981). Cells proliferate as a monolayer of attached cells. Proliferation may slow or stop as the monolayer becomes "confluent," or when a single layer of cells covers the entire culture surface (Todaro *et al*, 1965; Fisher and Yeh, 1967; Holley and Kiernan, 1968; Shutze and Mora, 1971; Holley, 1975).

Many tumorigenic cell lines appear to have lost the anchorage dependence of normal cells and can be characterized by their ability to form colonies in soft agar (Stoker *et al*, 1968; Freedman and Shin, 1974). Anchorage-independent cell lines can be maintained as continuously proliferating cultures in liquid suspension media (Freshney, 1987).

Most normal cells, with the exception of stem cells which may differentiate into several potential cell types as required by the organism, remain highly specialized throughout their life span (Buick and McCulloch, 1985). Transformed or malignant cells, however, often lose their differentiated properties (Yaffe, 1968; Pierce, 1979). Malignant cells often maintain high glycolytic rates compared to their normal cell counterparts (Shrivastava and Quastel, 1962). Excessive glycolysis and the accumulation of large quantities of lactic acid occurs in the presence of adequate oxygenation and active respiration (Crabtree, 1929; Dikens and Simer, 1930). It was first suggested that such "aerobic glycolysis" occurs due to a deficit or "injury" of respiration (Warburg, 1956). It has subsequently been postulated that excess glycolytic flux may be due to a lack of regulation among key glycolytic enzymes (Arany *et al*, 1981; Wenner, 1975), such that pyruvate is generated more rapidly than required for energy production *via* the TCA cycle. This excess pyruvate is converted to lactate, which accumulates in the culture medium.

B. Hybridomas and monoclonal antibody formation.

"Hybridomas" are hybrid cells resulting from the fusion of antibody-producing immune cells and immortal, or cancerous myeloma cells (Kohler and Milstein, 1975). Spleen cells isolated from an immunized donor are fused to the "immortal" myeloma using Sendai virus (Kohler and Milstein, 1975) or polyethylene glycol (Eshhar, 1985) fusion techniques. Successful fusion products retain their ability to synthesize antibody of defined specificity while assuming the cancer cell's ability to proliferate indefinitely in culture.

1. Immune cells and antibodies. The vertebrate immune system provides protection against potentially harmful or infective agents (Greaves *et al*, 1973; Jerne, 1973), responding to foreign material in the bloodstream with the formation of specific antibody products (Urso and Makinodan, 1963).

Foreign material, or antigen, entering the circulation is trapped by macrophages and becomes concentrated in the lymphoid organs (Kruse and McMaster, 1949; Waldmann and Howard, 1979). The antigen is internalized and cleaved. An antigen fragment is bound to an immunoglobulin for re-release (Greaves *et al*, 1973; Feldman, 1978). The immunoglobulin-antigen complex binds to receptors on immature T lymphocytes to stimulate proliferation and differentiation into the T helper cell. Differentiated T helper cells are lymphocytes which serve to help or assist in the further antigen-dependent differentiation of B lymphocytes and T effector cells (Waldman and Howard, 1979).

Effector T cells produce and present cell surface antibody. They migrate outside of the lymph organ to interact with antigen or cellular targets (Jerne, 1973; Waldman and Howard, 1979). Since recognition by, and binding of, these effector T cells results in the lysis of the foreign or infected cell, they are also referred to as cytotoxic T lymphocytes.

T helper cells also stimulate the differentiation of B-lymphocytes into antibody secreting plasma cells (Feldman, 1978; Waldman and Howard, 1979). *In vivo*, antibody circulates freely to bind the antigen target. This antibody is, in turn, recognized by macrophages (Greaves, 1973) which engulf and destroy the invading or infected cell.

Hybridomas are often generated from B-cells. B-cells secrete antibody into the bloodstream, and when fused with the cancerous myeloma, secrete antibody into the culture medium.

Antibodies are proteins composed of 2 heavy and 2 light peptide chains (figure 4) (Edelman and Gally, 1964; Edelman, 1970; Porter, 1974). The heavy chains are linked *via* two disulfide bonds and each light chain is attached to a heavy chain *via* a disulfide linkage. Variable and constant regions of the peptide sequence serve to provide antigen and host recognition, respectively (Edelman, 1970; Sakano *et al*, 1979). The antigen binding sites are composed of the variable regions of each chain (Edelman, 1970), which also determine the antigenic specificity of the antibody molecule.

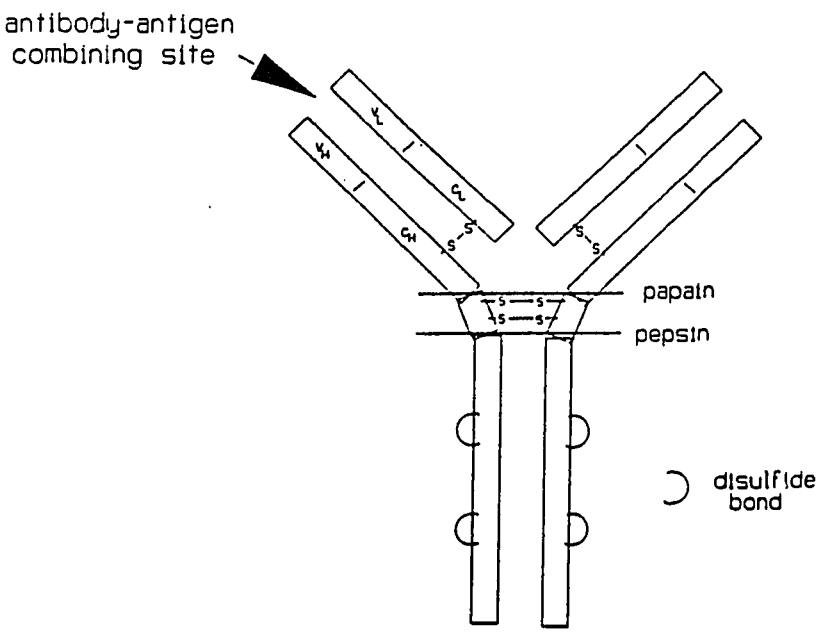

Figure 4. The antibody molecule. Antibodies consist of two heavy and two light peptide chains. The heavy chains are linked to each other via two disulfide bonds and each light chain is linked to a corresponding heavy chain through a disulfide bond. Each chain is composed of variable and constant protein regions. The variable regions of each chain combine to form the antigen recognition site. The constant regions of the heavy chain contain two intramolecular disulfide bonds.

2. Hybridoma cell growth characteristics. B-cell hybridomas are attachment-independent and can be grown and maintained in suspension or spinner flask culture (Eshhar, 1985). Hybridomas are generally grown in DMEM or RPMI 1640 supplemented with 2 mM glutamine. Cell growth can be adapted to serum concentrations as low as three to five percent, and in most cases synthetic serum supplements can be substituted for fetal bovine serum (Eshhar, 1975; Murakami, 1989).

Hybridoma cells were originally created and are now exploited for their production of antibodies directed against specific antigens of interest. According to the clonal selection theory of antibody production (Burnett, 1959), any single immune cell, or culture of cells derived from a single immune cell, secretes one discrete antibody. Antibody generated from a single hybridoma clone is, therefore, referred to as a "monoclonal" antibody (MAb), indicative of the fact that each hybridoma cell line produces only one type of antibody directed against a single haptan on the immunizing antigen.

Antibodies (and monoclonal antibodies) are constitutive products of immune cells. Following differentiation, they are secreted throughout the lifetime of the immune cell. *In vivo*, once B cells differentiate into antibody-producing plasma cells, they do not divide again prior to cell death. This occurs one to two days after differentiation (Feldman, 1978; Waldman and Howard, 1979). *In vitro*, maximum hybridoma MAb yields are obtained from suspension cultures following at least one day after the suspension has reached the

stationary phase of growth (Eshhar, 1985), and the rate of growth either slows or stops. The relationship between cell growth and antibody production is, however, unclear. It has been suggested that production levels increase with decreases in the growth rate occurring in response to lowered medium serum content (Heath *et al*, 1990). Other investigators have suggested that the growth parameter which correlates most closely to antibody production levels is oxygen, although peak MAb production levels were found to occur at the stationary phase of culture (Racher *et al*, 1990). Other data, however, show *both* cell growth and MAb yields to be increased significantly when murine hybridomas are cultured in the presence of murine ascites fluid. Little has been published, however, as to the regulatory mechanisms controlling MAb production or the extent to which the distribution of cellular energy changes by the presence of serum factors or proliferation. Large scale production of MAbs is traditionally carried out in serum-supported cultures of continuously dividing cells (Eshhar, 1985; Adamson *et al*, 1987).

C. Hollow fiber bioreactors for the growth and maintenance of hybridoma cell lines.

Initially, hybridomas were injected into mice and grown as ascites. The ascites fluid contained the antibody of interest (Chandler, 1987), although in relatively low quantities that can prove difficult to isolate in pure form. As more uses have been found for monoclonal antibodies, the need for large scale methods of cell production and product isolation has also grown (Seaver, 1983). More

recently, stirred tank fermenters (Lebherz 1983), air lift fermenters (Creuger, 1987), ceramic matrices (Putnam, 1983), hollow fiber reactors (Knazek *et al*, 1972), and roller bottle culture (Seaver, 1983) have been used for hybridoma growth and MAb production. Hollow fiber culture systems most closely resemble the true state of tissue morphology (Knazek *et al*, 1972; Hopkinson, 1985). Antibodies are concentrated within the circulating medium and removed from the cell mass, thus facilitating isolation and purification. For these reasons, hollow fiber bioreactors are preferred within the biotechnology industry, providing a means of large scale cell culture and product formation with relative ease of purification.

1. History and description. In the early 1970's, hollow fiber bioreactors were developed for the growth of mammalian cells *in vitro* (Knazek *et al*, 1972). These early bioreactors were patterned after *in vivo* tissue morphology. Capillary beds were simulated by culturing cells between a series of selectively permeable cellulose acetate fibers enclosed within a glass tube. The reactor was enclosed within a continuous medium perfusion circuit, as shown in figure 5 (Knazek *et al*, 1972). Bioreactor systems have subsequently been modified for the analysis of cell growth using NMR spectroscopy (Gillies *et al*, 1986 and figure 6). The hollow fibers run axially through a polycarbonate shell. Fiber ends are potted within an epoxy resin such that the fiber lumina remain open for the perfusion of medium. Cells grow outside the fibers, within the extracapillary space (ECS). Pores within the fibers allow the passage of cell nutrients and wastes, each according to their

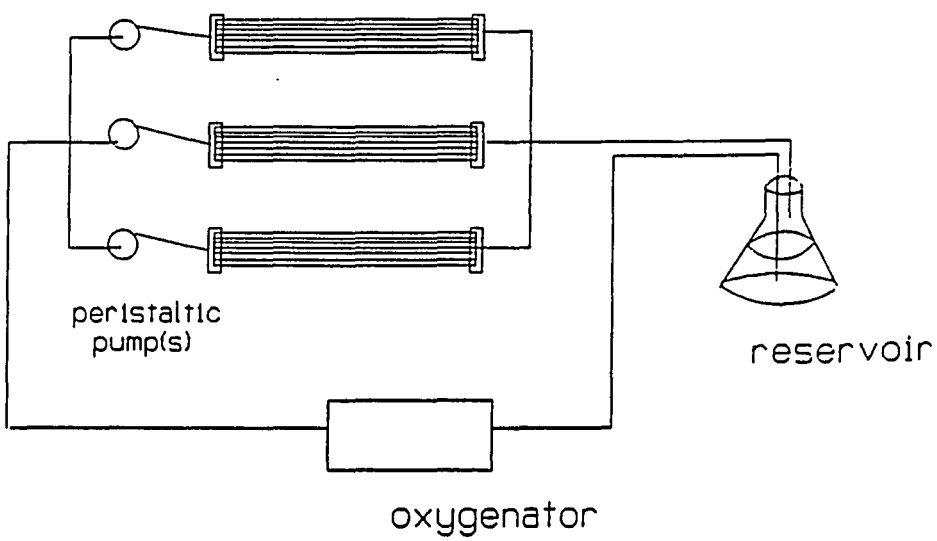

Figure 5. Knazek's perfusion circuit (Knazek *et al*, 1972). Cell culture units consist of a bundle of one or more types of hollow fibers sealed into each end of a glass tube by silicone rubber or epoxy resin. Units were arranged either in parallel (as shown) or in series. Nutrient medium was stored in a 125 ml flask and oxygenated prior to being pumped through the fiber bundles.

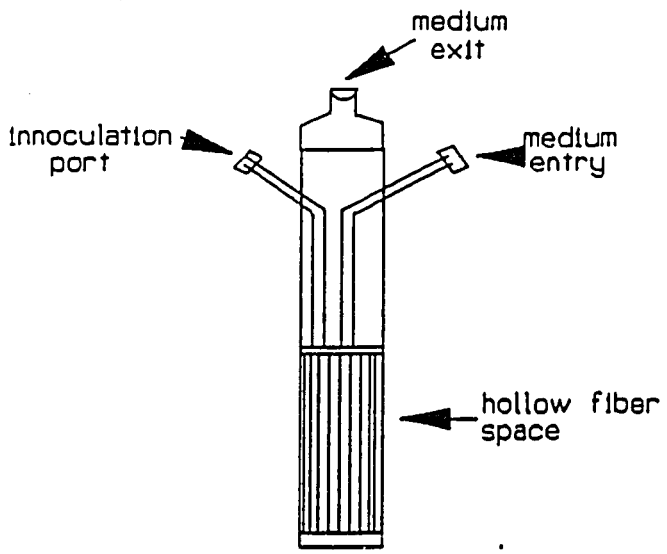

Figure 6. Hollow fiber bioreactor used for NMR studies. Cell culture units consist of a bundle of semipermeable hollow fibers encapsulated within a polycarbonate shell. Medium enters *via* the medium entry port, where it feeds directly to the bottom of the reactor and is forced up through the fibers. Medium from the exit port feeds back into the central perfusion vessel.

respective concentration gradients. The nutrients are consumed by cells within the ECS. Wastes enter into the fiber lumen by diffusion and are perfused away from the cell mass.

2. Bioreactor growth systems and their uses. Hollow fiber bioreactors have proven successful for the large scale production of microbial (Ollis, 1983; Suzuki *et al*, 1983) and mammalian (Glacken, 1983; Hopkinson, 1985; Anderson and Gruenberg, 1987; Anderson and Gruenberg, 1987; von Wedel, 1987; Handa-Corrigan, 1988) cells in culture. Bioreactor technology has permitted the cultivation of near tissue density cell cultures (Knazek *et al*, 1972; Hopkinson, 1985; Handa-Corrigan, 1988). Such systems are ideal for the study of cell systems *via* NMR spectroscopy, since they are able to generate the high local cell densities required for *in vivo* metabolic studies.

Bioreactor systems have been especially useful for the production of MAbs and other products of biological interest. The high cell densities produced yield high titers of the product of interest. As the secreted product diffuses into the perfusate, it collects within the medium reservoir to allow isolation of the product with relative ease.

D. Nuclear magnetic resonance (NMR) and *in vivo* NMR spectroscopy.

NMR phenomena were first reported by Rabi in 1936 (Rabi, 1936). Experiments performed in 1946 by Bloch and Purcell (Bloch, 1946; Purcell *et al*, 1946) later led to the development of NMR as a spectroscopic technique. NMR has subsequently been used to exploit the magnetic characteristics of atomic nuclei to characterize physical and environmental properties of molecules and perform quantitative

determinations (Gadian, 1982). It has been successfully applied to studies of living systems and used in medical diagnostics (Gadian and Radda, 1981; Gadian, 1982; Bottomly, 1990).

1. Basis of NMR. All nuclei with an odd number of protons or neutrons possess a net spin. Each nucleus has the property of internal magnetic momentum, or spin (Fukushima and Roeder, 1981; Gadian, 1982). A nucleus is, therefore, similar to a small bar magnet rotating about its own axis, as pictured in figure 7 (Gadian, 1982). In order to understand the nature of NMR phenomena and the ability to obtain information from this property of some molecules, it is necessary to discuss both the quantum mechanical and classical aspects of these molecular systems. For a more complete treatment of NMR theory see Abragam, 1960; Slichter, 1980; and Gadian, 1982.

The magnetic moment of a nucleus is related to, and has the same direction as, the angular momentum. The magnitude of the nuclear magnetic moment (u) is given by the equation:

$$u = gp$$

where p is the angular momentum and g is the gyromagnetic ratio. The gyromagnetic ratio is a constant, different for each nuclear isotope (Abragam, 1960; Slichter, 1980; Fukushima and Roeder, 1981; Gadian, 1982)

a. Quantum mechanical description of NMR phenomena. According to quantum mechanics, the angular momentum of any atomic nucleus may have only discrete values (Abragam, 1960; Gadian, 1982). These values are specified by the quantum number I, usually referred to as the spin

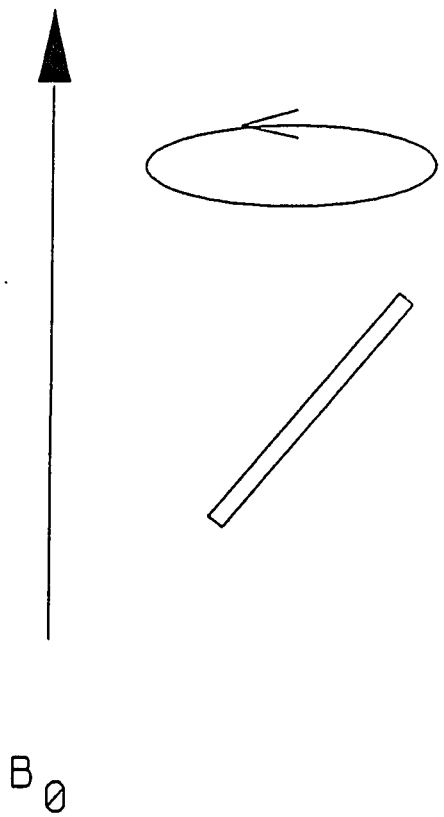

Figure 7. A nucleus within a standing magnetic field. When placed within a magnetic field, any nucleus with a magnetic moment and corresponding angular momentum will not align itself exactly parallel to the field. The nucleus precesses about the field (B_0) with the angular frequency (W_0), also known as the Larmour frequency.

of the nucleus. The nuclear angular momentum (p) is determined by the equation:

$$p = (h/2\Pi)[I(I + 1]^{1/2}$$

where h is Plancks constant, equal to 6.626×10^{-34} joule-sec.

The nuclear spin, I, may have only integer or half integer values. I is defined as:

1) An integer for nuclei with an odd number of protons and neutrons (e.g. ^{2}H).

2) Zero for nuclei with equal numbers of protons and neutrons (e.g. ^{4}He).

3) A half-integer (e.g. 1/2, 3/2, 5/2...) for nuclei with odd mass numbers (e.g. ^{1}H, ^{31}P).

Angular momentum is a vector quantity with both magnitude and direction. To specify direction, it is necessary to introduce the quantum number m, which specifies discrete orientations in Cartesion space. The angular momentum in the z direction (p_z) is given by the equation:

$$p_z = mh/2\Pi$$

where m is equal to I, I-1...-I.

If, for example, a nucleus with half-integral spin is placed within a magnetic field (B_o), it acquires energy (E) as a result of the interaction between B_o and the magnetic moment (u). The magnitude of this energy of interaction is given by:

$$E = -u_z B_o \text{ or } -(g)mB_o.$$

The nuclear energy levels are, therefore, split into 2I+1 states by the field. The energy difference between adjacent quantum states is:

$$\Delta E = B_o h/2\Pi$$

Transitions between energy states are induced with the application of an oscillating magnetic field (B_1) perpendicular to B_o in the xy plane (figure 8). To induce transitions, the field must oscillate with an energy equal to the energy difference separating adjacent states. Since $\Delta E = hv$, then $v_o = gB_o/2\Pi$. If the angular frequency w_o is equal to $2\Pi v_o$, then $w_o = gB_o$. This equation expresses the "resonance condition" for NMR experiments, where w_o is equal to the Larmour frequency.

Since g differs for each nuclear isotope, differing nuclei resonate at differing frequencies. Due to the strengths of B_o conventionally used, these frequencies lie in the radiofrequency range, and B_1 is referred to as the radiofrequency (rf) field.

For all spins, the distribution of nuclei among the possible energy states is determined by the Boltzman equation. For an I = 1/2 nucleus, the relative number of spins in the + 1/2 and - 1/2 spin states is given by the equation:

$$n-/n+ = \exp(-\Delta E/kT)$$

where T is the absolute temperature and k is the Boltzman constant, 1.38×10^{-23} Joule/degree. At $25^{o}C$, $\exp(-\Delta E/kT)$ is very close to one, and the populations often differ by less than 1 in 10^4 spins. Absorption of energy from the incident B_1 field is dependent on a population

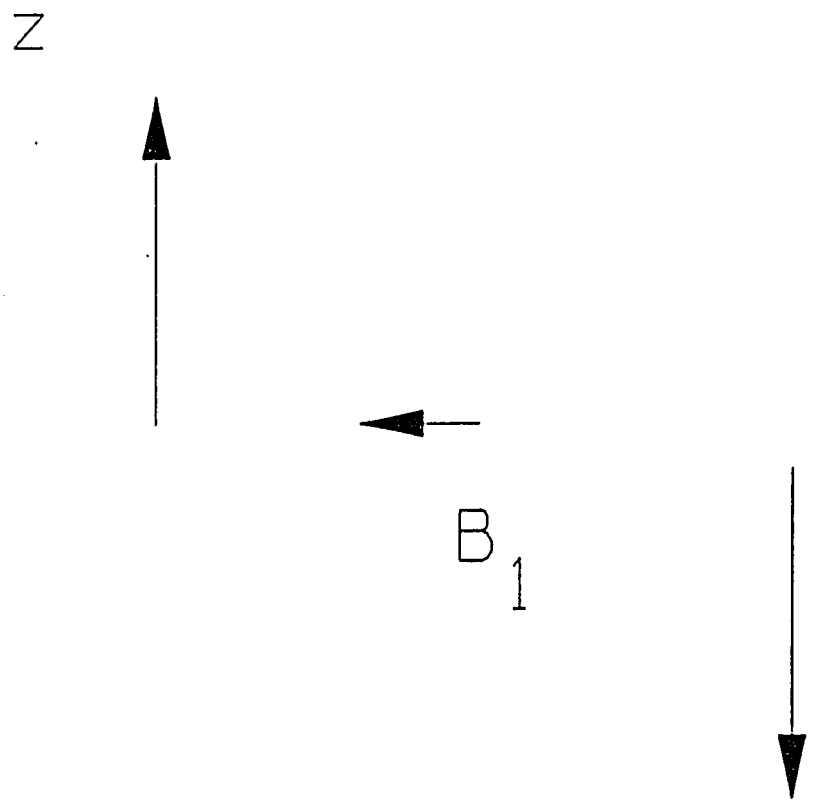

Figure 8. Transitions among nuclear spin states. Transitions are produced with the application of an oscillating magnetic field in the xy plane, perpendicular to the standing magnetic field and the net nuclear magnetization vector. This oscillating magnetic field is generated using an electromagnetic current oscillating at the Larmour frequency of interest. Due to the field strengths of B_1 usually employed, this freqency lies within the radiofrequency (rf) range and is referred to as the rf pulse.

difference existing between the two states. This small difference leads to a weak absorption of energy and a relatively low sensitivity of NMR.

b. Classical description of NMR phenomena. When placed within a magnetic field, a nucleus with a magnetic moment will align itself with the field. Since the spinning nucleus possesses angular momentum, it will not align itself exactly parallel to the field. Instead, it precesses about the axis of the field with the angular frequency W_o. This frequency, also known as the Larmour frequency, is the same as that derived from quantum theory. Therefore, $W_o = gB_o$.

Typically, samples used for NMR study consist of a large number of nuclei. All nuclei precess about B_o in the same direction, with no preferred orientation within the xy plane perpendicular to the B_o field. As such, the spins are phase incoherent. Nuclei may align in either direction with respect to B_o, the z axis. Due to the thermodynamic constraints described by the Boltzman equation, slightly more nuclei orient themselves with the field than against it, with slightly more nuclei in the lower energy state.

Since there is no preferred orientation within the xy plane, the net component of magnetization within the xy plane is zero. The sum of all magnetization vectors, however, yields a vector parallel to the z axis (figure 9).

c. Origin of chemical shift. The resonance frequency of any NMR-visible nucleus is proportional to the magnetic field (B_{eff}) experienced by the nucleus, where

$$B_{eff} = B_o(1 - \sigma).$$

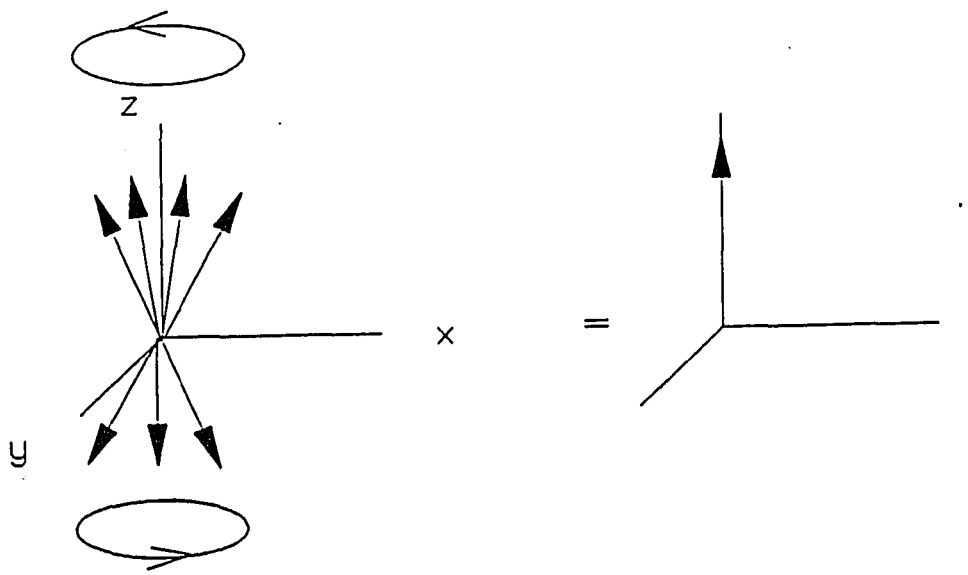

Figure 9. Net magnetization vectors from a sample of spinning nuclei. Samples within a standing magnetic field consist of a large number of individual nuclei, each spinning as described in figure 6. Spins are randomly aligned within the xy plane, and slightly more nuclei are aligned with the field than against it (see text). When individual contributions to the net magnetization are summed, the x and y components cancel, leaving the net magnetization aligned with the positive z axis.

The constant $(1-\sigma)$, represents the electronic shielding experienced by the nucleus. Electronic shielding lessens the field observed by the nucleus. The shielding tensor (σ) is a dimensionless constant whose magnitude is generally less than 10^{-4}. Nuclei of the same isotope in different electronic environments have different values of σ, and, therefore, experience different magnitudes of B_{eff}. For this reason, the same isotope in differing electronic environments will resonate at slightly different frequencies.

Chemical shift values are typically expressed in parts per million (ppm) relative to the resonance frequency of a reference compound. The ppm value is equal to $(\nu_s-\nu_r)$ Hz/ν_r MHz, where ν_s and ν_r represent the resonance frequencies of the sample and reference nuclei, respectively. This value, δ, is termed the chemical shift and represents the difference between shielding constants among nuclear centers. Nuclei with lower chemical shift values (upfield of the reference) experience a higher degree of shielding, and *vice versa*. The terms "upfield" and downfield" are remnants from continuous wave NMR spectroscopy and refer to the direction of the chemical shift. In Fourier transform NMR, a more strongly shielded nucleus experiences a reduced field and resonates at a lower frequency. Therefore, increased shielding produces an upfield shift, with lower resonance frequencies and chemical shift values.

Referring to resonances in terms of chemical shifts, rather than frequencies, stems from the use of different B_o field strengths in NMR experiments. The resonance frequency (in Hertz) of any nucleus is

at 200 megahertz (MHz) in a 4.7 Tesla magnet, 400 MHz in a 9.4 Tesla magnet and 500 MHz in an 11.7 Tesla magnet. Similar differences are observed among other nuclei. The derivation of the chemical shift value produces a value independent of field strength (Gadian, 1981; Slichter, 1980; Abragam, 1960).

d. Perturbation of spins. In order to measure NMR visible parameters, it is necessary to first perturb the nuclear spins within the sample. In order to visualize how this perturbation occurs, it helps to consider the "rotating frame," a frame of reference rotating at a rate equal to the resonance frequency w_o. If within this rotating frame, one applies a static field, B_1, along the x axis, the nuclear magnetization will begin to precess about B_1 with the angular frequency gB_1. This occurs because B_1 is the only apparent field experienced within the rotating frame. If this field is applied for a time t_p, the nuclei will rotate through an angle $\theta = gB_1t_p$ as shown in figure 10.

Within the laboratory frame, B_1 must correspond to a field that rotates around the z axis with an angular frequency w_o. This field is perpendicular to the z axis and generated by the passage of an oscillating or alternating current through a transmitter coil surrounding the sample.

2. Relaxation processes. Once tipped into the xy plane by the B_1 field, the nuclear spins, initially random, become phase coherent in the xy plane. After the B_1 pulse, the spins continue to precess about the z axis. This rotating magnetization creates an inductive electromotive

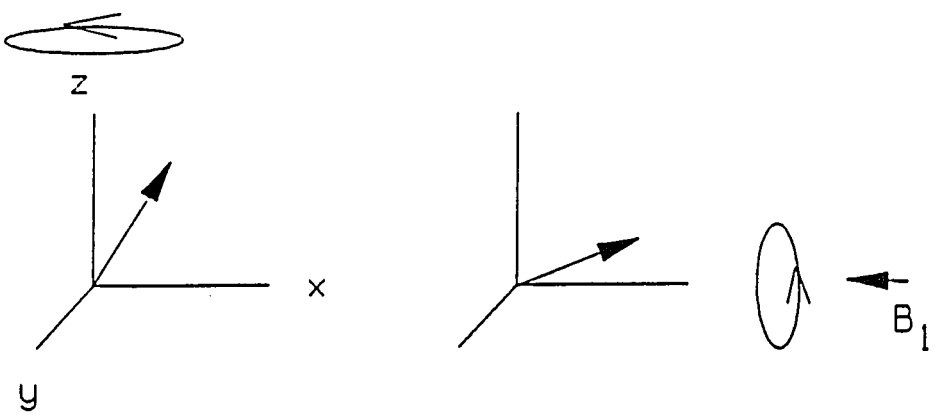

Figure 10. Perturbation of spins. Within the "rotating" frame of reference (see text), the oscillating magnetic field, B_1, is the only fieled experienced by the spinning nucleus. The nucleus, therefore, begins to precess about this field at the Larmour frequency. The net vector of magnetization (figure 9) therefore tips into the xy plane. The magnitude of this tip angle is proportional to the pulse length (in seconds).

force at the resonance frequency within a receiver radiofrequency coil. The voltage relaxes back to thermal equilibrium, with the time constants T_1 and T_2, respectively. The signal generated is a "free induction decay" of amplitude vs. time. Fourier transformation of this decay generates a spectrum of amplitude vs. frequency.

a. T1 relaxation. Once the nuclei have been tipped away from the z axis, the spin system will relax to its position of thermal equilibrium along the z axis (figure 11). This process is known as spin-lattice relaxation. The rate of this relaxation, $1/T_1$, is a measure of the ability of the lattice to absorb specific quanta of energy from the tipped nuclei.

b. T2 relaxation. Once the radiofrequency pulse aligns the spins along the x axis, the spins continue to precess at the Larmour frequency. Due to small inhomogeneities in this precessional frequency, the individual nuclei "fan out" in the xy plane (figure 12). This decay occurs with the time constant T_2, also known as the spin-spin relaxation time. Any process enhancing T_1 relaxation will induce these chemical shift "micro-heterogeneities," and T_2 is, therefore, always less than or equal to T_1.

3. Measurement of NMR phenomena. Once the nuclear spin ensemble has been tipped into the xy plane, it continues to precess about the z axis. This oscillating magnetic field in the xy plane induces an oscillating current in a radiofrequency coil which surrounds the sample. The oscillating, or alternating, current is a radiofrequency signal which decays due to T_1 and T_2 relaxation processes.

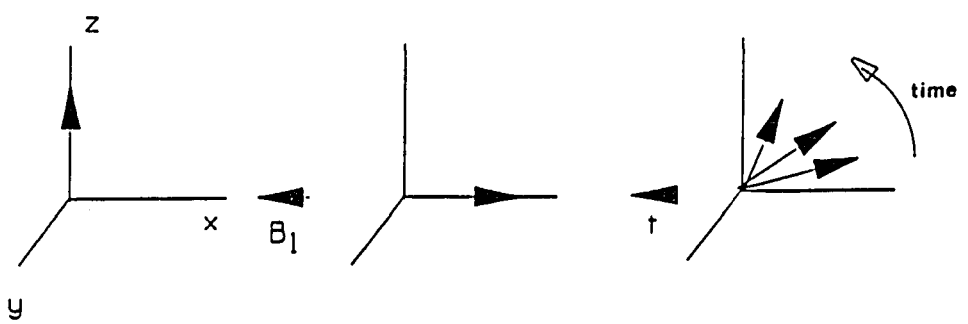

Figure 11. T_1 relaxation. After the perturbation of spins such that they are tipped towards the xy plane, the magnetized nuclei can donate their energy to the surrounding molecular lattice. By doing so over time (t), the net magnetization vector relaxes back to its position of thermodynamic equilibrium parallel to the z axis.

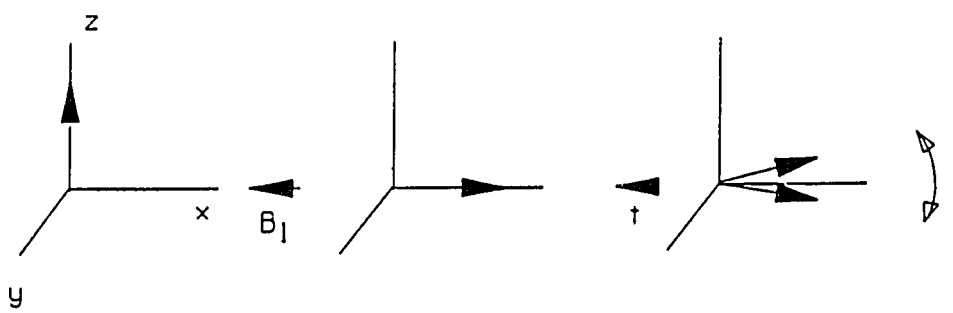

Figure 12. T_2 relaxation. Once tipped into the xy plane, the individual nucelar spins become "coherent" within the rotating frame of reference. "Microheterogeneities" in the precessional frequency cause the individual spins to "fan out' within the xy plane.

a. Saturation of spins. Radiofrequency signals are only generated from magnetizations oscillating in the xy plane. Magnetization vectors aligned with the + or - z axis will not be observed. Thus, due to the isotropic distribution of spins, no spins are observed prior to the application of an rf pulse with its associated B_1 field. Similarly, no signal will be observed from a sample whose magnetization has been tipped 180 degrees, or π radians, to become aligned with the -z axis. Alternatively, a series of rf pulses can be applied to eliminate the Boltzman population difference between the spin up and spin down states. Saturation can be achieved with a series of short pulses, each producing a flip angle of 1-10^{o}, separated with a short (200-400 usec) interpulse delay. During the interpulse delay, T_2 relaxation mechanisms cause the spins to "fan out" in the xy plane before they are tipped again by the next pulse in the series. After repeating this process a large number (10,000-20,000) of times, the Boltzman population difference is eliminated and the individual spins are de-phased and distributed randomly throughout Cartesian space. Thus, the net sum of the individual magnetizations is zero and no signal is observed. By adjusting the pulse length and transmitter power, pulses can usually be designed to specifically saturate any spectral region of interest (Forsen and Hoffman, 1963; Morris and Freeman, 1978).

4. General applications. All applications of NMR spectroscopy are based on the ability to assign resonances to specific nuclear centers (Abragam, 1960; Slichter, 1980; Gadian, 1982; Ernst *et al*, 1987). The

relative ease or difficulty of this identification is due, in large part, to the nature of the sample studied. For example, ^{1}H spectroscopy of a purified protein will generate a complex spectrum. Assignment of peaks to their respective amino acid residues can prove extremely difficult. This fact has largely been responsible for the development of multi-dimensional NMR spectroscopy, used primarily for the identification of resonances within complex molecules and studies of molecular conformation (Ernst *et al*, 1987; Bax and Lerner, 1986). In contrast, ^{31}P spectra of biological samples such as cells, tissues, and cell extracts are much simpler. Due to limits on the sensitivity of the instrumentation currently available and sample size limitations, only those compounds present at relatively high concentrations can be observed within the time limits that living samples can traditionally be maintained for study (Gadian and Radda, 1981). This is limited to inorganic phosphate, phosphoesters, and in some cases, phosphocreatine (Gadian, 1982).

NMR spectroscopy has been successfully applied to the study of biological systems. Addition of ^{13}C-labelled glucose to perfused organs and whole animals, has visualized pathways of metabolite flux through glycolysis (Ugurbil *et al*, 1979; Den Hollander, 1979; Bailey *et al*, 1981; Neurohr *et al*, 1983) gluconeogenesis (Cohen *et al*, 1979a), glycogen synthesis (Alger *et al* 1981; Stevens *et al*, 1982; Sillerud and Shulman, 1983; Canioni *et al*, 1983), the citric acid cycle (Bailey *et al*, 1981; Chance *et al*, 1983), and amino acid metabolism (Cohen *et al*, 1979b). In addition, it has been suggested that tumors can be

differentiated from non-malignant tissue on the basis of ^{13}C spectra (Halliday *et al*, 1987; James *et al*, 1990).

^{31}P spectroscopy has been used to study of cell and tissue bioenergetics and metabolism (Shulman *et al*, 1979; Gadian, 1981; Neeman *et al*, 1987). Although used less frequently, proton spectroscopy has also been used to observe metabolites *in vivo* (James *et al*, 1990; Williams *et al*, 1985).

a. Observation of system couplings. The NMR signal produced by any NMR-visible center is sensitive to the spins of neighboring nuclei (Abragam, 1960; Gadian, 1981). For example, a carbon-13 nucleus may have a neighboring proton. This proton may have either a spin up (+1/2) or down (-1/2) orientation. These possible orientations produce slightly different electrical environments, and therefore slightly different resonance frequencies for the nucleus under consideration. Thus, ^{13}C spectra will consist of a series of multiplets. Each multiplet represents the spin distribution among neighboring protons. Such carbon-proton, or heteronuclear, system couplings can be eliminated from a spectrum by inducing transitions rapidly, such that the carbons of interest experience a random field from all surrounding protons (Abragam, 1960; Gadian, 1982; Slichter, 1980; Bodenhausen *et al*, 1976). Alternatively, a nuclear spin may affect the environment of another located closely in space, although not directly connected through a covalent bond (Abragam, 1960; Gadian, 1981). Such coupling becomes especially important when performing spectroscopy of large, conformation-dependent molecules, such as proteins.

b. System conversion rates. Homonuclear decoupling methods can be applied to systems of non-equivalent, chemically exchanging, NMR centers. These methods have proven important in the determination of *in vivo* reaction rates (Brown and Ogawa, 1977; Matthews *et al*, 1981; Gadian *et al*, 1981; Shoubridge *et al*, 1982; Thoma and Ugurbil, 1987; Neeman *et al*, 1987; Eldar and Degani, 1989).

If two nuclei are exchanging such that A→B, "saturation" of the "A" spins will result in a decreased spectral intensity of "B". During the process of system perturbation and signal collection, "A" is being continuously converted to "B", and thus, the saturation of "A" is being transferred to "B". The newly formed molecules of "B" will also be "saturated," and effectively invisible to the receiver coil. Therefore, the intensity of "B" observed will decrease by an amount proportional the rate of the disappearance of "B." According the multisite exchange model of Neeman *et al* (1987), the fractional change in signal intensity ($\Delta M/M_O$) is equal to the product kT_1, where k and T_1 represent the rate constant for the disappearance of "B" and the observed spin-lattice relaxation time, respectively. This situation becomse more complicated in cases where "B" is involved in a multisite reaction mechanism. For example, where A $\xrightarrow{k1}$ B $\xrightarrow{k2}$ C the observed decrease in B will be proportional to k2, the rate of disappearance of "B".

Saturation transfer methods have been used to determine rates of the biologically important creatine kinase reactions of muscle and heart (Ugurbil *et al*, 1986; Hsieh and Balaban, 1987; Eldar and Degani, 1989). Such studies are important in that they provide physiological reaction

rates as they occur within a relatively undisturbed tissue and under physiological conditions.

5. Problems to be overcome when applying NMR to physiological systems. NMR has been developed, and primarily used, for the high resolution spectroscopy of isolated chemical compounds in solution. Although it has been applied to living samples, this field has developed more slowly.

a. Signal-to-noise considerations. Due to the small energy differences involved in NMR, it is a relatively insensitive technique (Abragam, 1960; Gadian, 1982). This is especially true of physiological systems, in which metabolites of interest tend to exist in millimolar or micromolar concentrations. These low concentrations usually require a large number of additive acquisitions so that the signal becomes visible over the noise inherent in the system (Gadian, 1982). NMR signals are coherent, whereas the system noise is random. The addition of repetitive spectra, therefore, results in an accumulation of the coherent signal while the noise tends to cancel itself. Increasing the number of acquisitions n-fold will increase the signal-to-noise ratio by the square root of n. Increasing the number of acquisitions is a common method of increasing the signal to noise ratio (S/N), especially when time resolution is not important to the sample under study (Abragam, 1960; Gadian, 1982). Time resolution can be more important in the study of physiological samples, in which cells and tissues must be maintained in a healthy and viable steady-state throughout signal aquisition.

One way to avoid the S/N problems associated with *in vivo* systems is to use a nucleus present at a high concentration in the cell or tissue of interest. This is the case with proton NMR of H_2O, which is 110 M in protons. Proton NMR is commonly used to generate images of soft tissues such as brain, cartilage, and muscle (Hoult, 1984; Bottomly, 1990). Proton images based on the water resonance are clinically important for the diagnoses of tumors and other tissue abnormalities (Bottomly, 1990). The large concentration of water in tissues, typically 55 molar, makes it difficult to obtain proton images or spectra of other compounds of potential interest. Proton metabolite spectra can, and have been obtained, although the spectra are relatively complex and difficult to interpret (Yoshizaki, 1981; Williams *et al*, 1985; Bloom *et al*, 1986; James *et al*, 1990).

b. Cell density. Since cell metabolites usually exist in relatively low concentrations, large numbers of cells are required for the collection of *in vivo* spectra. NMR signal intensities are proportional to sample concentrations. This parameter is, in turn, related to the density of cells within the sample (Gadian *et al*, 1979; Gadian, 1982). Tissues are densely packed aggregates of cells with a density of approximately 3-5 x 10^8 cell/ml. This density is unmatched by model systems of cells in culture. Perfused organs have, therefore, been used in a majority of physiological and *in vivo* NMR studies.

Such organ studies have provided valuable information about organ function and physiology, although they do have serious drawbacks. All tissues consist of several cell types. The functional cells of interest

(e.g. liver, kidney, or muscle) co-exist with cells performing auxillary or supporting roles, such as fibroblasts, endothelia, and circulating blood cells. Tissues are a heterogeneous mixture of cells experiencing a range of metabolic conditions arising from differences in circulation, oxygen availability and nutrient supply. NMR cannot differentiate between the various cell types and generates an average spectrum that cannot be ascribed to a single cell population.

More recently, hollow fiber bioreactors have been developed for use within NMR spectrometers (Gillies *et al*, 1986; Fernandez *et al*, 1988; Gillies *et al*, 1989). These bioreactor systems can grow and maintain cell densities of greater than 10^8 cell/ml, approaching the densities found in tissue (Gillies *et al*, 1989). One advantage of bioreactor systems is that homogeneous cell cultures may be grown for study, whereas any tissue consists of several cell types. NMR cannot differentiate between the various cell types and generates an average spectrum that cannot be considered representative of a single cell population.

c. Tissue and culture maintenance. In order to perform physiological studies of cells and tissues, these samples must be maintained in a system which closely approximates their true *in vivo* state (Gillies *et al*, 1989). Tissues can be studied *in situ* by, placing excitation and receiver coils outside the animal and over the area of interest, or surgically exposing the organ and wrapping the coil around the tissue (Ackerman *et al*, 1980; Gonzalez-Mendez *et al*, 1985; Balaban *et al*, 1986; Friederich and Freeman, 1986; Wolff *et al*, 1990). Excision

of the organ is usually performed for signal-to-noise considerations when ^{31}P or ^{13}C spectra are desired. Similar studies have been performed using tissues that have been removed and are maintained using perfusion systems for the supply of nutrients and oxygen (Jacobus *et al*, 1977; Matthews *et al*, 1981; Thoma and Ugurbil, 1987). A problem with these studies is that the tissues are moribund and are, therefore, not in a steady state.

With the development of bioreactors for use with NMR instrumentation (Gillies *et al*, 1986; Fernandez *et al*, 1988; Gillies *et al*, 1989; Heath *et al*, 1990), more emphasis has been placed on the growth of cell cultures for NMR studies. These systems are more complex and require constant monitoring. When performing whole animal studies, nutrient supply and tissue oxygenation are regulated by the animal's physiology, with little outside intervention. To perform studies of actively proliferating cell cultures, all aspects of cell growth must be monitored and adjusted over time (Gillies *et al*, 1989)

6. Applications to biological systems. Many of the problems encountered when applying NMR to cellular systems have been overcome sufficiently to allow successful investigations of cell metabolism (Gillies *et al*, 1986; Gillies *et al*, 1989).

a. Metabolite labeling. The addition of ^{13}C-labeled substrates to cultures of living cells will result in the subsequent labelling of metabolic intermediates or end-products. Most of these substrates are, however, too low in concentration to be observed using *in vivo* cell

preparations. Concentrated extracts from labeled cells have, therefore, been used to elucidate or confirm metabolic pathways.

b. Metabolite concentrations. Since NMR signals are proportional to concentration, NMR can be used as a non-destructive monitor of changes in metabolite concentration in response to tissue stress, trauma, and ischemia. ^{31}P-NMR has been used to monitor ischemia-induced changes in ATP levels in organs and tissue (Chance *et al*, 1987; Martin *et al* 1987; Zimmer *et al*, 1987). Similar studies have provided information as to the changes in phosphocreatine levels occurring in exercising muscle (Brown *et al*, 1990).

c. Intracellular pH. The chemical shift of inorganic phosphate (P_i) is sensitive to changes in pH. In the absence of large amounts of extracellular phosphate, it can be used as an effective indicator of intracellular pH. Such studies have been largely performed in muscle, where the endogenous presence of the pH-insensitive phosphocreatine resonance provides a chemical shift reference for the P_i resonance. Tissues lacking phosphocreatine usually require the addition of an exogenous chemical shift reference.

Inorganic phosphate is not a convenient pH indicator for cell cultures. Cell cultures are traditionally grown in the presence of phosphate salts. In the absence of a large plasma membrane pH gradient, intra- and extracellular phosphate co-resonate such that the large extracellular peak masks that of the intracellular pool. P_i can be removed from the extracellular space, but cells cannot be maintained under this condition for long periods of time. In addition, healthy

cells have a low internal P_i content which may increase the difficulty of determining intracellar pH from the chemical shift of this relatively low signal.

d. Tissue studies. ^{1}H, ^{13}C, and ^{31}P NMR have each been applied to studies of intact, excised, or perfused tissues. ^{1}H NMR is used primarily to generate images of tissue and organs. Proton spectra of brain have, however, demonstrated metabolic responses in the form of increased lactate concetration in the visual cortex in response to focal stimulation (Sappy-Marinier *et al*, 1990). Proton spectroscopy of normal and cancerous prostate glands has revealed low levels of citrate in the malignant condition, while all phosphorous resonances were poorly resolved when compared to spectra from healthy volunteers (Thomas *et al*, 1990).

F. Rationale--Proliferating cells and monoclonal antibody production.

In order for cell division to occur, proliferating cells need to increase their energy production rate for the purpose of doubling all existing cellular components. This is evidenced, in part, by the up-regulation in metabolism and synthetic events that are observed in response to growth-factor or serum stimulation of cell division (Prescott, 1968; James, 1984).

Throughout the cell cycle, metabolism and molecular syntheses are tightly regulated such that macromolecules are produced only when and as needed (Prescott, 1968). Similarly, the metabolic energy, or ATP, required to drive these syntheses is produced only as it is needed. In many respects, one may view the energetic state of the dividing cell as

geared for the ATP production required for cell syntheses, and eventually, division. The cell may preferentially synthesize those cell substrates required for division or division-associated processes.

Monoclonal antibodies (MAbs) are constitutive products of hybridoma cells and are not required in order for division to take place. The direct effects of cell division and the concommitant upregulation in metabolism on MAb yields remains unknown. Since MAbs are not required for the successful progression of cell division, MAb synthesis may, in fact, be "down regulated" so that any available cellular energy may be used for those processes required on order for division to take place.

1. Significance. As a result of their potential uses in biochemistry and medicine, MAbs and their production have developed an ever-increasing importance. The requirements for efficient MAb production are, however, poorly understood. MAbs are usually produced in large-scale, actively proliferating hybridoma cultures and harvested once the culture reaches the "stationary" phase of growth. This can prove expensive, even when serum-free media preparations are used. This may also be unnecessary, since proliferation may not provide the most efficient or cost-effective means of product formation.

2. Hypothesis. Proliferation may not enhance MAb yields. Proliferating cells may, in fact, produce MAbs less efficiently than healthy non-proliferating cultures, since they are not needed in order for division to occur. To address this hypothesis and better characterize hybridoma cell metabolism and energetics, this report

compares energy production among static and proliferating hybridoma cultures. The distribution of cellular energy among several pathways critical to cell division and maintenance has also been investigated.

This research combines traditional biochemical methods for the determination of substrate (glucose, oxygen) consumption and product (lactate, MAb) formation with the more novel applications of NMR spectroscopy to problems of bioenergetics. NMR spectroscopy provides an alternative method for the measurement of cell growth in bioreactor culture, as well as a potentially direct determination of ATP synthesis rates.

The NMR studies presented here have been performed using hybridoma cultures grown and maintained in hollow fiber culture. These studies, therefore, provide a means of evaluating and comparing the relatively physiological and commercially significant bioreactor growth systems with suspension cultures, in terms of growth rates, substrate consumption, and product formation.

II. Materials and Methods.

A. Cell culture.

All experiments were performed using EPO8F7 hybridoma cells. EPO8F7 cells are an Sp/2 derived mouse hybridoma, developed and donated by Amgen, Boulder CO. EPO8F7 cell secrete F12, a mouse antibody directed against human erythropoietin.

Cells were grown and maintained in RPMI 1640. Standard RPMI 1640 (Sigma), with L-glutamine and sodium bicarbonate, supplemented with 5% Nu-serum (Gibco) was used for maintenance of stocks and studies of cell growth in suspension culture. Non-proliferating or slow-growing cultures were produced by amino acid (leucine) or serum deprivation. Leucine limitation was produced by inoculating log-phase healthy cultures at a density of approximately 5 x 10^5 cells/ml into RPMI medium, deficient modification (Sigma) lacking sodium bicarbonate, glutamine, leucine, lysine, and methionine. All compounds except leucine were resupplemented to their normal RPMI 1640 concentrations (Freshney, 1987). Low level leucine supplements were added in culture preparation. Serum deprivation studies were performed after inoculating healthy, log phase cells into serum-free or conditioned medium.

To determine the Nu-serum concentration which best supports the growth of EPO8F7 cells, cells were harvested from log-phase stocks and resuspended in serum-free medium at densities of 2 x 10^4 or 2 x 10^5 cells/ml. Suspensions (0.5 ml) were added to each well of a 24-well miniplate (Falcon). An additional 0.5 ml of medium and serum was added to yield serum supplements of 0 to 10%. Cells were incubated for 48

hours at 37° C in a 5% CO_2, 95% air incubator (VWR/IR). Prior to counting, the cells were aspirated several times in a Pasteur pipet to fully resuspend them. Fifty percent of a 0.1% trypan blue solution was added to assess individual well viabilities and the cell number determined by hemocytometer count.

Bioreactor cultures were maintained in low phosphate RPMI 1640. Medium was prepared from scratch, weighing out the individual medium components required for 20 liter quantities. All components were dissolved at the time of medium preparation. The Na_2HPO_4 concentration was reduced to 1 mM and the buffering capacity of the medium restored with 5.5 mM HEPES. 1 mM dimethylmethyl phosphonate (DMMP, Sigma) was added as a concentration and chemical shift standard. Medium pH was adjusted to 7.30. Penicillin and streptomycin sulfate (Sigma) were added to insure maintained sterility of the bioreactor culture.

All media were filter sterilized immediately following preparation.

Stock cultures were maintained in spinner flask culture. When performing or preparing experiments, cells were harvested in the log phase of growth, between 2 and 6 x 10^5 cell/ml.

B. MAb determination.

MAb titers were determined using the enzyme-linked immunosorbant assay (ELISA) technique. MAb-containing medium was added to 96-well microtiter plates "blocked" or coated with a rabbit-anti-mouse (R α M) antibody. Plates were incubated for one hour at 37°C and erythropoeitin-horse radish peroxidase (HRPO) conjugate added to the

wells. The R α M antibody block binds the MAb of interest and the EPO-HRPO conjugate binds the MAb to be assayed. Following another incubation for 30 minutes at 37°C, any excess conjugate is rinsed away with phosphate buffered saline (PBS; Freshney, 1987). A mixture of 3,3',5,5'-tetramethylbenzidine and hydrogen peroxide was used as the colorigenic substrate for the peroxidase reaction, turning blue in the presence of peroxidase labelled antibodies. Reactions were allowed to proceed for 5 to 10 minutes, or until a visible color change was observed. Reactions were stopped with 0.5 M H_2SO_4. Reaction progress was determined photometrically, using well absorbances at 450 nanometers. This value is proportional to the peroxidase product concentration, related to the reaction rate, and determined by the amount of enzyme conjugate bound to the wells. All ELISA reagents and blocked microtiter plates were supplied by Amgen, Boulder CO.

C. Inhibitor studies.

Protein, DNA, and RNA syntheses were inhibited with 100 uM cycloheximide (CHX, Campisi and Pardee, 1984), 2 mM thymidine (Bresnick *et al*, 1964) and 10 uM 5,6-dichlororibofuranosyl-benzimidazole (DFB; Campisi and Pardee, 1984), respectively. Each of these inhibitors has been previously shown to inhibit the pathways of interest. One millimolar ouabain was used for the inhibition of Na^+/K^+ transport (Buckhold-Shank and Egan-Smith, 1976). Inhibitors were dissolved at a concentration of 1 M (0.1 M in the case of DFB) in DMSO to facilitate their addition to cell suspensions.

All inhibitors were used individually for determinations of inhibitor-induced changes in the glycolytic flux and oxygen consumption rate. In addition, CHX, thymidine, and ouabain were added in pairs to assess the degree to which inhibition of any one pathway affects other energy-consuming pathways.

D. Oxygen consumption measurements.

Cells were harvested from log-phase or leucine-limited cultures, centrifuged at 100 x g and resuspended in fresh (standard or 0.5 mg/l leucine medium). Final cell densities were approximately 3 x 10^6 cells/ml. This suspension was transferred to a YSI instruments standard bath assembly (model #5301) for measurement of O_2 consumption. Oxygen levels in the suspension were monitored using a Clark-type oxygen electrode and biological oxygen monitor (YSI instruments, model 5300). Percentage O_2 saturation was recorded on a Houston analog plotter. Plotter response was calibrated using media equilibrated to 5% CO_2, 95% air at 37^o C. The solubility of oxygen in tissue culture medium was adapted from the method and calculations of Schumpe *et al* (1978) for the solubility of oxygen in electrolyte solutions. Inhibitors were added to the suspension once the O_2 level had reached 50 to 70% of its pre-inhibition value.

E. Glucose consumption/lactate production.

Cells were harvested from log-phase or leucine limited cultures, centrifuged at 100 x g, and resuspended in fresh (standard, leucine free, or 20% conditioned) medium. Final cell densities were approximately 4 x 10^6 cell/ml. Glucose and lactate concentrations in

the suspension were determined at 5 to 10 minute intervals over a 60 to 90 minute period using a YSI instruments clinical glucose/lactate analyzer (model #2000). Determinations were performed in the presence and absence of metabolic inhibitors. Consumption rates were also determined over longer time periods in stock suspension culture using Sigma enzymatic test kits.

F. Analysis of data.

Pre- and post-inhibition rates of oxygen consumption were used to calculate relative inhibitor-induced decreases in consumption. To correct for day-to-day variations observed among pre-inhibition O_2 consumption rates, the mean and standard deviation for O_2 consumption in the absence of inhibition were calculated using all pre-inhibition values. On any given day, if more than 50% of the pre-inhibition values were found to lie outside the range of the standard deviation, these daily values were averaged. This average was used to calculate a normalization constant by dividing the daily average by the overall average determined from all of the pre-inhibition values. Individual pre- and post-inhibition consumption rates were normalized using this constant. This process was repeated, using the normalized values, until a majority of the pre-inhibition rates determined on any given day were found to lie within the new standard deviation range. This treatment does not affect the overall mean and was performed only to allow comparisons between scalar, rather than relative, values.

A similar procedure was used to determine glucose consumption and lactate production rates in the absence of inhibition. Means of glucose

consumption and lactate production were used to calculate daily averages. These averages were used to calculate normalization constants, and all rates normalized using these values.

1. Estimation of ATP production. ATP production rates were estimated from measurements of glucose, lactate, and O_2 consumption or production, assuming the production of 1 ATP per lactate and a P/O_2 ratio of 6.0 (Lehninger, 1949; Lehninger, 1954; Chance, 1956; Lynch and Balaban, 1987a and 1987b). This yields the maximum for ATP production for cells utilizing glutamine as an energy source.

G. Radiolabel studies.

Tritiated (methyl ^3H) thymidine, (5,6-^3H) uridine and (1-^{14}C) leucine were obtained from ICN Biomedicals. Ten ml cell suspensions containing 10^6 cells were incubated in 50 ml culture tubes for 5 minutes at 37°C using various concentrations of the inhibitor of interest. The relevant label was added (approximately 1 uCi/ml of tritiated species, or 0.1 uCi/ml of ^{14}C-leucine) and the suspensions incubated another 20 minutes at 37°C. Ten ml of 5% perchloric acid was added to each culture tube and precipitates allowed to form overnight. Protein and DNA precipitates were obtained by centrifuging the samples for 10 minutes at 850 x g. The pellets were washed twice in 95% ethanol. RNA pellets were obtained by centrifuging 10 minutes at 1500 x g and washing the pellets twice in 0.1 M HCl. Pellets were collected on glass fiber filters (Whatman GF/C) and radiolabel analyzed by scintillation counting of the filters in the presence of 5 ml liquid scintillation fluid (Aquasol, DuPont).

To assay ^{14}C-leucine uptake (as opposed to incorporation) 0.1 uCi/ml was added to samples of 10^6 cells. Samples were incubated for 20 minutes at 37°C. Cells were removed from suspension by centrifuging for 5 minutes at 100 x g. The cells were washed twice in 5 ml of ice-cold RPMI 1640. Five milliliters of 5% perchloric acid was added and precipitates allowed to form overnight. The precipitate was removed by centrifuging the samples for 10 minutes at 850 x g and the supernatants assayed for radioactivity as discussed.

H. Mithochondrial control studies.

To investigate the effects of inhibitors on cellular respiratory mechanisms alone, inhibitors were added to crude suspensions of mitochondria. Rat liver mitochondria were prepared according to the proceedure of Schneider (1948). Rats were killed by decapitation, the livers removed and chilled in ice-cold 150 mM (isotonic) KCl. After cooling, the livers were blotted, weighed, and homogenized in isotonic (8.5 g/100 ml) sucrose. Livers were coarsely chopped and homogenized using a Potter-Elvehelm homogenizer.

The homogenate was centrifuged for 10 minutes at 600 x g to sediment cell nuclei. The mitochondria-containing supernatant was added to RPMI 1640 equilibrated to 5% CO_2, 95% air, and 37° C immediately prior to the measurement of oxygen consumption. The RPMI/mitochondrial suspension ratio used was 3:1.

I. Hollow fiber bioreactor systems.

1. Construction. Hollow fiber bioreactor housings were composed of polycarbonate shells of 1.4 mm thickness, 28 cm in length, and 25 mm in

diameter. The capillary bed consists of 1410 composite fibers of cellulose acetate and cellulose nitrate 90 um thick and 3 mm in diameter. Bioreactors were supplied by Microgon, Inc.

Fiber ends are potted within an epoxy resin such that the fiber bed remains stationary and fiber lumina are open for the passage of perfusion medium. Cells are inoculated into, and remain within, the 14.4 ml extracapillary space between the resin at each fiber end (figure 6).

Medium feeds into the reactor *via* polyurethane tubing which extends through the center of the capillary bed and to the bottom of the reactor. Medium is forced upwards, through the fibers, and exits through a central port at the top of the reactor. The inoculation port, through which cells are added, extends into the extracapillary space.

2. Perfusion system. Medium is continuously perfused through the reactor as shown in figure 13. The perfusion vessel is contained within a constant temperature cabinet maintained at approximately 42^{o}C. The temperature was controlled *via* a temperature controller connected to a heat source consisting of three 100 Watt light bulbs. The temperature is sensed *via* a thermocouple link, the lights shutting off once the temperature rises 0.2^{o}C above the set point and relighting when the temperature drops 0.2^{o}C below the set point. Using this method, the medium within the bioreactor could be maintained at 37 ($\pm$ 0.2 ^{o}C).

Medium is forced from the perfusion vessel to the bioreactor *via* tygon tubing, using a peristaltic pump. On leaving the perfusion vessel, the medium flows through a flow meter and hollow fiber

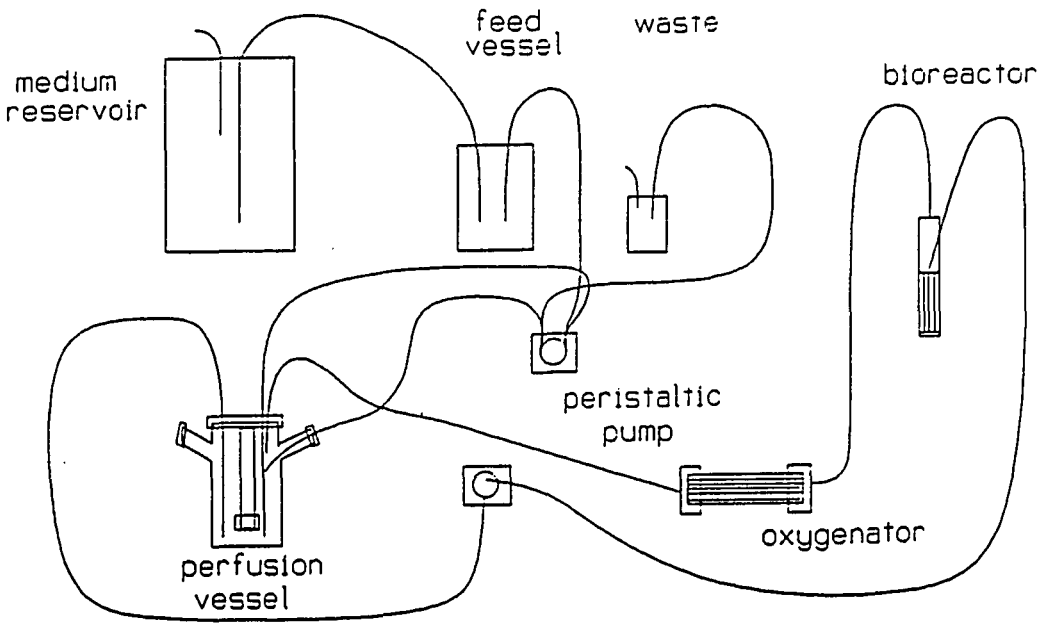

Figure 13. Perfusion system. Medium is cycled from the main perfusion vessel through the hollow fiber bioreactor and back again. Prior to the medium return to the vessel, it passes through a hollow fiber membrane oxygenator supplied with gas of a defined composition. In this way, the medium within the vessel remains adequately oxygenated at all times. Fresh medium is continuously pumped into the perfusion vessel. Simultaneously, wastes accumulating within the vessel are bled away. By adjusting this "bleed-and-feed" rate as the culture grows, it is possible to maintain nutrients, wastes, and medium pH at concentrations supportive of cell growth. The feed vessel is supplied by a large (20 l) medium reservoir. Any medium supplements (such as serum) are added to the medium once it has been transferred from the reservoir and into the feed vessel.

oxygenator (Kinentek, Inc., St. Louis, MO) connected to a tank of defined gas mixture (e.g. 5% CO_2, 20% O_2, 75% N_2), prior to reaching the bioreactor. Medium flow rates were set between 100 and 150 ml/min.

Nutrient concentrations are maintained in the perfusion vessel using a continuous "bleed and feed" mechanism. Fresh medium is pumped into the perfusion vessel while waste medium is continually bled away. It is possible to maintain nutrient levels at any desired level with adjustment of this "bleed and feed" rate as the cells within the reactor grow. Any serum or growth factors desired are added to the 2-3 liter feed vessel, which is, in turn, supplied by a larger (20 l) medium reservoir (figure 13).

3. Sterilization and maintenance of bioreactor sterility. All glass vessels and tubing in the bioreactor loop were autoclaved at 121°C for 30 minutes. Bioreactors, oxygenators, and medium flow meters were sterilized with ethylene oxide gas followed by sterile aeration. Once the perfusion system was assembled, it was allowed to cycle with medium for several days prior to inoculation with cells. This was to insure that any toxic remnants from the gas sterilization were rinsed away, as well as to serve as a final sterility check prior to the addition of cells.

4. Bioreactor inoculation. Cultures (1-2 l) were grown to a density of 4 to 6 x 10^5 cell/ml to supply an inoculation stock of approximately 10^9 cells. Sterile tubing connects the spinner flask stock to the bioreactor inoculation port and is secured with polycarbonate luer fittings (figure 14). The peristaltic pump used for perfusion was

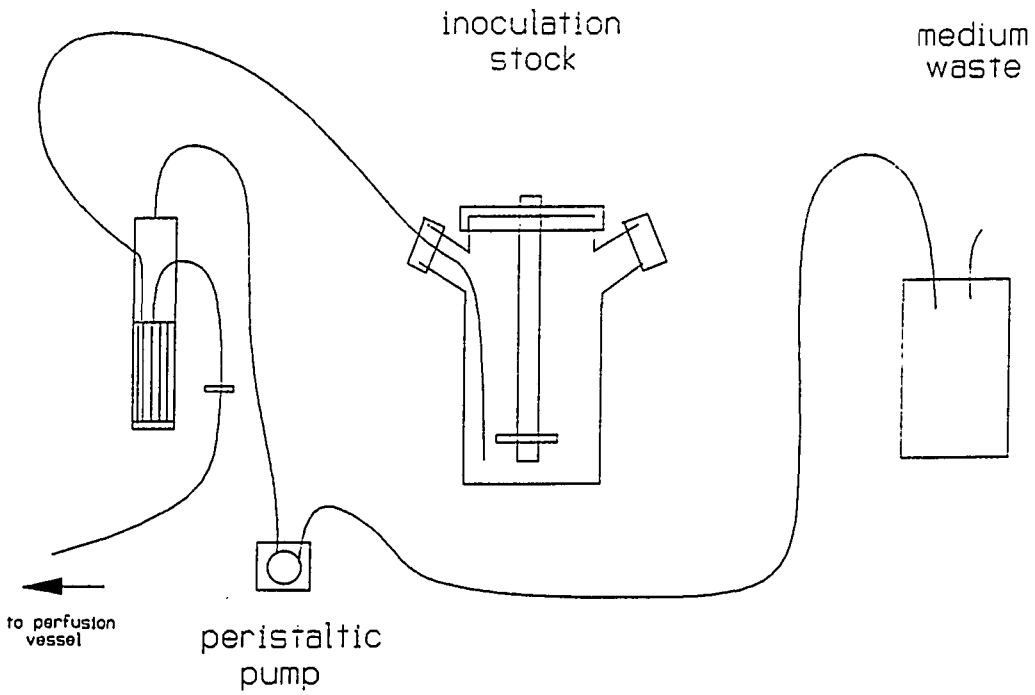

Figure 14. Inoculation set up. To draw cells into the reactor, a peristaltic pump draws medium out of the reactor *via* the exit port at an approximate rate of one liter per hour. The medium entry port is clamped shut, and a sterile line of tubing extends from the innoculation port to a suspension culture of 2-5 x 10^5 cell/ml. The cell suspension is drawn into the reactor. The cells, which cannot cross the fibers, remain trapped within the extracapillary space. Excess medium from the suspension culture is pumped into the waste reservoir and removed.

reversed to draw medium out of the reactor *via* the exit port. The medium entry port was clamped shut. As medium was drawn out of the reactor, the cell suspension was drawn in. Medium crosses the fibers, is pumped into the perfusion vessel, and bled away. The cells could not cross the fibers, and remained trapped in the extracapillary space.

J. NMR instrumentation and experiments.

All NMR experiments were performed on a Bruker AMX 400 WB spectrometer operating at 161.97 MHz for phosphorus. To monitor cell growth, ^{31}-P spectra were obtained at 6 to 10 hour intervals. These one hour spectra were generated with the accumulation of 3600 transients of 14 microseconds (14 us = 20^{o}) separated by a 1 second delay. The intensity of the gamma-ATP peak relative to the system noise or the 2.5 mM dimethylmethylphosphonate (DMMP) internal standard was used to indicate increases in cell number.

Saturation-transfer experiments were performed using a DANTE saturation pulse train at the spectral frequency to be saturated (Bovey, 1988). This was comprised of 16,000 60 usec pulses of 40 dB transmitter attentuation and a 250 usec inter-pulse delay. This presaturation sequence lasted for a total of 5 seconds. An excitation pulse of 14 usec and a 0.11 second acquisition time, during which WALTZ decoupling (Bovey, 1988) was performed, was used to collect spectra. A one second recycle delay was used prior to the application of the next presaturation and acquisition seqence. Spectra consisted of 640 transients and required one hour for collection.

Transfer rates were determined using the multisite exchange model described by Neeman *et al* (1987). Upon the saturation of any one resonance (e.g. gamma-ATP) the fractional change in signal intensity ($\Delta M/M_o$, where M_o is equal to the control saturation at equilibrium), is proportional to the corresponding rate constant, such that $\Delta M/M_o = kT_1$, where k and T_1 represent the rate constant and observed spin-lattice relaxation time, respectively.

Spin-lattice relaxation times were determined according to the progressive saturation technique (Gadian, 1982; Bovey, 1988), using a (90^o-acquire-t_d) pulse sequence. This method is appropriate for nuclei which have T_2 values much smaller than T_1, a condition true for most biological systems. This sequence is designed such that a series of 90^o pulses establishes a dynamic equilibrium between rf absorption and spin-lattice relaxation. The magnitude of the steady state signal (after early signals are discarded) depends on the interval (t_d) between pulses according to the equation:

$$M_o - M_t = M_o \exp(-t/T_1)$$

This method is less accurate than the more conventionally used inversion recovery (180^o-t-90^o) pulse sequence for the determination of T_1 values. Since time resolution was important in the bioreactor studies of cell growth, throughout which T_1 values may be changing, this method was chosen over the more generally accepted inversion recovery method.

III. Results.

A. Cell growth.

To determine the serum concentration which best supports EPO8F7 growth in suspension culture, cells were grown using serum supplements ranging from 0 to 10 % (figure 15). Following 48 hours in miniwell culture, all wells showed increases in cell number. The cell numbers produced in response to serum supplementation appeared to plateau at approximately 5% Nu-serum supplementation. Relative MAb titers were also determined as a function of Nu-serum concentration in the high and low density miniwell cultures (figure 16). Antibody yields appeared to be independent of the added serum concentration, as well as the initial inoculum size.

To insure that no significant differences existed between cell cultures grown using 5%, as opposed to 10% Nu-serum supplements, cell growth rates were determined in 5% and 10% Nu-serum cultures (figure 17). Low density (approximately 10^4 cell/ml) suspension cultures were prepared with 5% and 10% Nu-serum supplements, respectively. Five and ten percent cultures were inoculated at the same density and determinations of cell number performed in parallel. Cultures were counted at 4 to 6 hour intervals and cell number plotted as a function of time. In both cases, cell densities were found to double at 16 hour intervals. No significant differences were observed among the growth curves produced by the 5% and 10% Nu-serum supplements. In addition, the two cultures consumed glucose and produced lactate at similar rates (figures 18a and b). The initial concentration of medium lactate was

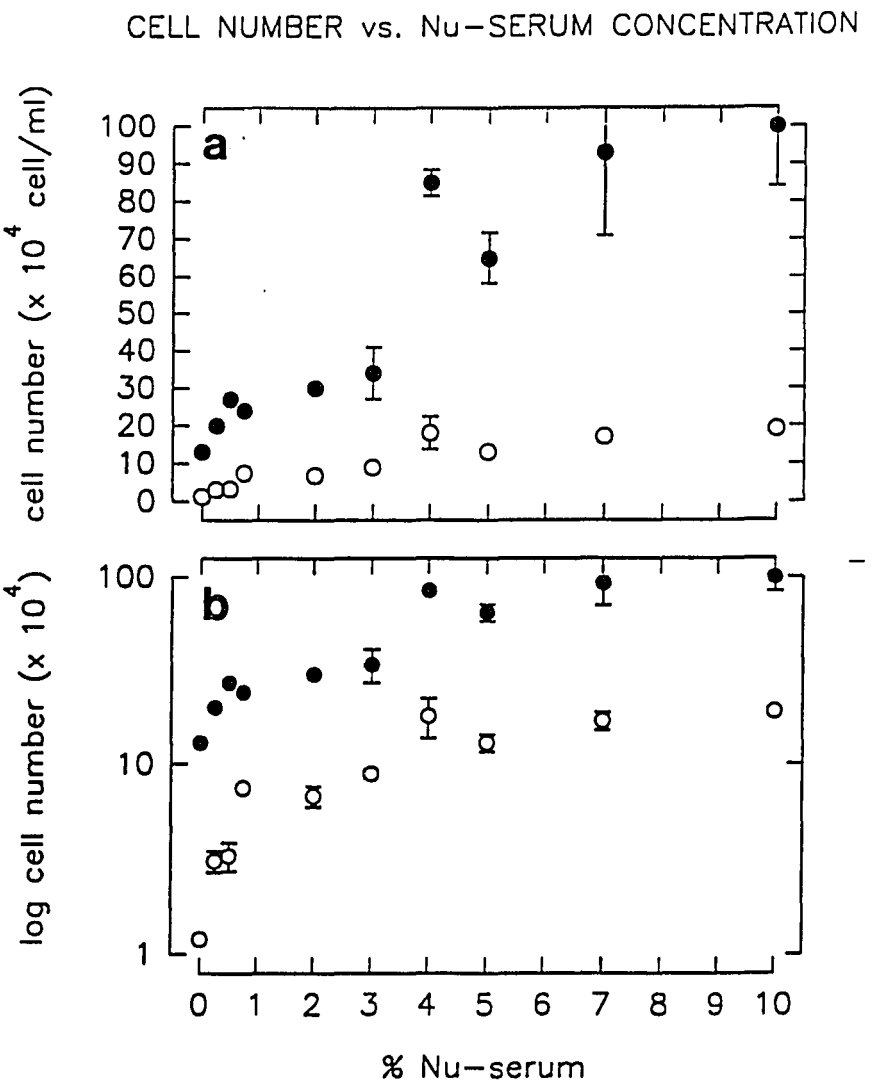

Figure 15. Cell number *vs.* Nu-serum concentration. Miniwell cultures were initiated at 10^4 (open circles) and 10^5 (filled circles) cells/ml. Cultures were prepared and counted as described in "Materials and Methods." Increases in cell number are plotted as a function of serum concentration. Low density cultures show only modest increases in cell number, while the higher density wells demonstrate more dramatic increases as a function of serum concentration. In both cases, however, cell numbers appear to plateu between 4% and 5 % Nu-serum supplements.

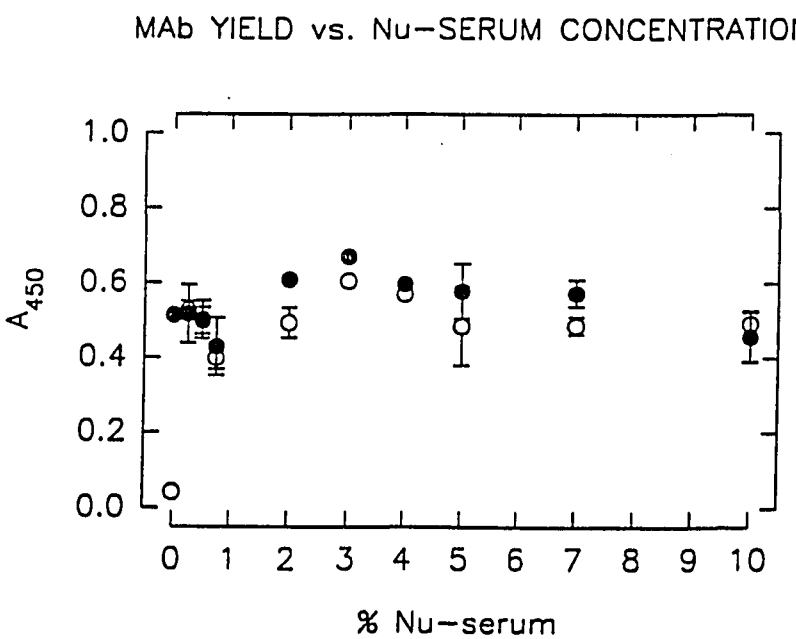

Figure 16. MAb yield vs. Nu-serum concentration. Media supernatants were collected from miniwell cultures as described in the text. ELISA assays (see Materials and Methods) were used to determine relative antibody yields. Low and high density cultures, plated at 10^4 cells/ml (open circles) and 10^5 cells/ml (filled circles) produced similar MAb yields. MAb titers also appeared to be serum-independent.

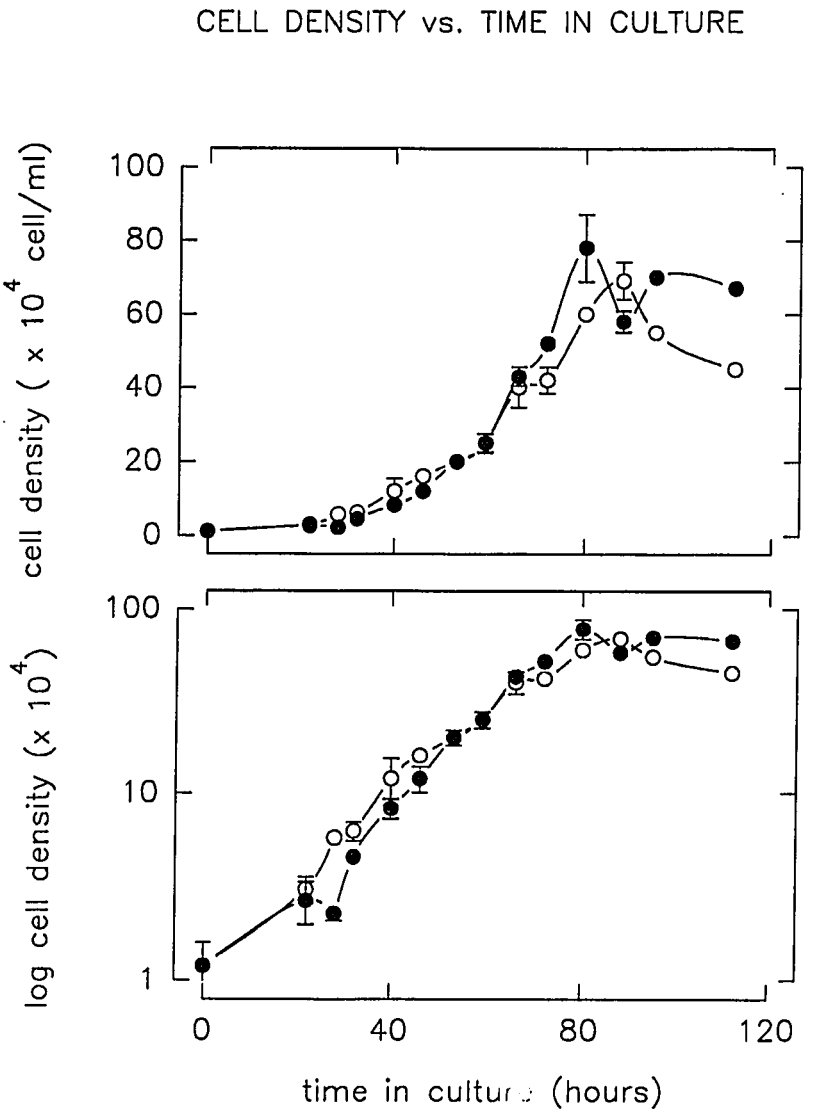

Figure 17. Cell density vs. time in culture. Cell density was determined as a function of time in 5% (open circles) and 10% (filled circles) Nu-serum culture. The cell cultures were innoculated at the same density and determinations performed in parallel. Growth rates did not differ appreciably between the two cultures.

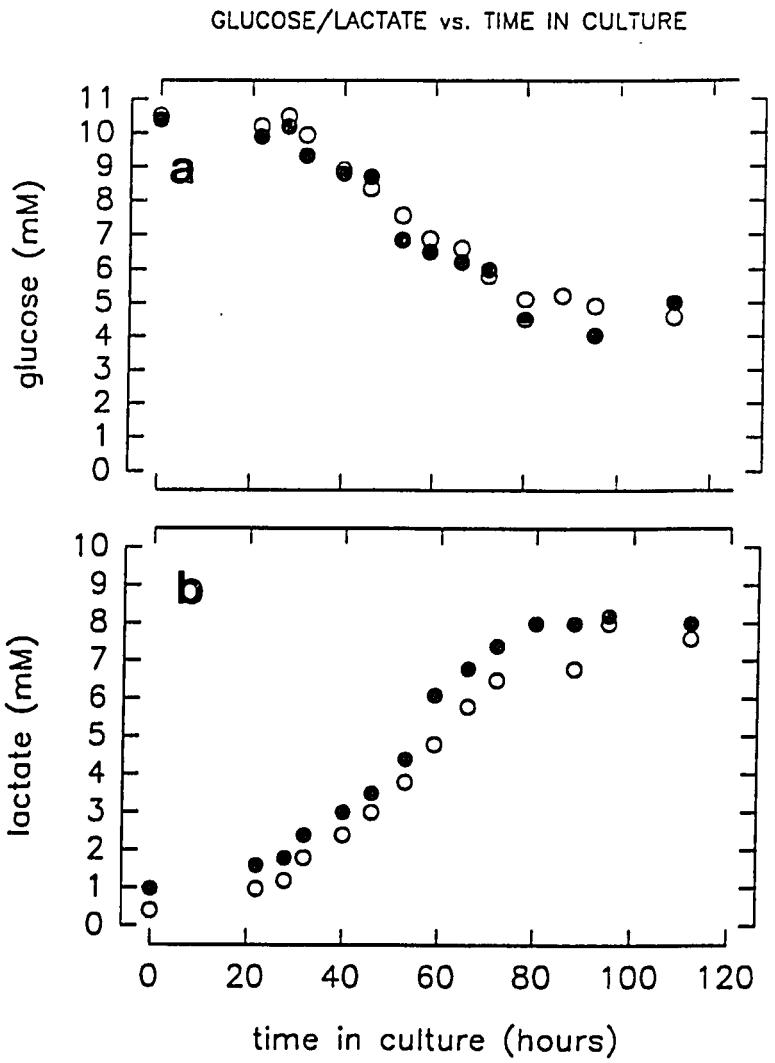

Figure 18. Glucose/lactate *vs.* time in culture. Glucose and lactate concentrations were determined as a function of time in 5% (open circles) and 10% (filled circles) Nu-serum cultures, using Sigma enzymatic test kits, as described in Materials and Methods. The data presented here were obtained from the same cultures as used to obtain the information presented in figure 14. Cultures were sampled for glucose and lactate determinations at the same points as used for determinations of cell density. Rates of glucose consumption and lactate production do not appear to differ between the two serum concentrations studied.

slightly higher in the 10% Nu-serum culture (figure 18b). This is due to lactate present within the serum itself being diluted to a lesser extent given the higher serum concentration. Determinations were performed using Sigma enzymatic test kits, as described in Materials and Methods. When observed under the microscope, cells grown under the two culture conditions appeared identical, with the reduced serum concentration producing no noticeable morphological differences.

Since the 5% and 10% Nu-serum cultures were identical in all respects studied, 5% supplements were used for the maintenance of all stock cultures and the production of proliferating cultures for further study. Numerous determinations of cell number as a function of time, were used to firmly establish the doubling time near 16 ($\pm$ 2) hours, with the cells reaching a maximum density near 10^6 cells/ml. At this point, medium glucose is depleted to approximately 5 mM, the concentration of lactate is near 9 mM, and the cells lose viability rapidly. Resuspension of the cells in fresh, serum-supplemented medium did not prevent this loss in viability.

B. Non-proliferating cultures.

In an attempt to produce either slow growing or non-proliferating cultures, miniwell cultures were prepared in the absence of serum. Low density cultures of 10^4 cells/ml in serum free RPMI 1640 did not grow, and the culture died within 12 hours of inoculation. With an inoculum of 10^5 cells/ml, however, cell growth was noticeable within 4 hours (figure 19). The growth of the higher density culture in the absence of

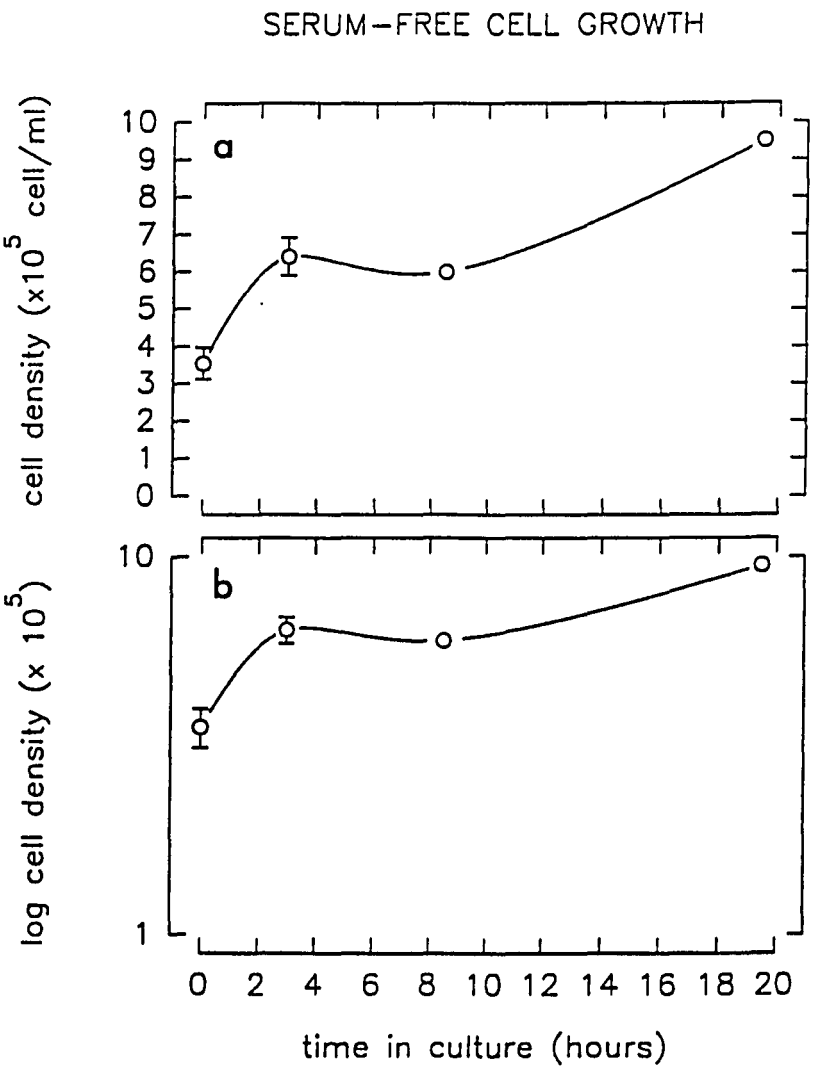

Figure 19. Serum-free cell growth. Log phase cells at a density of 10^5 were inocculated into miniwell culture and cell number was determined by hemocytometer count after 48 hours at 37°C, as described in Materials and Methods.

serum initially suggested the production of autocrine growth factors by the cell mass.

1. Leucine limitation studies. Since the cells appeared to grow in the absence of serum, more severe measures were considered necessary to inhibit proliferation. Low levels of an essential amino acid can provide the culture with a sufficient concentration to allow the synthesis of proteins necessary for cell survival, but not for the large increases in protein synthesis required for division. Similar deprivations have been used to limit culture growth by other investigators (Prescott, 1968). For these studies, cells were deprived of leucine.

Cell number was assessed as a function of leucine concentration in miniwell culture (figure 20). Cultures were incubated with leucine concentrations ranging from 0 to 50 mg/l. Given as little as 0.1 mg/l leucine, the cell number remained near the original inoculum size. At this density, culture viability was 81%. A concentration of 0.5 mg/l produced slight increases in cell number, and the viability increased to 84%. None of the cultures showed greater than 87% viability. Given concerns as to the viabilities of suspension cultures grown with leucine concentrations as low as 0.1 mg/l, 0.5 mg/l was chosen for further study.

Suspension cultures of approximately 5 x 10^5 cells/ml were inoculated into RPMI 1640 with a leucine concentration of 0.5 mg/l. Cultures were counted at 2 to 3 hour intervals. In the first cultures studied, cell number increased slowly during the first eight hours of

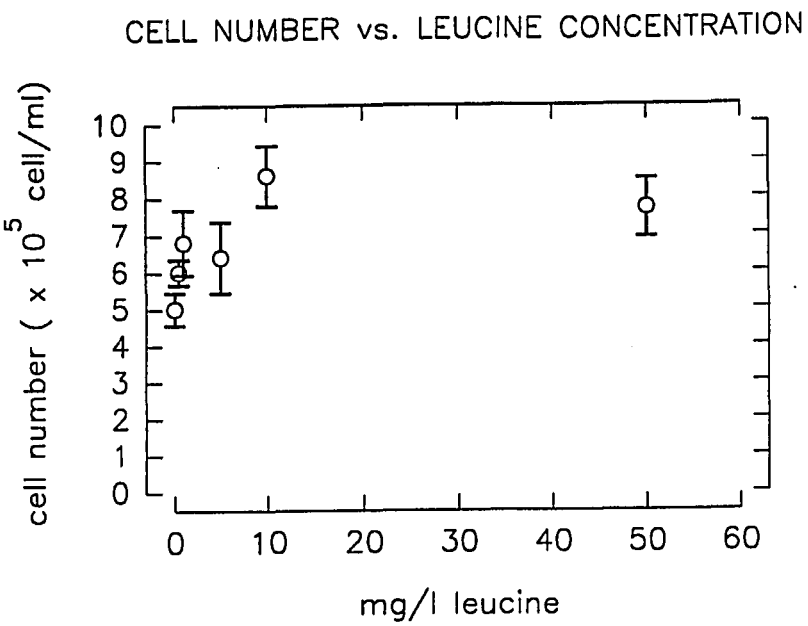

Figure 20. Cell number *vs.* leucine concentration. Cell number was determined as a function of leucine concentration following 24 hours in miniwell culture (described in Materials and Methods).

culture. During this time, the mitotic index of the culture decreased from 15% to 6%, while cell viability remained greater than 90%. After the eighth hour in culture, the cell number and mitotic index remained relatively constant until the 12th hour in culture, when culture viability began to decline. By the 14th hour post-inoculation, the cell population was only 70% viable. This loss in viability seemed to be due to leucine depletion, and could be postponed by the addition of 0.5 mg/l leucine at the eighth hour of culture (figure 21). On the basis of this information, 0.5 mg/l leucine RPMI was used for the production of slow-growing cultures. Cells were harvested between 8 and 12 hours following culture inoculation. Once culture viability dropped below 90%, the cultures were discarded. Relative increases in cell number as a function of time, accumulated from a large number of experiments, are shown in figure 22. Note that the cell number in low leucine medium remained relatively stable while there were clear increases in cell number in serum supplemented medium.

2. Serum deprivation studies. To limit the growth of cells hormonally, as opposed to using the amino acid limitation discussed, low-serum medium was investigated for its ability to produce slow- or non-growing cultures. Low-serum (0.2%) medium is traditionally employed to stop the growth of cells in culture and/or synchronize the growth response (Freshney, 1987). In contrast to the results obtained in miniwell culture, however, low-serum suspension cultures ranging from 0.2 to 1% Nu-serum content did not grow, but began to lose viability within the first four hours following culture inoculation. This was found

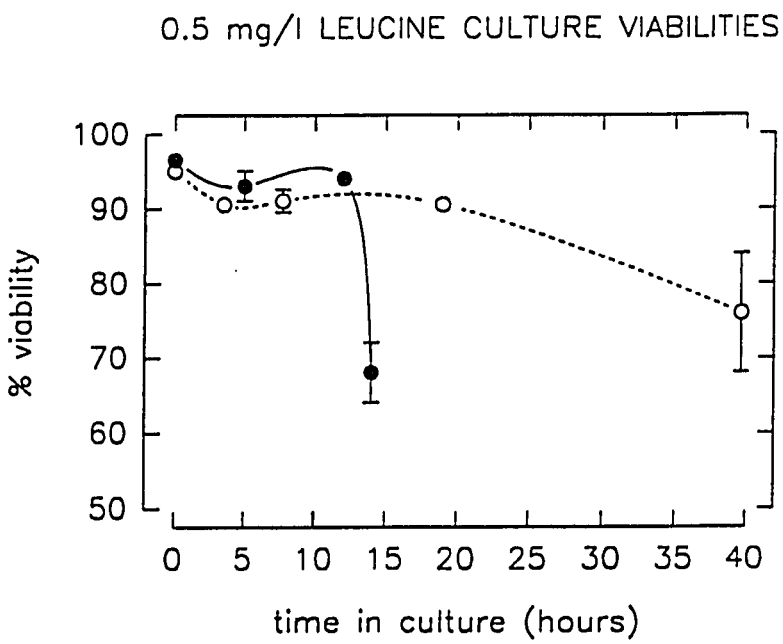

Figure 21. 0.5 mg/l leucine culture viabilities. Cell viabilities were determined by trypan blue exclusion. Cells were maintained in 0.5 mg/l leucine suspension culture and sampled at the times indicated. An additional 0.5 mg/l of leucine was added at the eighth hour of culture in some experiments (open circles) or no addition was made (filled circles).

observed in both low and high density cultures, inoculated at densities of 10^5 and 5 x 10^5 cells/ml, respectively.

When the cultures were counted, and culture viabilities determined using trypan blue exclusion (see Materials and Methods, a large number of the trypan-blue stained cells were mitotic in appearance. Following eight hours post- inoculation, cultures were less than 50% viable. These data appear to conflict with the observations of serum-free, leucine limited miniwell cultures, in which viability remained high for approximately 24 hours.

Since earlier experiments had suggested the production of autocrine factors (e.g. the apparent proliferation of serum-free miniwell cultures), supplements of conditioned medium were considered as a possible means of slowing growth in suspension. Conditioned medium was collected from log phase cells at a density of approximately 5 x 10^5 cells/ml. Cells were removed from the suspension by centrifugation (see Materials and Methods) and the conditioned medium supernatant decanted and stored. Suspension cultures were prepared in serum-free RPMI 1640 with a 20% supplement of conditioned medium. Cultures were prepared to a density of approximately 4 x 10^5 cells/ml, and cell number determined at four to six hour intervals. During the first 16 hours in culture, cell number was found to increase slowly. Between 18 and 28 hours in culture, the cell number remained relatively stable and the mitotic index decreased to 6%. After the 30^{th} hour in culture, however, the cells begin to lose viability and the culture died by the 40^{th} hour post inoculation. Relative increases in cell number as a function of time

are shown in figure 22, where they can be compared to those results obtained in proliferating and 0.5 mg/l leucine cultures.

Cells were harvested for further study between 18 and 24 hours following culture inoculation. Cells were counted several times throughout this period, throughout which cell number and culture viability remained stable.

C. Cellular growth rates.

As shown in figure 17, cell cultures proliferating in RPMI 1640 + 5% Nu-serum double every 16 (± 2) hours. This translates to a specific growth rate of 0.10 (± 0.04) hr^{-1}, determined from multiple experiments similar to those shown in figure 22. In contrast, cells in low leucine medium grow only slightly, with a rate of 0.02 (± 0.04) hr^{-1}. Following the 18^{th} hour in conditioned medium, cultures show a similar specific growth rate of 0.4 (± 0.04) hr^{-1}. Standard deviations were determined from the sums of squares in the linear least squares determination of growth rates. The difference in these growth rates is also reflected in their respective mitotic indices of 14% found for proliferating cultures, as opposed to the value of 6% determined for both leucine-limited and conditioned medium cultures. This information is summarized in table 1.

Table 1. Specific growth rates and mitotic indices.

Condition	Growth rate*	Mitotic index
RPMI 1640 + 5% Nu	0.10 ± 0.04	14 ± 3%
0.5 mg/l leucine	0.02 ± 0.04	6 ± 3%
20% cond. med.	0.04 ± 0.04	6 ± 4%

*$hour^{-1}$

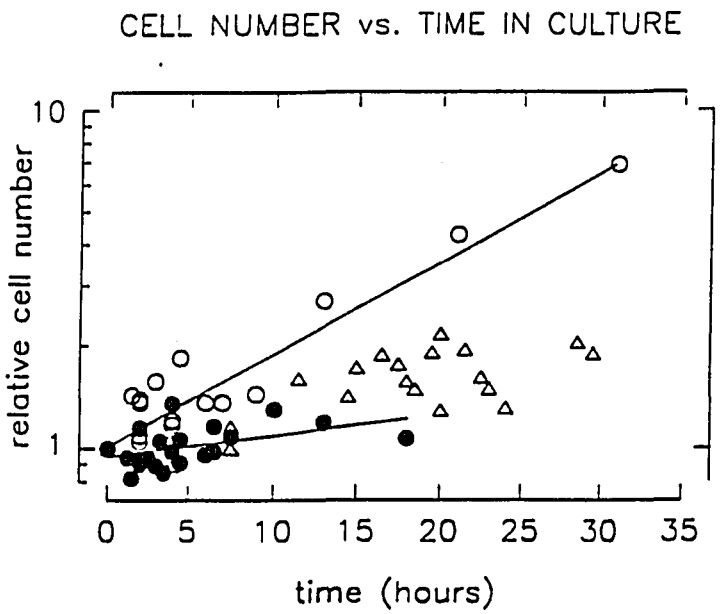

Figure 22. Cell number vs. time in culture. Data were collected from many cultures to assess the relative growth rates of proliferating, leucine-limited and conditioned medium cultures. Relative cell numbers (in percent) at the specified times were normalized to the density of cells at time 0. Proliferating cultures (open circles) demonstrate significant increases in cell density as a function of time while leucine-limited (filled circles) and conditioned medium (open triangles) cultures demonstrate only slight and perhaps insignificant increases as a function of time. The respective growth rates are summarized in Table 1.

D. Serum-free cultures.

Since miniwell cultures were found to proliferate in the absence of serum, suspension cultures of 2 x 10^5 cells/ml were prepared to determine cell growth rates in the absence of serum. Following 6 hours in serum free culture, however, culture viability had dropped to 60%. Culture viability declined slowly thereafter, and the cultures were discarded. These data appear to conflict with the observations of serum-free, leucine limited miniwell cultures, in which viability remained high for approximately 24 hours.

E. MAb production and protein synthesis rates.

MAb production levels among leucine-limited and conditioned medium cultures are dramatically lower than found among serum-stimulated cultures (figures 23a-c). The low leucine cultures demonstrate decreased rates of MAb production as a function of time (figure 23a). Since the larger yields found among proliferating cultures could have been due to increases in cell number, product yields were evaluated as a function of culture densities (figure 23b). In addition, specific product yields were determined using the amount of product formed with respect to the increases in cell number occurring between sampling points. In all cases, the specific MAb production was found to be lower among the non-proliferating (i.e. leucine limited and conditioned medium) cultures.

MAb production levels among the leucine-limited and conditioned medium cultures appear similar when taken as a simple function of time

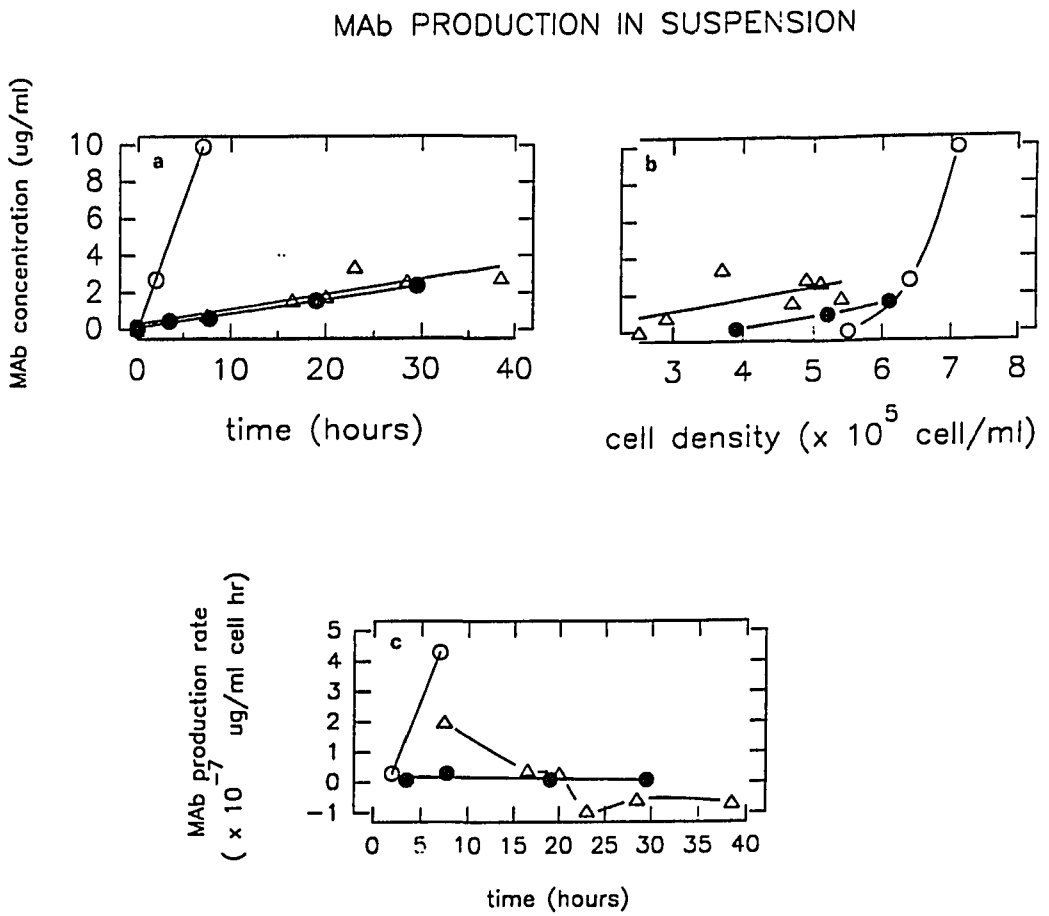

Figure 23. MAb production in suspension. MAb yields were determined as a function of time in proliferating (open circles), leucine-limited (filled circles), and conditioned medium (open triangles) culture. Medium supernatants were diluted 1:50 in PBS, and the diluted samples subjected to enzyme-linked immunosorbant assay (ELISA). The amount of F12 in each sample was determined from a standard cruve of ng F12 *vs.* A_{450} prepared on the same blocked microtiter plate (see Materials and Methods). In b, these data are plotted as a function of cell number at the time of culture sampling. In c, the amount of antibody newly formed in culture between the time points between sampling was divided by the time elapsed to yield a specific production rate in ug/ml/hour.

or cell density. Specific MAb production levels (shown in figure 23c), however, differ in that the specific production among the conditioned medium cultures decreased steadily, with absolute MAb levels showing small decreases as a function of time. This contrasts with the results found among leucine-limited cultures, in which the specific antibody production as a function of time and cell number was close to zero, although MAb levels in the suspension did not appear to decrease.

Since this difference could be due to differential rates of protein synthesis, rates of ^{14}C-leucine incorporation into acid-insoluble material were determined in proliferating, leucine limited, and conditioned medium cultures (figure 24a and b). These studies of protein synthesis were performed over 4 hours, suspending the cells in fresh medium. To correct for the differing leucine concentrations in the media used, ^{14}C-leucine was added to generate similar specific activities between the media. Under these conditions, ^{14}C-leucine incorporation rates were found to be 4.09 $\pm$ 0.71 and 1.06 $\pm$ 0.56 cpm/min (deviations determined from the sum of the squares) in proliferating and leucine-limited cultures, respectively. In a parallel experiment to compare the leucine incorporation rates of proliferating and conditioned medium cultures, proliferating cultures were found to have an incorporation rate of 36.14 $\pm$ 1.56 cpm/min, and 20% conditioned medium cultures a rate of 14.85 $\pm$ 2.31 cpm/min.

Since these differences in protein synthesis rates could be due, in part, to differences in amino acid transport among the

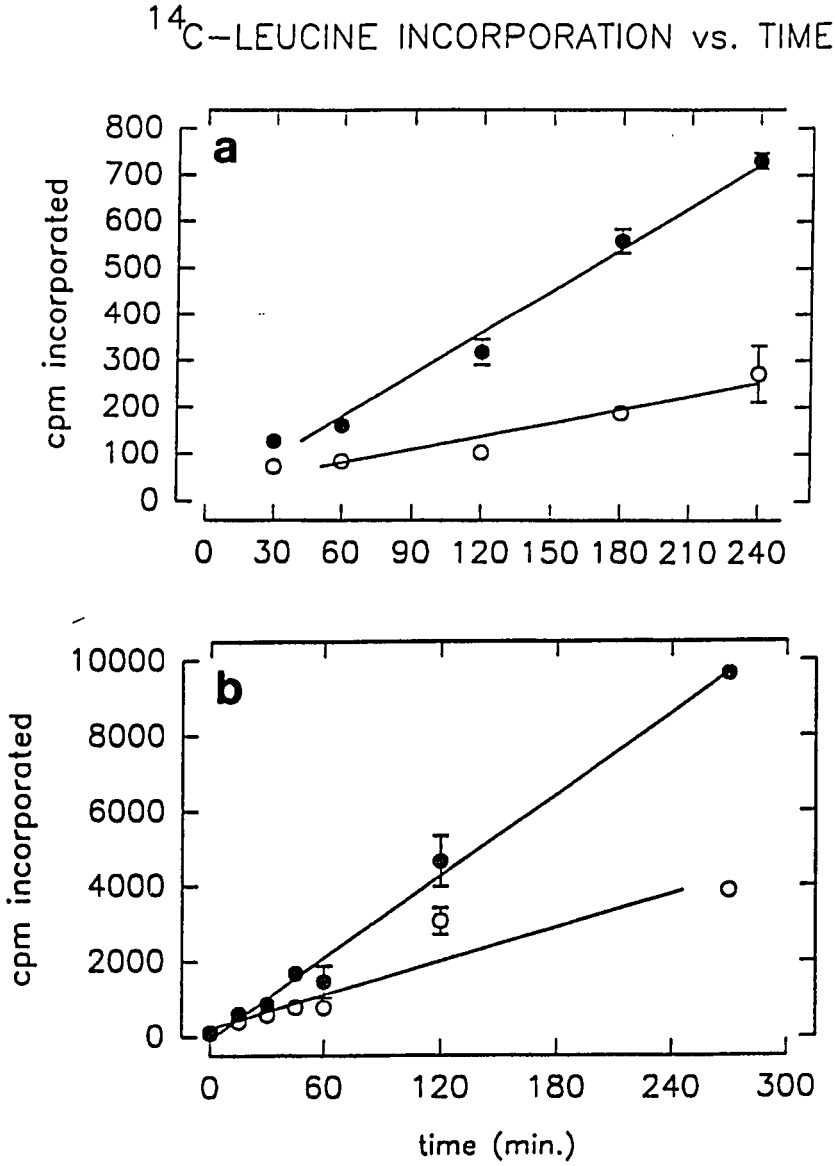

Figure 24. ^{14}C-leucine incorporation *vs.* time. ^{14}C-leucine incorporation data (Materials and Methods) were used to compare protein synthesis rates in proliferating (filled circles) and leucine-limited (open circles) cultures (a) or proliferating (filled circles) and conditioned medium (open circles) culture (b). Specific activities of radioactivity were the same in all samples studied.

cell cultures, ^{14}C-leucine uptake was compared among serum stimulated and leucine-deprived cultures (figure 25).

Leucine-limited cultures were found to take up much less ^{14}C-leucine than the serum-stimulated cultures (figure 25 and table 2). The decreased availability of intracellular leucine may, therefore, have effects on amino acid availability which may at least partially explain the differences observed in protein and MAb synthesis. Conditioned medium cultures, however, showed no significant difference in leucine uptake when compared to the proliferating cultures maintained in RPMI 1640 + 5% Nu-serum (figure 25), and a different explanation must be found for the differences observed in protein and MAb synthesis levels.

Table 2. ^{14}C-leucine incorporation and uptake.*

Condition	cpm incorporated ($\times 10^{-3}$)	cpm uptake
RPMI 1640 + 5% Nu	4.09 ± 0.71	1333 ± 108
0.5 mg/l leucine	1.06 ± 0.54	920 ± 29
20% cond. med.	1.68 ± 0.26	1490 ± 125

*Relative levels determined from the experiments presented in figures 24 and 25.

F. Energy distribution among suspension cultures.

1. Inhibitor studies. Inhibition of cellular pathways critical to cell growth and survival was used to assess the distribution of cellular energy in proliferating and leucine-limited cultures. To determine the best inhibitor concentrations, protein, DNA, and RNA synthesis levels were determined in the presence of varying concentrations of ouabain, cycloheximide (CHX), thymidine, and DFB, respectively.

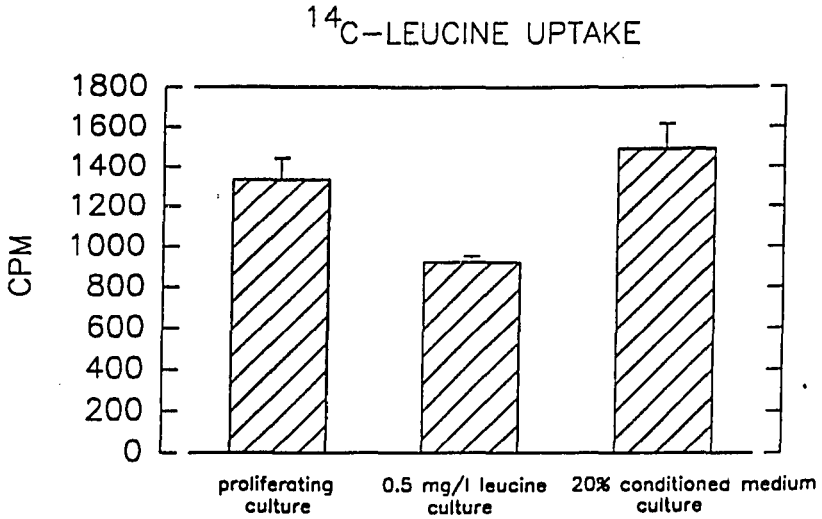

Figure 25. ^{14}C-leucine uptake. Leucine uptake, in terms of total CPM taken into cells but not used for the synthesis of proteins, was compared among proliferating and growth limited cultures as described in the text. Leucine-limited cultures appear to incorporate significantly less of the amino acid, while no significant difference exists between the uptake of proliferating and conditioned medium cultures. These data are summarized in table 2.

^{14}C-leucine incorporation into acid insoluble material was determined as a function of CHX concentration (figure 26). Incorporation drops to baseline levels at a CHX concentration of 25 uM. DNA synthesis was assessed using the incorporation of ^{3}H-thymidine as a function of the excess thymidine concentration (figure 27). In the cell, excess thymidine is phosphorylated by thymidine kinase. The distal product of the kinase, thymidine triphosphate, serves as a feedback inhibitor for the kinase, the rate determining step in DNA synthesis (Bresnick *et al*, 1964). Since the inhibitor concentration differed among the samples studied, ^{3}H thymidine incorporation, as a function of thymidine concentration was studied within samples of similar specific activity. Thymidine incorporation was found to drop to baseline levels when cells were given an excess thymidine concentration of 1 mM. In figure 28, ^{3}H-uridine incorporation into RNA was used to assess the inhibition of RNA synthesis as a function of the DFB concentration. DFB is a relatively specific inhibitor of messenger RNA synthesis (Campisi and Pardee, 1984). ^{3}H-uridine incorporation reaches its minimum levels above the baseline values observed previously, possibly due to the synthesis of other forms of RNA. This minimum incorporation occurs when cells are given 60 uM DFB. One millimolar ouabain is generally accepted as an inhibitor of Na^{+}/K^{+} exchange (Shank and Smith, 1972). To insure that 1 mM ouabain produced maximum metabolic inhibition, oxygen consumption studies were performed in the

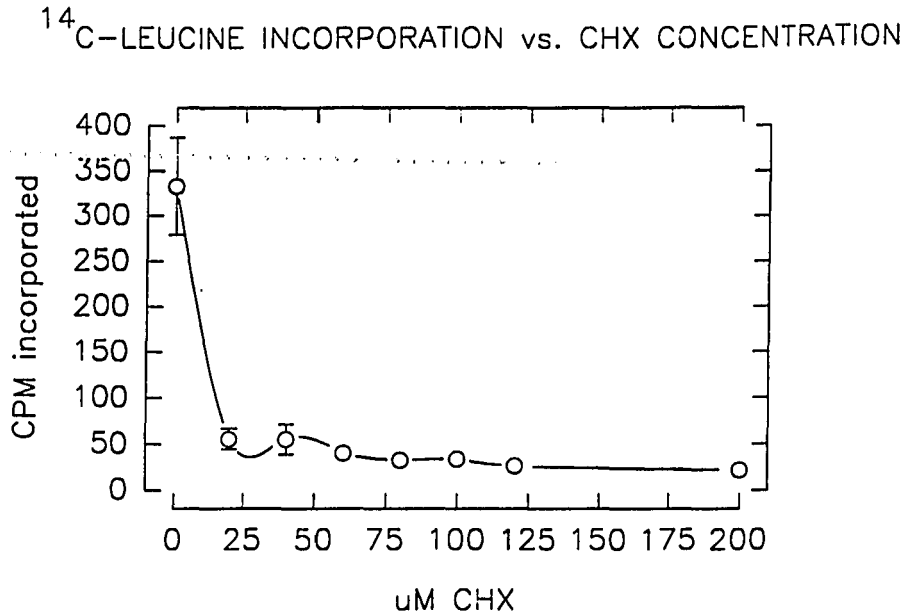

Figure 26. ^{14}C-leucine incorporation *vs.* cycloheximide concentration. Protein synthesis was assessed using ^{14}C leucine incorporation into acid insoluble material, as described in Materials and Methods. 10^6 cells were incubated with CHX concentrations ranging from 0 to 200 uM CHX, and leucine incorporation plotted as a function of concentration. ^{14}C leucine incorporation drops to low levels at CHX concentrations as low as 25 uM. 100 um CHX was used in all inhibition studies.

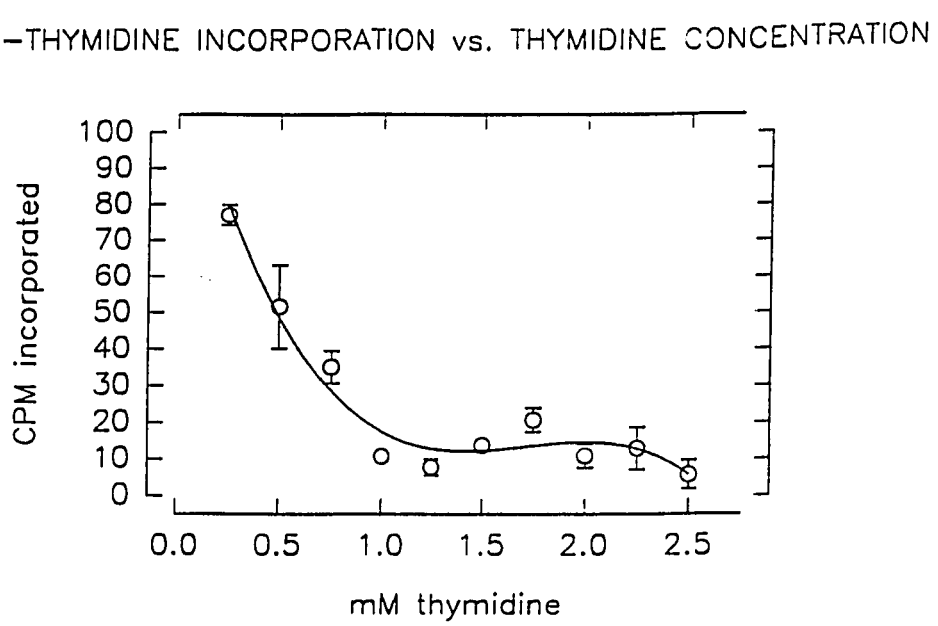

Figure 27. ^{3}H-thymidine incorporation vs. thymidine concentration. Experiments were performed as described in Materials and Methods. CPM ^{3}H-thymidine incorporated into DNA was determined as a function of the excess thymidine concentration. DNA synthesis appears to drop off, with CPM values being very close to the baseline values determined among radioactivity blanks, at a concentration of 1 mM. 2 mM thymdidine was used in all inhibition studies.

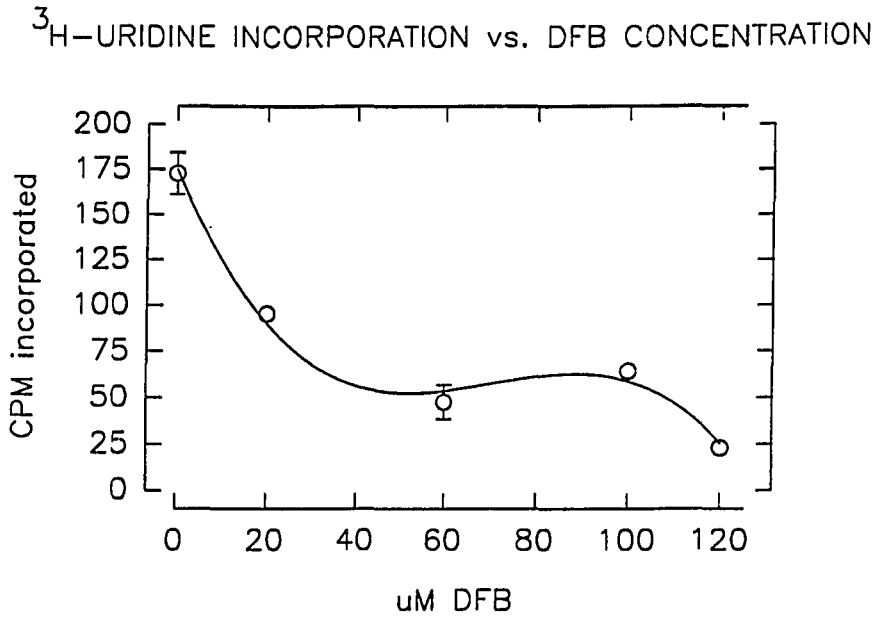

Figure 28. ^{3}H-uridine incorporation vs. DFB concentration. Experiments were performed as described in Materials and Methods. Relative RNA synthesis levels were extrapolated using values of ^{3}H-uridine (CPM) incorporated in RNA. RNA synthesis decreases and stabilizes near a concentration of 60 uM DFB. Since DFB is believed to be a relatively specific inhibitor of hn RNA synthesis (Campisi and Pardee, 1984), the residual radioactive counts incorporated are believed to arise from the synthesis of other forms of RNA.

presence of 1 mM and 2 mM ouabain (figure 29). The respective degrees of inhibition were not significantly different between the two concentrations studied.

All subsequent studies of inhibitor-induced changes in metabolism were performed using concentrations of 100 uM cycloheximide, 100 uM DFB, 2 mM thymidine, and 1 mM ouabain.

Control experiments were performed to ensure that the inhibitors used did not affect mitochondrial oxygen consumption directly. Oxygen consumption was monitored in crude mitochondrial suspensions (see Materials and Methods). The inhibitors discussed were added once the oxygen level had reached 40-50% of its original concentration. As shown in figure 30, these additions did not affect oxygen consumption rates significantly, and any inhibition occurring was no greater than that observed when the inhibitor solvent (DMSO) was added alone.

2. Oxygen consumption studies. Proliferating cells consumed oxygen at a rate of 3.4×10^{-15} mol/min/cell. This compares to rates of 0.8 to 8.0×10^{-15} mol/min/cell determined for other mammalian cells in culture (Miller *et al*, 1987). This rate decreased immediately on the addition of inhibitors, examples of which are presented in figure 31. Oxygen consumption values are summarized in table 3. The values presented in table 3 represent the mean of multiple determinations. Inhibition of protein, DNA, and RNA synthesis reduced O_2 consumption by 29, 25, and 30%, respectively. Inhibition of the Na^+/K^+-ATPase reduced oxygen consumption by 29%. The sum of these values is over 100%, and could,

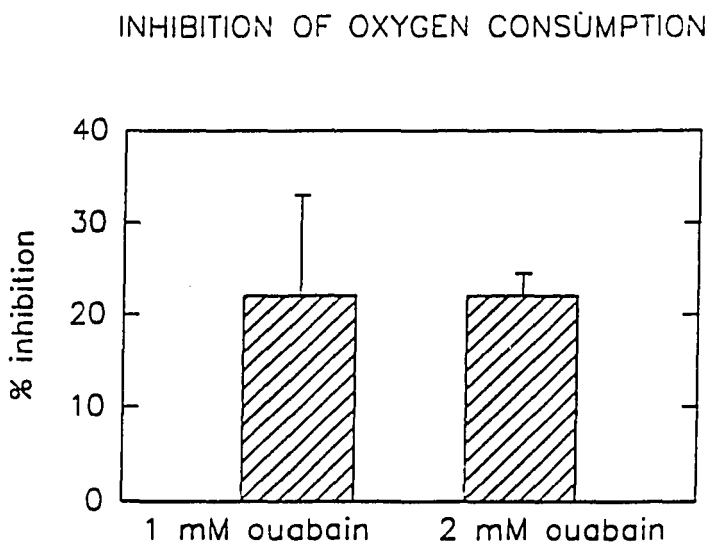

Figure 29. Inhibition of oxygen consumption. To insure that 1 mM ouabain maximally inhibits Na^+/K^+transport (as was determined by comparing the decrease in oxygen consumption produced by inhibition) oxygen consumption was compared among cells incubated with 1 and 2 mM ouabain, respectively. Oxygen consumption did not differ between the two oaubain concentrations used.

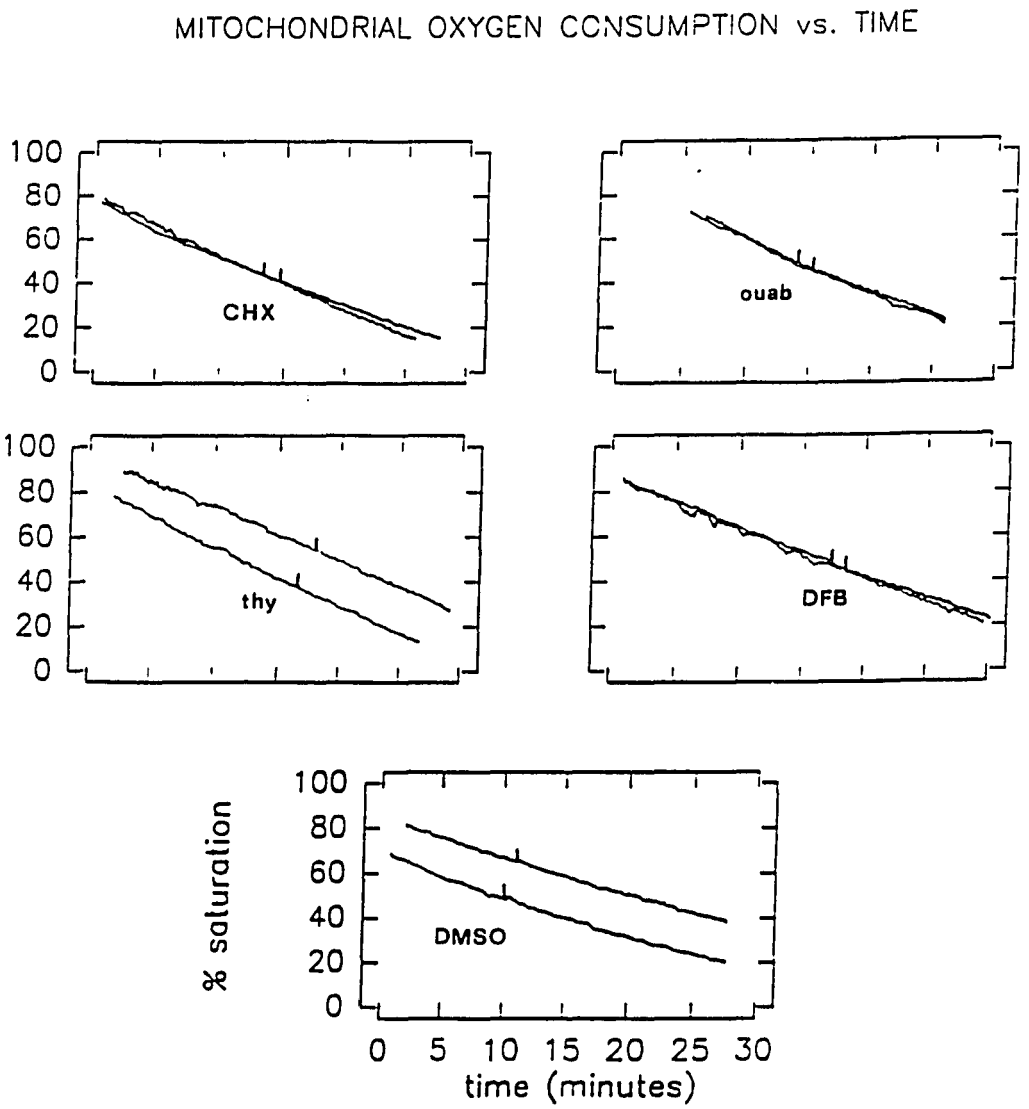

Figure 30. Mitochondrial oxygen consumption *vs.* time. Oxygen concentration was determined as a function of time in crude suspensions of rat liver mitochondria (see Materials and Methods). When the oxygen concentration had reached 40-50% of its original saturating value, inhibitors (see Materials and Methods) were added to assess their effects on mitochondrial oxygen consumption alone. None of the inhibitors added was seen to exert any significant effect.

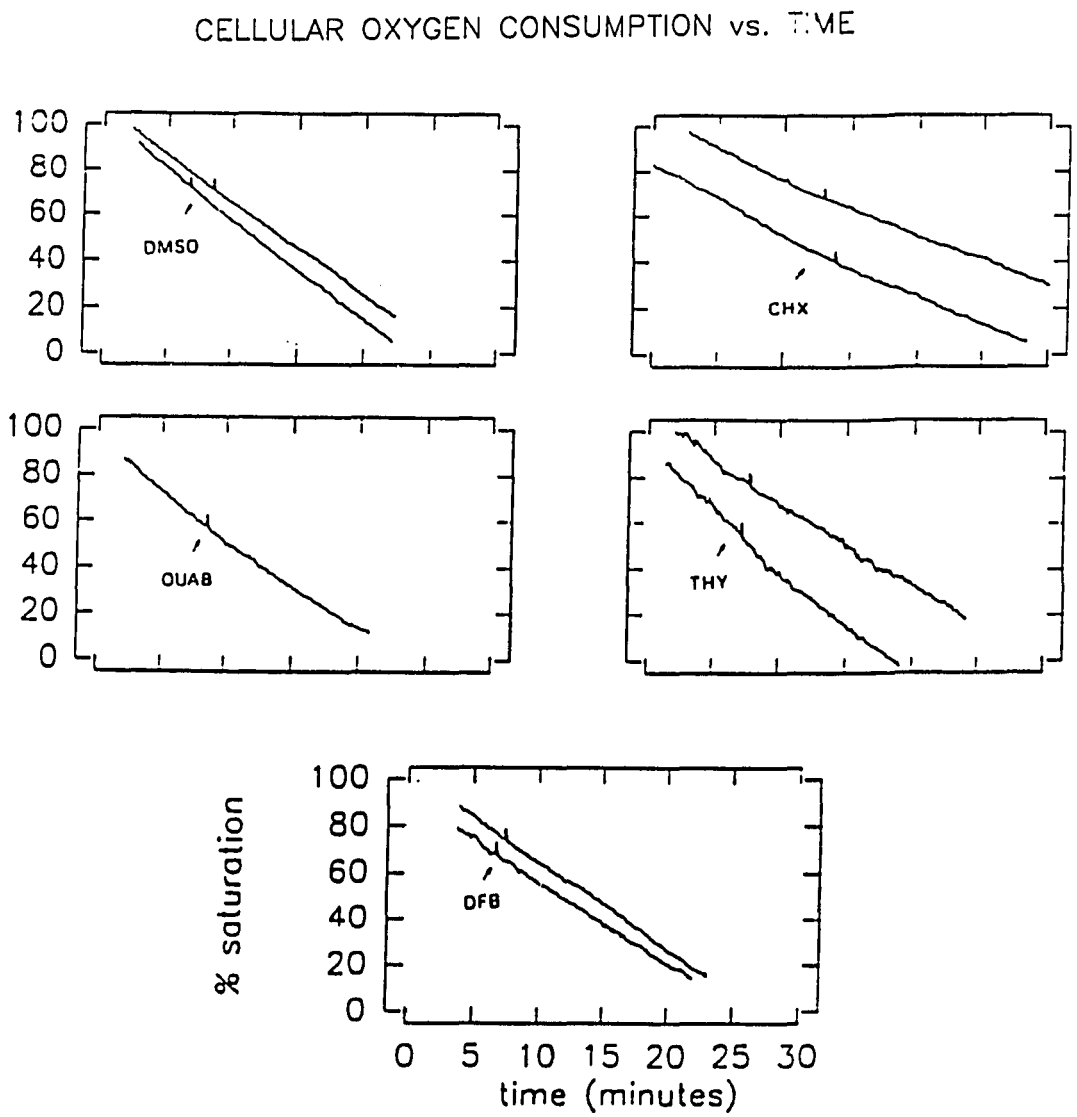

Figure 31. Cellular oxygen consumption *vs*.time. Oxygen consumption measurements, determined from the decrease of the medium dissolved oxygen concentration as a function of time (see Materials and Methods). All measurements shown are examples of O_2 consumption observed in proliferating cultures maintained in RPMI 1640 + 5% Nu-serum. All cells were harvested from stocks in the log phase of growth. Inhibitors were dissolved in DMSO prior to addition to the cell suspension. DMSO alone had no effect on oxygen consumption. Cycloheximide (CHX, 100 uM), ouabain (ouab, 1 mM), thymidine (thy, 2 mM), and dichlororibofuranosyl benzimidazole (DFB, 100 uM) each resulted in a decreased rate of oxygen consumption (summarized in table 3). Similar results were found among non-proliferating cultures, although pre-inhibition rates of oxygen consumption differed, as did the degrees to which oxygen consumption was altered by the inhbiitors.

therefore, account for all of the cell's energy requirements if there were no significant cross-talk between the pathways.

Cycloheximide, ouabain, and thymidine were added in pairs to assess the degree to which inhibition of any one pathway affects the energy consumption of others, or the degree of "cross talk" between the pathways studied. Simultaneous inhibition of protein synthesis and Na^+/K^+ transport reduced oxygen consumption 38%, as compared to the 58% expected from each inhibitor when used alone. This 20% discrepancy could indicate a significant degree of cross talk between protein synthesis and Na^+/K^+ transport. Simultaneous inhibition of DNA synthesis and Na^+/K^+ exchange reduced oxygen consumption 42%, as compared to the 54% expected on the basis of the single-inhibition data. Simultaneous inhibition of protein and DNA synthesis reduced O_2 consumption by only 37%, as opposed to the expected decline of 54%. Due to the rather large confidence limits associated with this data, these discrepancies must be considered insignificant.

Leucine-limited cultures consumed oxygen at a rate of 2.1×10^{-15} mol/min/cell, 38% more slowly than the actively proliferating cultures (see table 3). Inhibition of protein synthesis reduced oxygen consumption 34%, while inhibition of DNA or RNA synthesis did not reduced oxygen consumption. Inhibition of the Na^+/K^+-ATPase, reduced O_2 consumption 21%. This distribution differed dramatically from that observed among proliferating cultures, with the individual inhibitions totalling only 55%.

DNA and RNA syntheses in leucine-limited cultures consumed a smaller proportion of the total oxidative energy. Protein synthesis consumed a larger proportion, although this translated into a smaller value in terms of absolute ATP consumption. Inhibition of the Na^+/K^+-ATPase reduced oxygen consumption to approximately the same degree as observed in proliferating cultures. This may indicate a relatively constant role of the transporter in terms of the fraction of cell energy it needs to drive cellular processes. Again, however, due to the decreased levels observed for oxidative ATP production among leucine-limited cultures, the absolute amount of energy consumed by the transporter is less than that observed for the proliferating cultures.

The oxygen consumption data obtained under conditions of simultaneous inhibition of pathways in leucine-limited cultures were variable. Inhibition of protein synthesis and Na^+/K^+ transport reduced oxygen consumption to the same degree as the inhibition of protein synthesis alone. When protein and DNA synthesis were inhibited simultaneously, the decrease in the oxygen consumption rate was not different from the decrease observed with cycloheximide alone. The observed decrease in oxygen consumption observed in response to the inhibition of DNA synthesis and Na^+/K^+ was not different from that observed in response to the inhibition of Na^+/K^+ transport alone. Since all of these experiments have been performed under acute conditions, more complex interactions have been discounted.

Twenty percent conditioned medium cultures were found to consume oxygen at a rate of 3.8×10^{-15} mol/min/cell. This rate is not

significantly different from that determined for proliferating cultures. Inhibition of RNA synthesis and Na^+/K^+ transport reduced oxygen consumption by 35% and 26%, respectively. Inhibition of protein and DNA synthesis did not reduce oxygen consumption significantly.

The use of combined inhibitors again produced unexpected results (see Table 3). The effects were not additive, and the observed decreases are not significantly different from the decreases observed under conditions in which single inhibitors were used.

Table 3. Oxygen consumption measurements.

Complete medium	oxygen consumption*	C.L.	ATPox*	% decrease
control (37)	3.4 +/- 0.3	0.1	20	--
100 uM CHX (6)	2.4 +/- 0.3	0.2	14	29
1 mM ouabain (6)	2.4 +/- 0.2	0.1	14	29
2 mM thy (6)	2.6 +/- 0.2	0.1	16	25
100 uM DFB (4)	2.4 +/- 0.2	0.2	15	30
CHX + ouab (4)	2.1 +/- 0.1	0.2	13	38
CHX + thy (7)	2.2 +/- 0.5	0.3	13	37
ouab + thy (4)	2.0 +/- 0.3	0.4	12	42
Leucine-limited medium				
Control (28)	2.1 +/- 0.4	0.1	13	--
100 uM CHX (6)	1.4 +/- 0.4	0.3	8.7	34
1 mM ouab (4)	1.6 +/- 0.2	0.2	10	21
2 mM thy (3)	1.9 +/- 0.2	0.4	12	NS
100 uM DFB (4)	1.8 +/- 0.4	0.5	11	NS
CHX + ouab (4)	1.4 +/- 0.4	0.7	8.7	31
CHX + thy (4)	1.6 +/- 0.1	0.2	9.7	24
ouab + thy (4)	1.7 +/- 0.2	0.2	10	19
20% conditioned medium				
Control (30)	3.8 +/- 0.7	0.3	23	--
100 uM CHX (4)	3.2 +/- 0.1	0.2	17	NS
1 mM ouab (4)	2.8 +/- 0.8	0.6	19	26
2 mM thy (4)	3.3 +/- 0.7	0.6	20	NS
100 uM DFB (4)	2.5 +/- 0.7	0.5	15	35
CHX + ouab (4)	2.9 +/- 0.4	0.6	17	26
CHX + thy (4)	3.0 +/- 0.2	0.3	18	21
ouab + thy (4)	2.8 +/- 0.4	0.7	17	26

* fmol/min/cell

C.L.-Confidence levels determined using the student's t test at a 95% confidence level.

Numbers in parentheses represent the number of determinations.

3. Glucose consumption and lactate production. Proliferating cultures of EPO8F7 cells consumed glucose and produced lactate at rates of 10 x 10^{-15} and 17 x 10^{-15} mol/min/cell, respectively (see table 4 and figure 32a and b). If it is assumed that all lactate formed arises from the incomplete oxidation of glucose, then approximately 85% of the available cell glucose was converted to lactate. Rates of glucose consumption were generally lower in the presence of metabolic inhibitors (data summarized in table 4). Inhibition of protein synthesis, RNA synthesis, and Na^+/K^+ transport each reduced glucose consumption rates by 27% to 35%. Inhibition of DNA synthesis reduced glucose consumption by 27%. The simultaneous addition of inhibitors again reduced glucose consumption and lactate production much less than would be expected, based on the inhibition caused by each inhibitor alone.

Leucine-limited cultures consumed glucose much more slowly than the proliferating cultures, with average rates of 4.0 x 10^{-15} and 5.5 x 10^{-15} mol/min/cell for glucose consumption and lactate production, respectively (see table 4 and figure 32b). If it is again assumed that all lactate produced arises from glycolysis, here only 69% of the glucose consumed is converted to lactate. In the presence of metabolic inhibitors, any changes in glucose consumption and lactate production (table 4) were insignificant, as determined from the student's T test.

The conditioned medium cultures also glycolysed more slowly than the proliferating cultures, with rates of 5.4 x 10^{-15} mol/min cell for glucose consumption and 4.4 x 10^{-15} mol/min cell for lactate production.

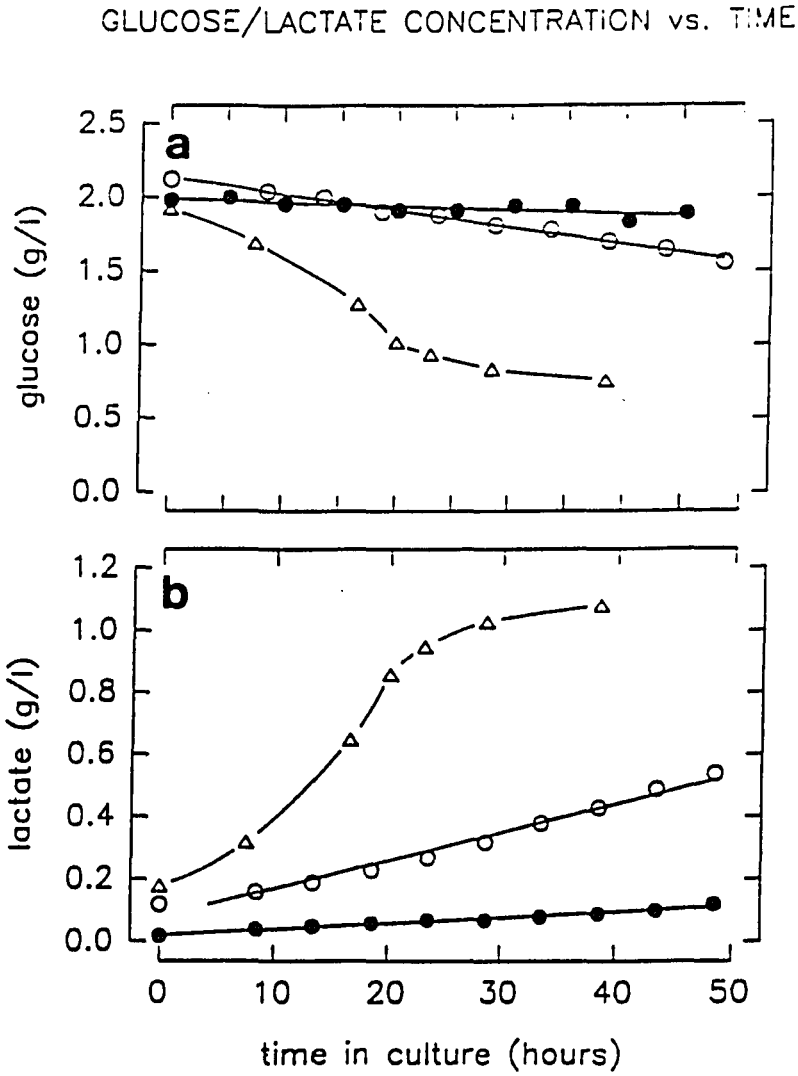

Figure 32a and b. Glucose/lactate concentration *vs.* time. Glucose and lactate concentrations were determined in suspensions of approximately 2 x 10^7 cells/ml, using a YSI Instruments glucose/lactate analyzer, described in Materials and Methods. Rates were determined in proliferating (open circles), leucine-limited (filled circles), and conditioned medium (open triangles) cultures. Proliferating cells were metabolically more active. Respective rates of glucose consumption and lactate production are summarized in table 4.

These values are again much less than those observed in proliferating culture, but do not differ significantly from the rates determined among leucine-limited cultures. In this case, however, only 40% of the consumed glucose was observed to be converted to lactate. Evaluation of glucose consumption and lactate production throughout the 40 hours from culture inoculation to culture death, however, revealed an increase in glucose consumption and lactate production that lasts until approximately the 18^{th} hour post-innoculation. At this point, glucose consumption decreased to a rate comparable to that found among the leucine limited cultures. The inhibition data suggested that protein and DNA synthesis consumed 22% and 27% of the energy derived from glycolysis, respectively. Glucose consumption was unaffected by the inhibition of RNA synthesis, while inhibition of the Na^+/K^+-ATPase decreased glucose consumption approximately 22%. In all cases in which inhibitors were added in pairs, lactate production rates (on which glycolytic ATP production rates were based) are again seen to decrease less than would be expected on the basis of the single inhibition data. The apparent decreases in the glucose consumption rates, were, however larger than expected given the sums calculated from the single inhibition data. It must be emphasized, however, that these observed decreases can only be suggested, given the fact that the standard deviations and confidence limits determined are relatively large.

Table 4. Measurements of glucose consumption and lactate production.

Complete medium	glu*	C.L.	lac*	C.L.	ATPgly	% change
control (21)	10.2	1.0	17.4	2.0	17	--
100 uM CHX(5)	7.0	0.8	10.8	1.9	11	-38
1 mM ouab (5)	6.2	1.7	11.0	4.0	11	-38
2 mM thy (6)	7.4	1.9	13.6	3.3	14	-22
100 uM DFB(4)	7.4	1.7	11.7	0.7	12	-33
CHX + ouab(4)	5.5	0.4	10.4	0.4	10	-40
CHX + thy(3)	6.9	0.9	12.7	0.6	14	-21
ouab + thy(3)	6.4	0.1	12.4	0.8	12	-28
Leucine-limited medium						
control(10)	4.0	0.8	5.5	1.0	5.5	--
100 uM CHX(4)	4.2	1.0	7.9	2.7	7.9	+44
1 mM ouab(4)	4.9	0.8	8.0	2.3	8.0	+46
2 mM thy(4)	5.4	0.5	9.0	0.7	9.0	+65
100 uM DFB(4)	5.9	1.4	10.3	1.7	10.3	+88
CHX + ouab(4)	4.6	0.3	7.3	0.1	7.3	+34
CHX + thy (4)	4.1	0.3	7.8	0.2	7.8	+43
Ouab + thy(4)	4.0	0.5	6.6	0.3	6.6	+20
20% conditioned medium						
Control (10)	5.4	1.4	4.4	0.9	4.4	--
100 uM CHX(4)	5.0	1.1	3.4	1.1	3.4	-22
1 mM ouab (4)	4.2	0.5	2.8	0.1	2.8	-35
2 mM thy (4)	5.8	0.3	3.2	0.6	3.2	-27
100 uM DFB(4)	5.4	0.3	4.3	0.3	4.3	NS
CHX + ouab(4)	3.6	1.3	3.2	1.1	3.2	-26
CHX + thy (4)	4.1	1.5	4.1	0.6	4.1	NS
ouab + thy(4)	2.7	0.5	3.5	0.3	3.5	-19

* fmol/min/cell

C.L.-Confidence limits determined using the student's t test at a 95% confidence level.

Numbers in parentheses represent the number of determinations.

4. Extrapolated rates of ATP production. In proliferating cultures, the total rate of ATP production (as calculated from measurements of glycolytic flux and oxygen consumption) decreased dramatically upon the addition of metabolic inhibitors (see table 5). The largest changes were observed under conditions of cycloheximide inhibition of protein synthesis and ouabain inhibition of Na^+/K^+ transport, each inhibiting ATP production by 34%. Inhibition of RNA synthesis decreased ATP production by 31%, and inhibition of DNA synthesis by 23%. The sum of the individual inhibitor-induced decreases in energy production was over 100%.

The total ATP production of leucine-limited cultures, depending on the inhibition imposed, was seen to increase, decrease, or remain unchanged. Due to the apparent increases in glycolytic flux, increases in ATP production were suggested upon inhibition of nucleic acid synthesis, while inhibition of protein synthesis did not decrease ATP production. Ouabain inhibition of the Na^+/K^+-ATPase did not appear to change the overall rate of energy production. The simultaneous addition of inhibitors did not change ATP production significantly. This cannot readily be reconciled with single-inhibition data or those results obtained in proliferating cultures.

In all cases studied, the addition of inhibitors to conditioned medium cultures resulted in decreases in the total ATP production. Inhibition of protein and DNA syntheses produced decreases in ATP production much less than those observed within proliferating cultures. Inhibition of RNA synthesis and the Na^+/K^+-ATPase, however, both

produced decreases comparable to those observed in proliferating cultures. These apparant decreases must again, however, be called into question due to the rather large confidence limits calculated. The sum of these individual inhibitor-induced decreases in energy production does, however, approach 100%.

Some of the inhibitors seem to differentially affect glycolytic and oxidative production of ATP (see tables 3 and 4). Among proliferating cultures, cycloheximide inhibition of protein synthesis reduced the extrapolated glycolytic ATP production by 35%, while oxidative ATP production decreased by only 21%. Similar results are obtained from ouabain inhibition of Na^+/K^+ transport. Inhibition of DNA and RNA synthesis appeared to affect glycolytic and oxidative ATP formation equally. These data imply that glycolytic metabolism was more sensitive to alterations in protein synthesis and ion transport mechanisms than is oxidative metabolism. The two mechanisms appear to have equal sensitivity with respect to DNA and RNA synthesis. Due to the apparent anomalies among inhibitor-induced glucose consumption values in leucine-limited cultures, it is difficult to perform a similar analysis of the data. Among conditioned medium cultures, however, oxygen and glucose consumption appear equally sensitive to the inhibition of protein synthesis, while glucose consumption is most sensitive to the inhibition of DNA synthesis or Na^+/K^+ transport. Oxygen consumption appeared to be most sensitive to the inhibition of RNA synthesis, while glucose consumption was not affected significantly.

Table 5. Extrapolated ATP production rates.

	Complete		Deficient		Conditioned	
	ATP*	% change	ATP*	% change	ATP*	%change
Control	37	--	20	--	27	--
100 uM CHX	25	-34	18	--	20	-18
1 mM ouab	25	-34	18	NS	22	-26
2 mM thy	30	-36	21	NS	23	-15
100 uM DFB	29	-31	21	NS	19	-30
CHX + thy	23	-39	16	NS	20	-18
CHX + ouab	27	-29	18	NS	22	-33
ouab + thy	24	-35	17	NS	21	-22

* fmol/min cell

G. Bioreactor cultures.

1. Cell growth. ^{31}P spectra of cells growing in bioreactor culture demonstrate significant increases in the ATP resonances as a function of time. When inoculated with a relatively low cell number of approxmately 10^8 cells, cell growth begins after a 1-2 day lag period, and the cell number appears to increase with a doubling time of approximately 30 hours (figure 33a). This rate appeared to decrease slightly as the cell number increased (figure 34a).

The data presented in figures 33a and 34a represent a bioreactor inoculated with approximately 10^8 cells and allowed to grow continuously until growth spontaneously stopped at a global ATP concentration of 1.2 mM. In this case, cell growth had stopped due to the visible plugging of fibers within the reactor such that the cell mass could not obtain the nutrients required for continued growth. The reactor represented in figures 33b and 34b was inoculated with a higher (approximately

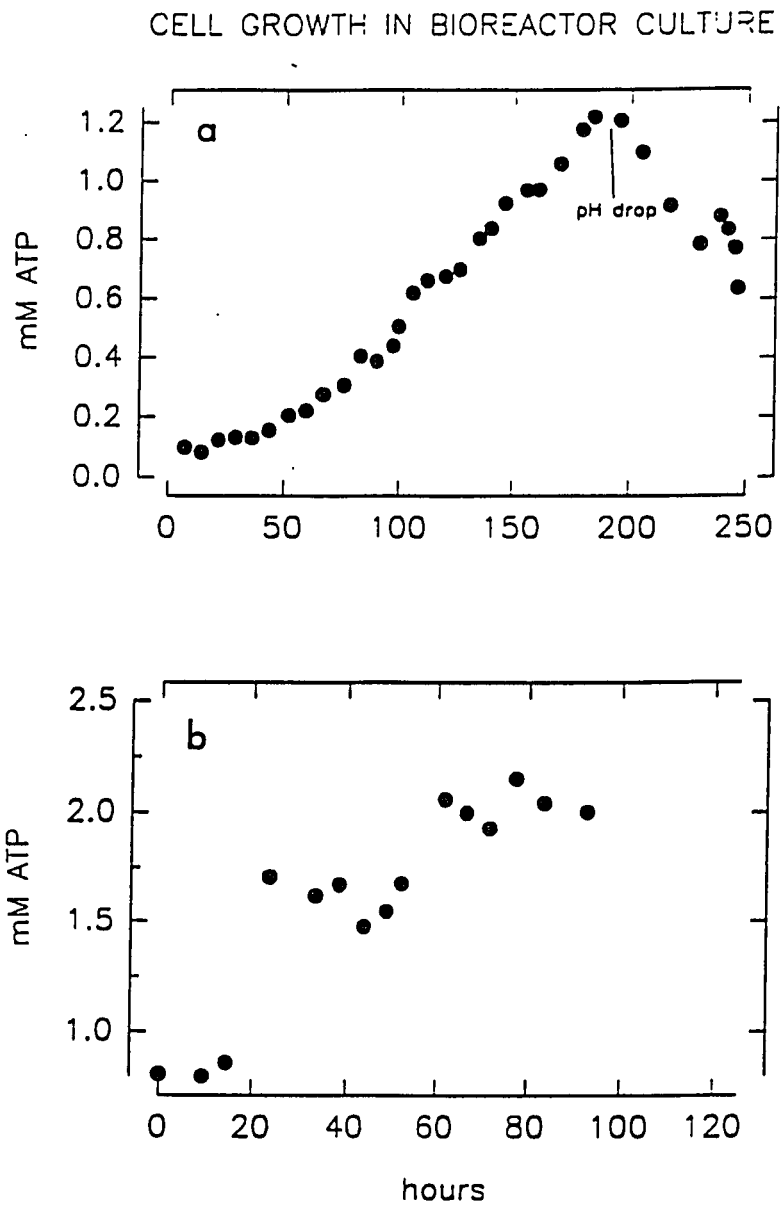

Figure 33. Cell growth in bioreactor culture. The integral of the gamma-ATP resonance (relative to the 2.5 mM DMMP standard) is plotted as a function of time in order to visualize culture growth rates (data from spectra similar to those shown in figure 36). The bioreactor in (a) was innoculated with a relatively low number (approximately 10^8) of cells and allowed to grow continuously until reaching its peak density near 1.2 mM ATP (see text). The bioreactor in (b) was innoculated with a higher number (approximately 4 x 10^8) of cells. At fifteen hours, cell growth was stopped with a 20% conditioned medium supplement. At 40 hours, growth was allowed to resume with the readdition of 2.5% Nu-serum.

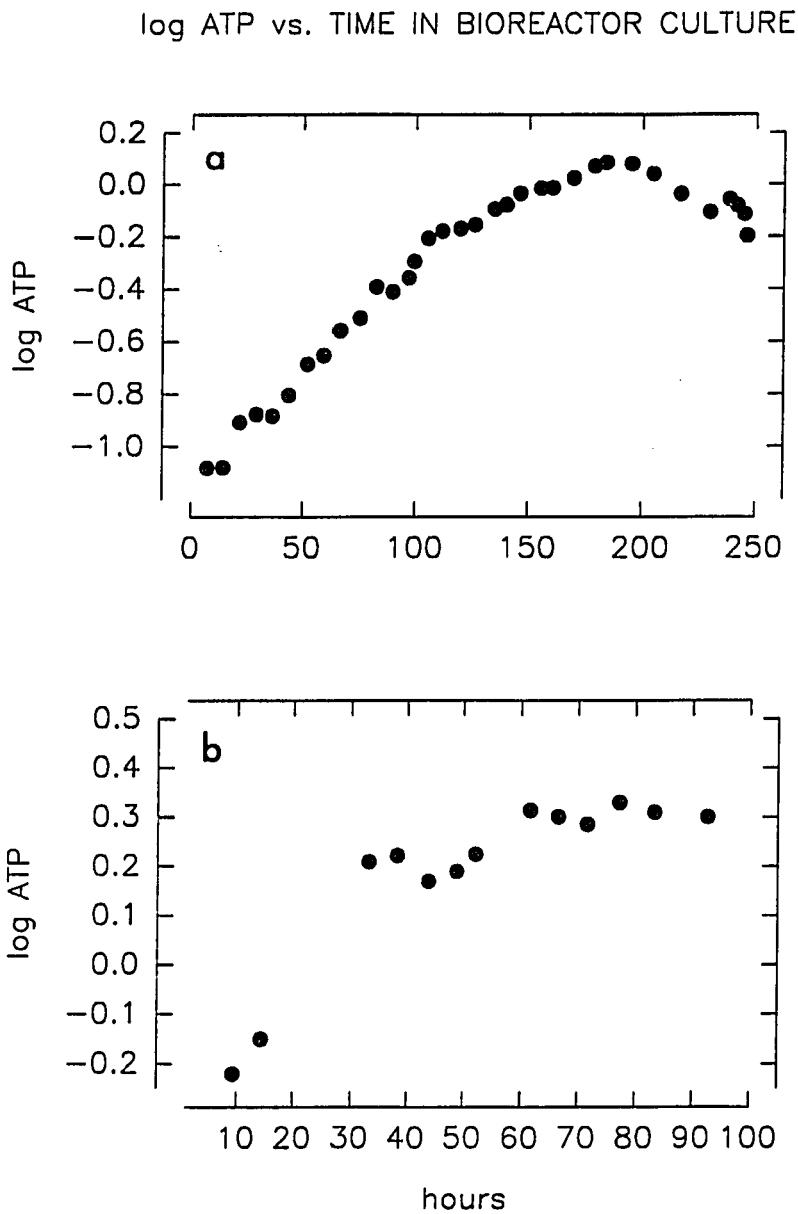

Figure 34. Log ATP *vs.* time in bioreactor culture. The data presented in figure 33 were logarithmized in order to linearize the respective growth rates.

4×10^8) number of cells. After 20 hours (between the 3rd and 4th data points in the figure), the bioreactor feed was changed to serum-free RPMI with a 20% conditioned medium supplement, in hopes of slowing or stopping cell growth. Further increases in the gamma-ATP signal did not occur until the 50th hour of culture, when the 2.5% Nu-serum supplement was replaced, and cell a slight amount of growth was found to occur (figures 33b and 34b).

During cell growth, increases in bioreactor glucose consumption and lactate production parallel increases in cell number. To ensure that the bioreactor cultures had a sufficient nutrient supply at all times, the medium "bleed and feed" rate was increased as the cells grew. Given these increases in the bleed and feed rate, glucose levels were maintained above 5.5 mM at all times. Under these conditions, medium lactate never rose above 8.5 mM (data not shown). Bioreactor cultures were found to convert 72 $\pm$ 10% of their available glucose to lactate, even when the culture medium was oxygenated with 60% O_2.

3. MAb production. MAb production in bioreactor culture did not correlate with growth or increases in cell density, but with periods in which the culture was stimulated with 2.5% Nu-serum (figure 35). This treatment does not necessarily correspond with growth. Serum readdition took place at 50 hours post-innoculation, and peak MAb production was observed after the 70th hour, when further increases in the global ATP concentration were not observed. This implies that it is not growth, but perhaps a specific serum factor, which is reponsible for MAb

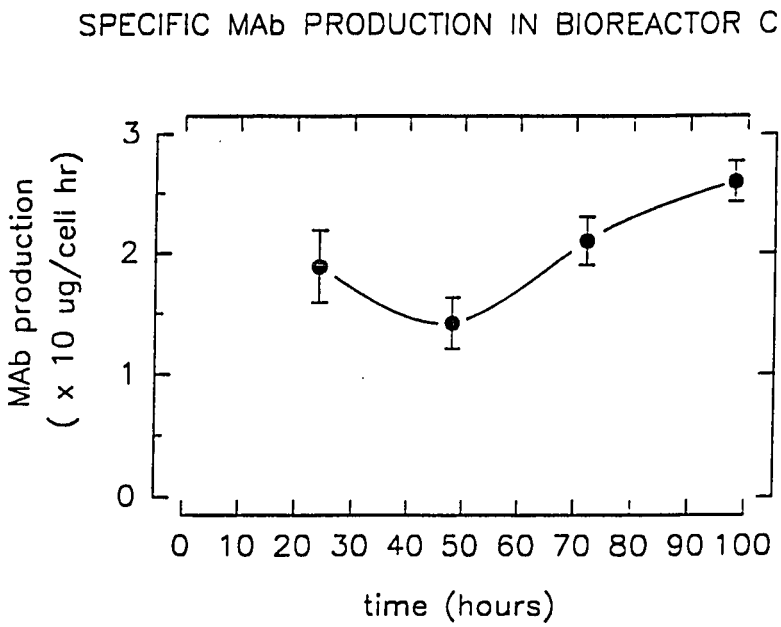

Figure 35. MAb production in bioreactor culture. MAb concentrations were determined in the perfusate collected from the bioreactor represented in figures 33b and 34b. The perfusate was diluted 1/100 in RPMI 1640 and ELISA assays performed as discussed in Materials and Methods. MAb yields appear to increase with increasing cell density and growth rate.

production. Overall, however, MAb production levels were much lower than those observed in suspension (figure 23).

4. Spectroscopic studies. Immediately following inoculation with approximately 10^8 cells, it was difficult to obtain meaningful ^{31}P-NMR spectra. Within 2 days, however, the alpha-, beta-, and gamma-resonances of ATP increased to visible levels and continued to increase throughout growth (figure 36). The relative intensity of the inorganic phosphate (P_i) peak increased as the ratio of intra- to extracellular volume in the reactor increased. This suggests that the intracellular P_i concentration is greater than 1 mM.

a. Magnetization transfer. Magnetization transfer experiments were performed as described in Materials and Methods, moving the transmitter frequency to selectively irradiate the frequency of interest. Since the resonances of interest (those to be saturated) were separated by a frequency difference of approximately 1200 Hz, control spectra were accumulated by placing transmitter frequencies 1200 Hz downfield of the gamma-ATP resonance and 1200 Hz upfield of the P_i resonance, respectively. Spectra in which the transmitter frequency was placed downfield of the ATP signal were used a controls for the P_i-saturated spectra, while the 1200 Hz upfield (of P_i) spectra were used as controls for the gamma-ATP saturations. In most cases, however, the control spectra did not differ significantly from each other.

T_1 values were determined by the method of progressive saturation, as described in Materials and Methods. This method was chosen over the more universally accepted inversion-recovery method because it offered a

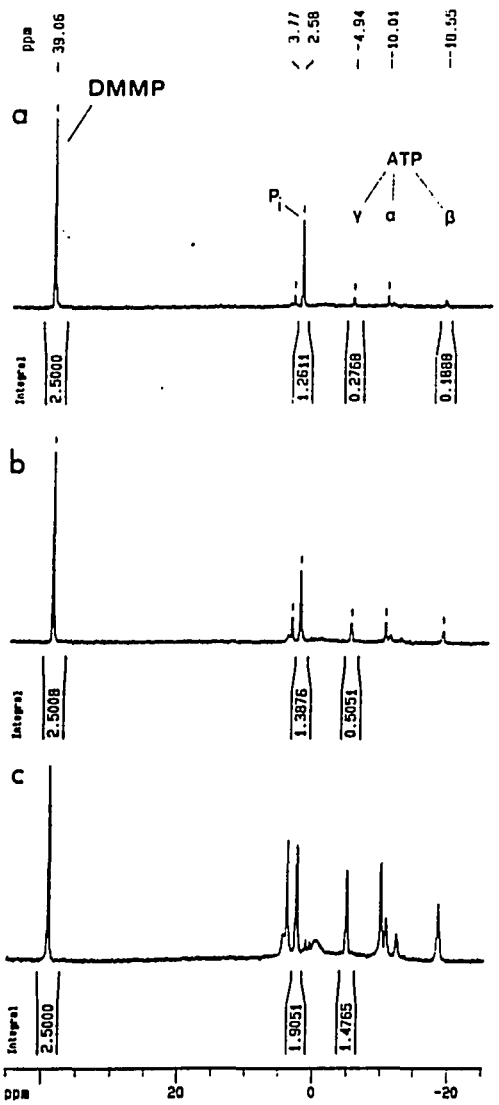

Figure 36. ^{31}P-NMR spectral changes associated with growth. Figures a-c represent spectra accumulated from bioreactors at various densities, demonstrating the increased spectral intensities that can be correlated with growth. Spectra "a" and "b" were acquired 66 and 100 hours, respectively, post-inoculation of the bioreactor whose growth data is presented in figure 33a. Spectrum "c" was acquired from the bioreactor presented in 33b, 40 hours post-inoculation. The key resonances indicated are: DMMP, dimethylmethyl phosphonate, a chemical shift and concentration standard, added to a conentration of 2.5 mM; P_i, inorganic phosphate; and the alpha-, beta-, and gamma-resonances of adenosine triphosphate (ATP).

more rapid means of T_1 determination. To insure that no significant differences existed between T_1 values determined by this method, the T_1 of inorganic phosphate (P_i) was determined in a cell-free bioreactor (although one containing dead-cell debris) using both methods. The T_1 determined *via* progressive saturation (3.72 $\pm$ 0.30 seconds) was not significantly different from that determined *via* inversion recovery (3.96 $\pm$ 0.74 seconds), and was well within the margin or error (as determined from the standard deviation) generated using the inversion recovery method.

To further establish the validity of the progressive saturation technique for this application, a data sample generated from a progressive saturation experiment is presented in figure 37. The magnetization (Mt) *vs.* tau (t) data demonstrates a logarithmic recovery of Mt with increasing tau values. Some scatter is apparent within the data, but this scatter is no greater than that observed in an inversion recovery experiment performed on a bioreactor containing cells (data not shown). When -ln(1-Mt) is plotted as a function of t, a straight line is generated (figure 37b). The slope of this line is equal to $1/T_1$. Using this method, it was possible to perform T_1 determinations in less than 4 hours, collecting 2 sets of T_1 data per saturation transfer experiment. T_1 values thus determined were averaged prior to calculating the exchange rates of interest. The more conventional determination of T_1 values by inversion recovery (assuming that the same number of tau values were used) would require 12 hours, decreasing the total amount of data that could be acquired in any given period of time.

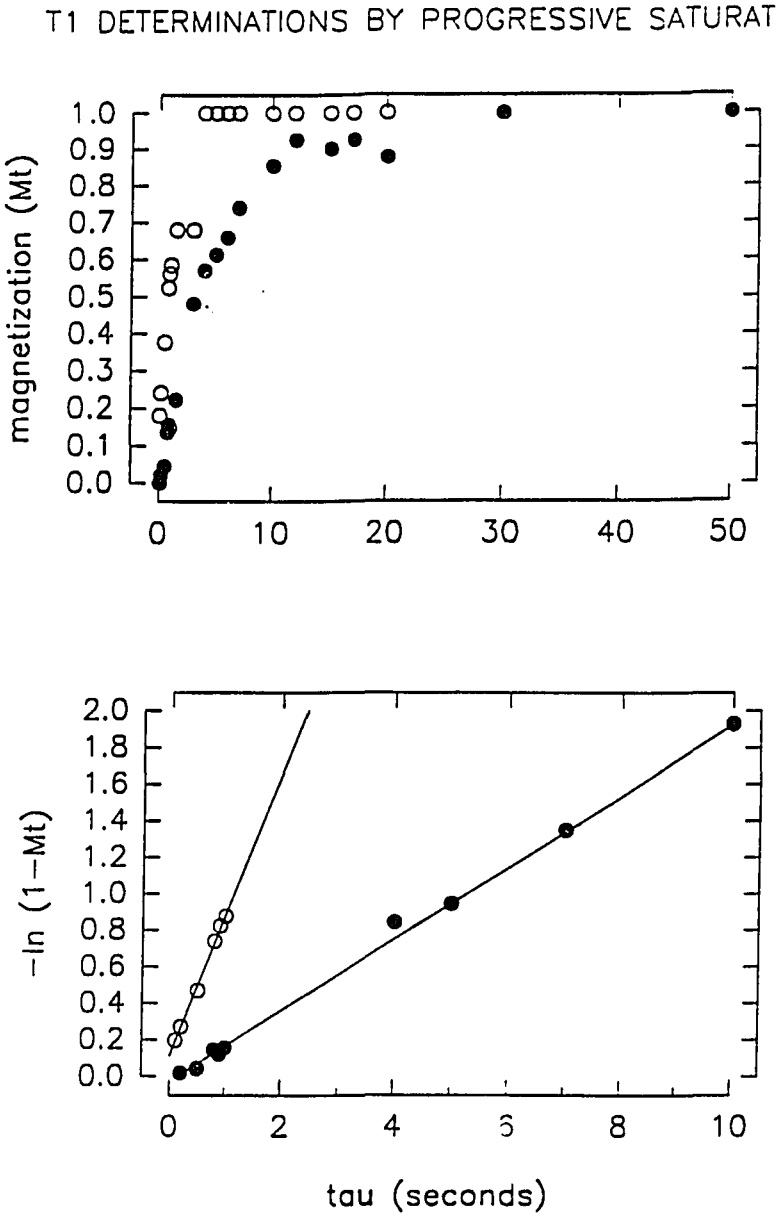

Figure 37. T_1 determinations by progessive saturation. In order to establish the validity of this method for the determination of T_1 values in bioreactor culture, a sample of magnitization *vs.* tau-value data is presented for a typical progressive saturation experiment (a). Open circles represent data obtained for the gamma-resonance of ATP, and filled circles data for the inorganic phosphate resonance. In (b), -ln (1 - Mt) has been plotted to generate a straight line. The slope of this line is equal to $1/T_1$.

In all saturation transfer experiments performed, saturation of the P_i resonance was observed to transfer the gamma-resonance of ATP and *vice versa* (shown in figure 39). According to the rate analysis of Neeman *et al* (1987), the fractional changes in signal intensity ($\Delta M/M_o$) occurring in response to saturation are proportional to the corresponding rate constants such that $\Delta M/M_o = kT_1$, where k is the rate constant of the exchange under consideration and T_1 is the apparent (measured) spin-lattice relaxation time of the saturationed resonance. The transfer rates (k) thus determined were normalized to account for changes in viable cell number by dividing by the ATP concentration (in mM) determined by comparison with the DMMP standard. Saturation transfer data and the corresponding rate constants determined are presented in table 6. ΔM values under conditions of P_i saturation represent the millimolar change in the observed intensity of the gamma-ATP peak and *vice versa*. Throughout bioreactor growth, the T_1 determined for the gamma resonance of ATP remained relatively stable, near 1.2 ($\pm$ 0.2) seconds. This value, therefore, was used in all determinations of k. The T_1 of P_i, however, decreased steadily as the bioreactor filled with cells. In this case, the T_1 values determined at the time of each saturation transfer experiment were used in the calculations performed.

Transfer rates determined in the low and high density bioreactor cultures are plotted as a function of specific growth rate (figure 38). Overall, increases in the transfer rate appear to correlate with

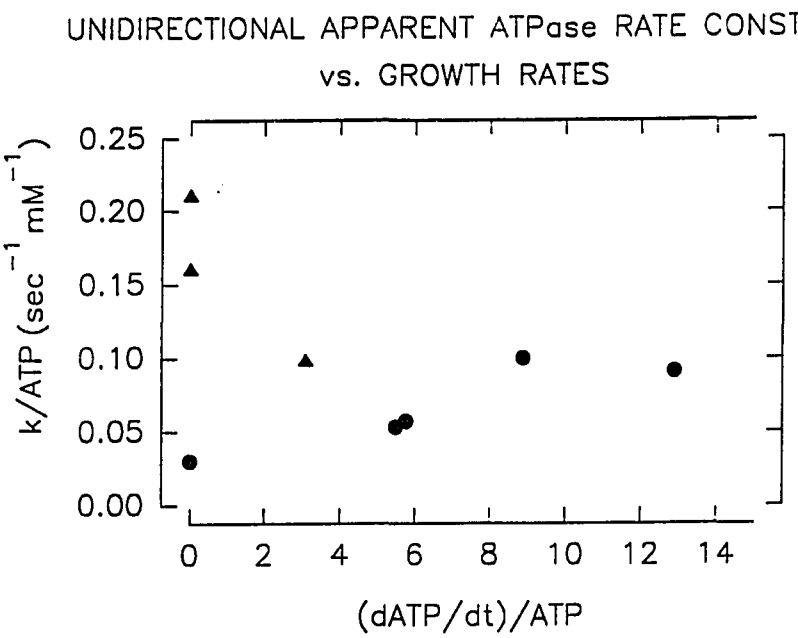

Figure 38. Unidirectional apparent ATPase rate constants *vs.* growth rates. Pi to gamma-ATP transfer rates have been plotted as a function of specific growth rate in low (triangles) and high (circles) density bioreactor culture. Increases in the P_i to gamma-ATP transfer appear to correlate with observed increases in the specific growth rate, while the gamma-ATP to Pi transfer appears unaffected by the growth rate of the bioreactor culture (see text).

increases in the growth rate, with the noticeable exception of two points which indicate ahigh transfer rate during periods of low growth. These points, however, were obtained from the bioreactor in which the fibers were visibly plugged, and may, therefore, represent an artifact created by this condition.

Table 6. Saturation transfer data*.

Hours	sat.	ΔM	ΔM/Mo	T1	k(sec.$^{-1}$)	k/ATP	(dATP/dt)/ATP
48	P_i	0.26	0.18	1.2	0.15	0.10	8.8
	ATP	0.31	0.16	5.9	0.027	0.019	
55	P_i	0.38	0.20	1.2	0.17	0.091	12.8
	ATP	0.34	0.17	5.4	0.032	0.017	
75	P_i	0.21	0.12	1.2	0.10	0.057	5.8
	ATP	0.31	0.15	4.9	0.03	0.016	
85	P_i	0.20	0.11	1.2	0.092	0.053	5.6
	ATP	0.48	0.21	4.3	0.049	0.022	
100	P_i	0.13	0.07	1.2	0.058	0.030	3.2
	ATP	0.17	0.08	4.3	0.019	0.094	

* M represents the change in the P_i or -ATP peak intensity (relative to the DMMP standard) oberved on application of a saturating pulse sequence to the -ATP (in the case of P_i) or P_i (in the case of -ATP) resonance

T_1 represents the spin-lattice relaxation time.

k is the rate of transfer from the irradiated to the observed nucleus.

k/ATP is the specific transfer rate in units of $sec^{-1}mmATP^{-1}$. This is the transfer rate normalized to the amount of ATP visible within the reactor (proportional, in turn, to the number of cells within the reactor.

(dATP/dt)/ATP represents the specific growth rate determined at the time of the saturation transfer experiment, equal to the millimolar change in ATP per hour and normalized to the average ATP concentration determined throughout the experiment.

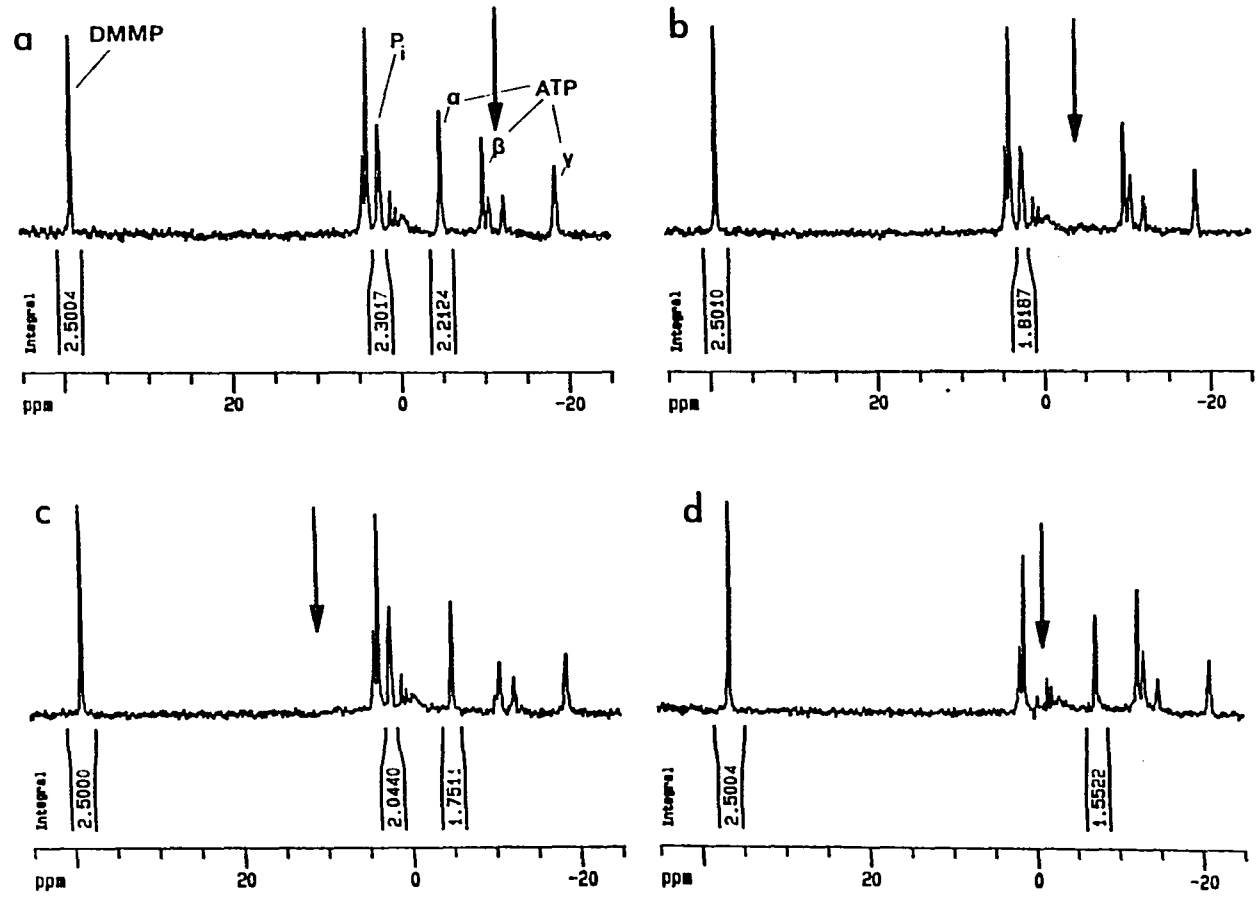

Figure 39. Representative ^{31}P-NMR saturation transfer spectra. Spectra were acquired with the application of a DANTE presaturation sequence (see Materials and Methods) at the positions indicated by the placement of the arrows in spectra a-d. For determinations of phosphate transfer rates, (a) served as a control for (b) and (c) served as a control for (d). In most cases, however, control spectra (a) and (c) were found not different.

IV. Discussion.

A. Cell culture.

1. Serum-supplemented growth. Maximal growth of EPO8F7 cells occurred with 5% Nu-serum supplementation. No obvious differences in cell growth rates or macroscopic cellular appearances were observed between EPO8F7 cells cultured in 5 and 10% Nu-serum. This is a relatively low concentration compared to other cell types, such as EAT or 3T3 cells, which are traditionally cultured with 10% fetal bovine serum (FBS), or some human and mouse cell lines which require 20% serum supplements (Sanford *et al*, 1948; Hayflick and Moorhead, 1961). This low concentration requirement, as well as the fact that cells which generally grow in 5% FBS require 10% Nu-serum, suggests that EPO8F7 cells are at least partially capable of autonomous growth support, perhaps due to the synthesis of autocrine growth factors.

The high and low density miniwell cultures demonstrate identical behaviors with respect to serum concentration (figure 15). The cell densities produced in response to serum addition plateau with a 5% Nu-serum concentration, after which no further dramatic increases are observed.

Serum-supplemented cultures have a cell doubling time of 16 hours (figure 17). This period is relatively short compared to many other cell lines routinely cultured, such as 3T3 cells and EAT cells with doubling times ranging from 18 to 36 hours (Todaro and Green, 1963).

In suspension culture, cells reach a maximum cell density of approximately 10^6 cells/ml (figure 17). Upon reaching this density, the

medium glucose concentration is reduced to approximately 5 mM, and medium lactate has accumulated to a concentration of approximately 9 mM (figures 18a and b). Initially, it was believed that upon reaching the peak cell density, cultures had depleted the medium of glucose and glutamine, energy sources essential for growth. Other investigators have found cultures limited by low concentrations of either glucose or glutamine to respond to increases in medium nutrient concentrations with increases in the culture growth rate (Miller *et al*, 1989a, b). EPO8F7 cultures, however, once having reached near-maximal density, do not resume growth when harvested and resuspended in fresh medium. In contrast, they lose viability within several hours.

2. Serum-free growth. Suspension cultures inoculated at a density of approximately 10^4 cells/ml into fresh, serum-free medium fail to grow, and begin to lose viability after several hours in culture. Higher density cultures, inoculated at a density of 2×10^5 cells/ml also begin to lose viability within 6 hours post-innoculation.

This result contrasts to those results initially found in miniwell culture, in which slight growth occurred among the higher density serum free cultures (figure 19). Due to the small, relatively localized volume of the miniwell culture, any autocrine factors produced by the cell mass may have been more immediately available to support the growth and survival of the cells, most of which had settled to the bottom of the miniwell. At the lower miniwell culture inoculum, these factors may not be produced at concentrations sufficient to promote growth.

3. Leucine deprived cultures. Leucine, an essential amino acid, was chosen as the substrate to deprive cells of, and thus, inhibit cell growth. The medium leucine concentration was decreased to 0.5 mg/l, 10% of that found in normal RPMI 1640 (Freshney, 1987). The effect of this limitation was initially studied for its ability to slow growth yet maintain a viable culture.

During the first 8 hours following inoculation into the 0.5 mg/l leucine culture, the mitotic index decreased steadily from 14% to 6%. Throughout this time, cell viability remained high (>90%). After the 12th hour in culture, the viability began to decrease due to extreme medium depletion. This loss in viability could be postponed with the re-addition of leucine at the 8th hour of culture (figure 21).

Leucine limitation, therefore, appears to reversibly limit or slow the growth of cells in suspension culture. After longer periods of leucine-deficient culture, however, re-addition of leucine is required to sustain culture viability.

These observations contrast with those experiments performed in serum-free suspension culture, in which cells lost viability after six hours in culture. Although serum-free suspension cultures lose viability rapidly, serum-free leucine deprived cultures retain their viability for as long as 12 hours. Leucine deprivation, therefore, may prevent cell entry into the mitotic cycle, effectively blocking mitosis at the "restriction point" of the cell cycle (Pardee, 1974). Alternatively, cell metabolism may be slower in the absence of leucine, thus, it would take longer for a cell to detect the absence of serum.

Analysis of cell number *vs.* time data obtained from multiple experiments (figure 22) demonstrates that cell number does not increase appreciably following inoculation into 0.5 mg/l leucine medium. The consistent decreases observed in the culture mitotic index indicate that significant changes are occurring within the culture. Changes in the mitotic index stabilize near the seventh or eighth hour of culture. Therefore, the cultures were not used for determinations of glycolytic flux or oxygen consumption rates until this time.

Although the cultures demonstrate a mitotic index near 6%, no further significant increases were observed in cell number. This low rate of mitosis may serve to replace cells which die as a result of the deprivation conditions, such that the cell number does not change over time. Cell viability does decrease slightly (from approximately 97% to 90%) during the deprivation. The deprivation may, therefore, have some unknown effects on cells at critical stages of the cell cycle. Since relatively few trypan blue-stained (dead) cells appear to be mitotic, the leucine deprivation may exert its most damaging effects on cells entering or undergoing the synthetic portions of the cell growth cycle.

4. Serum deprivation studies. Leucine deprivation is not necessarily the best means of limiting cell growth. More traditionally, arrest of cell growth is produced with a reduced serum concentration of 0.2% (Freshney, 1987; Prescott, 1968). Serum limitation is likely to more closely resemble physiological conditions, and would therefore be optimal for these types of studies. Due to the growth initially observed among serum-free miniwell cultures, however, this avenue was

not explored immediately, due to the success of the leucine deprivation experiments.

When low-serum (0.2-1%) medium was investigated for its potential ability to slow or stop growth in suspension, the cell cultures under study lost viability within four hours post-inoculation. Surprisingly, a large number of the dead cells (as determined from trypan blue exclusion) were mitotic in appearance. This finding disagrees with Pardee's restriction point hypothesis (Pardee, 1974), which suggests that once cells pass a restriction point commiting them to division, the subseqent removal of division-promoting factors will not effect the progression of those mitotic processes already initiated.

Since experiments in miniwell culture had suggested the possible production of autocrine factors supporting cell growth, 20% conditioned medium supplements were added to serum-free RPMI 1640 in hopes of producing a slow-growing culture. Following 18 hours in culture, cell growth slowed and the mitotic index dropped to six percent. The culture remained greater than 90 percent viable until the 28^{th} hour of culture, after which it lost viability rapidly. The survival of cells post-inoculation could not have been due to serum factors remaining in the medium. If the 20% supplement still contained its original 5% Nu-serum content, the Nu-serum concentration of the final culture would be 1%, a Nu-serum concentration which was found not to support culture viability.

5. MAb production. Contrary to the original hypothesis that non- or slow-growing hybridoma cultures would demonstrate a greater degree or more efficient MAb synthesis, MAb levels were lower among non-growing

(leucine limited and conditioned medium) cultures (figures 23a-c). This contrasts with the data presented in figures 15 and 16, where low serum concentrations produce low growth, although MAb levels remain high and appear to be serum-independent. Under the low-leucine conditions, therefore, leucine may not be present in concentrations sufficient for any syntheses other than those required for cellular repair. This is supported by leucine uptake and incorporation data, which demonstrate a lower rate of protein synthesis as well as amino acid uptake within the deprived cultures. Conditioned medium cultures, however, demonstrated low MAb synthesis levels even though all necessary medium components were present at their normal concentrations. This could imply that the presence of either serum or serum factors is required (regardless of a culture's proliferative state) in order for MAb synthesis to occur.

B. Energy distribution in suspension.

1. Rationale of inhibitor studies. In order to estimate the amount of glycolytic and oxidative energy consumed by cellular pathways, specific pathways were chemically inhibited and the resulting rates of glucose consumption, lactate production, and oxygen consumption determined. If ATP is produced in steady state, and only as needed, inhibition of any cellular pathway will reduce the total cellular energy consumption. This reduced energy need should be reflected in decreased rates of glycolytic flux and oxidative metabolism. The amount of energy otherwise consumed by an inhibited pathway should be approximately equal to the difference between cellular energy production rates determined pre- and post-inhibition. Since these experiments were performed under

acute conditions (within 30-60 minutes) the long-term effects of complex interactions among pathways would not be observed.

2. Oxygen consumption rates. Within proliferating cultures, oxygen consumption rates decreased immediately in response to any of the chemical inhibitions imposed (figure 30). Inhibition-induced alterations in oxygen consumption are summarized in table 3. Protein synthesis and Na^+/K^+ transport each consumed 21% of the energy produced from oxidative metabolism, while DNA and RNA synthesis consumed 25% and 30% of this energy, respectively.

The oxygen consumption rate of leucine-limited cultures was significantly less than their proliferating counterparts. Oxygen consumption rates decreased further in response to pathway inhibition. In some cases studied, the degrees of these decreases differed from those observed in proliferating cultures. The inhibition of protein synthesis reduced the oxygen consumption rate by approximately 30% of the total in each case (see Table 3). Since the total oxygen consumption, and therefore the total oxidative ATP production, was reduced among the leucine-deprived cultures, this 30% actually represent a smaller absolute decrease in ATP production than observed in proliferating cultures. Inhibition of Na^+/K^+ transport, also produced a decrease in oxygen consumption similar to that observed among the proliferating cultures. This may indicate a relatively constant role of the ion transporter which remains somewhat independent of the cell's proliferative state. The scalar differences in oxygen consumption due to Na^+/K^+ transport, however, reflected a decreased activity of the

transporter and perhaps a reduced requirement for transport-associated Na^+ influx.

Inhibition of DNA or RNA synthesis within the leucine-limited cultures did not effect oxygen consumption. Since non-proliferating cells have little or no need to synthesize DNA, this result is reasonable. Such cells should, however, synthesize a small amount of RNA to allow for the synthesis of required proteins. It may, therefore, be speculated that either the degree of RNA synthesis is too small to have significant contribution to the overall oxygen consumption rate, or that due to the medium deprivation of leucine, a substrate required for the synthesis of proteins, RNA synthesis is being inhibited by an unknown mechanism.

Inhibition of RNA synthesis and Na^+/K^+ transport in conditioned medium cultures produced decreases in oxygen consumption very similar to those observed in proliferating cultures. Inhibition of protein and DNA synthesis, however, were found to have no significant affect on oxygen consumption rates.

3. Glucose consumption studies. The inhibition-induced decreases in glucose consumption in proliferating cultures differed significantly from those observed among the oxygen consumption data. Inhibition of protein synthesis and the Na^+/K^+-ATPase produced larger relative decreases in glycolytic than oxidative ATP synthesis rates. This seems to imply that these pathways preferentially utilize the ATP generated *via* glycolysis. This may be due, in part, to the fact that both are

cytoplasmic processes, as is glycolysis, and ATP generated by glycolysis may be more readily available.

The possibility that Na^+/K^+ transport may be directly coupled to glycolysis has previously been suggested by Lynch and Balaban (1987a, b), who also observed glycolysis to be more sensitive to ouabain inhibition than is oxygen consumption. Thus, they hypothesized a specific coupling between glycolytic enzymes and the transporter.

When inhibitors were combined, the corresponding decreases in glucose consumption were not additive, and much lower than expected. This cannot be readily explained, unless glucose is being consumed for processes other than energy production, and the rates of these processes increase in response to metabolic inhibition.

The inhibition-induced changes in glucose consumption among leucine-limited cultures are more difficult to evaluate, since the addition of inhibitors appeared to result in increased rates of glucose consumption. This is not a logical result and may be an artifact of the rather large confidence limits determined for the data. The addition of inhibitors to conditioned medium cultures, however, consistently produced decreased rates of glucose consumption, as would be expected.

The inhibition of Na^+/K^+ transport produced a decrease in glucose consumption similar to that observed in proliferating cultures, again pointing to the central role of this pump in cell function. Inhibition of protein synthesis reduced glucose consumption less than observed in proliferating culture, while inhibition of RNA synthesis had no

significant effect on glucose consumption or glycolytic ATP production rates.

4. Extrapolated ATP production rates. Glucose and oxygen consumption data suggested that approximately one-half of the proliferating cells' energy originates from glycolysis. This could imply that the cells are oxygen limited or that glycolysis is not properly regulated by cellular control mechanisms. Since the cells are aerated, it can be concluded that glycolysis is not properly regulated, running at a rate faster than required to feed the TCA cycle to meet the cellular ATP demand. Thus, only a small amount of the pyruvate formed is utilized by the TCA cycle, and the remainder is converted to lactate. This may partially explain the large lactate production of EPO8F7 cultures.

Leucine-limited cultures generate only approximately 40%of their total ATP from glycolysis. This implies that the cells need proportionately less of their total energy from glycolytic sources, perhaps due to the decreased demand by pathways which preferentially utilize glycolytic energy.

Conditioned medium cultures generate even less, approximately one-fifth of their total energy, from glycolysis. This could again be due to a reduced energy demand by pathways utilizing glycolytic energy. Alternatively, the conditioned medium supplement may lack a serum factor or factors serving to upregulate glycolysis past the energy demand of the cell. Interestingly, these cells also convert glucose to lactate at a rate approximately half that of proliferating cultures, further

suggesting a hormonal mechansim for the regulation of glycolysis in this cell line.

Extrapolated total ATP production rates were significantly higher in proliferating than non-proliferating cultures, as shown in table 5. In proliferating cultures, ATP production rates decreased in response to all inhibitions imposed. On the basis of studies performed under conditions of multiple inhibition, metabolic cross-talk was significant between all pathways studied. The relative degrees of cross-talk were similar in each case studied, and can be considered indicative of cell metabolism. For example, the inhibition-induced decrease in cellular ATP demand observed on the simultaneous inhibition of protein synthesis and Na^+/K^+ transport (39%, as opposed to the 68% expected from the single-inhibition data) may demonstrate the importance of the transporter in maintaining the Na^+ gradient to allow Na^+-coupled amino acid transport, and ultimately protein synthesis. A similar coupling is observed between protein synthesis, without which enzymes are unavailable, and nucleic acid synthesis. The apparent cross-talk between inhibition of Na^+/K^+ transport and DNA synthesis is more difficult to understand. Inhibition of Na^+ transport could exert long-term effects on DNA synthesis *via* its effects on protein and enzyme synthesis. These experiments, however, were performed within a relatively short time frame in which it would not seem possible that such complex interactions could be observed.

Inhibition-induced changes in ATP production rates among leucine-limited cultures are skewed by the apparent increases observed in

glucose consumption rates in response to the addition of inhibitors. These changes, however, prove insignificant after a statistical T test and analysis of confidence limits. Even with the apparent increases in glucose consumption, inhibition of protein synthesis appeared to decrease ATP production slightly. This could be reasonably expected for a non-proliferating culture. Experiments in which inhibitors were combined demonstrate slight to no decreases in energy production. Nevertheless, given the anomalies found among glucose consumption data, no real conclusions can be drawn from these results.

The large variations found among the glucose consumption data in low-leucine cultures present a special problem. The standard deviations and confidence limits determined for these data lie in the same ranges as determined for the proliferating cultures. Since the absolute rates are significantly lower, however, these deviations amount to a larger percentage of the mean. This could possibly be overcome with a larger number of samples. Alternatively, these deviations may reflect a limitation of the methods used.

With the exception of DFB inhibition of RNA synthesis, all inhibitions imposed on the conditioned medium cultures produced a decrease in the extrapolated rates of ATP production which were lower than those observed for the proliferating cultures. The DFB-induced decrease in ATP production was not significantly different from that observed in proliferating cultures. This could indicate that even though the cultures have down-regulated their energy production levels and have slowed division, they continue to synthesize proteins required

within the cell. Combined inhibitor studies are seemingly anomalous in that the decreases observed in response to multiple inhibition were no greater than those observed when single inhibitors were used.

5. MAb synthesis with respect to protein synthesis and energy consumed in protein synthesis. MAb synthesis rates in leucine-limited and conditioned medium cultures were only 14% of that determined in proliferating cultures. In contrast, for the leucine-limited cultures, protein synthesis rates and levels of ^{14}C-leucine transport are 25 and 69% of the rates determined in proliferating cultures, respectively (table 2). Protein synthesis rates in conditioned medium cultures were 40% of that determined in proliferating culture, while leucine uptake levels were not significantly different. As determined from measurements of metabolic flux, approximately 13 x 10^{-15}, 2 x 10^{-15}, and 5 x 10^{-15} mol/min/cell of ATP were consumed for protein synthesis in proliferating, leucine-limited, and conditioned medium cultures, respectively. These ratios (approximately 20-50 % of the amount determined in proliferating culture) approximate the ratio of MAb production rates.

C. Bioreactor culture.

1. Culture growth rates. The relatively slow growth rate and extended cell doubling times of bioreactor cultures, suggested that the availability of nutrients to the cell mass may have been insufficient to promote the maximal growth rates observed in suspension. One potential suggestion for eliminating this problem would be to increase the number of fibers in the capillary bed so that individual cells within the

reactor could be assured of the nutrients required for growth. A shorter reactor would also insure that any possible nutrient gradients within the reactor were minimized. Such modifications would reduce the number of cells that could be housed within a reactor, but the efficiency of these studies would be improved through decreasing the rather large amount of medium required under present conditions. Unfortunately, the smaller cell number would also affect the quality of the NMR signals obtained. This might prove acceptable, however, if the signals obtained were indicative of a more healthy cell population.

The loop presented in figures 33a and 34a steadily increased in density (as determined by the intensity of the gamma-ATP signal) until near the 200th hour post-inoculation, at which time the bioreactor fibers had become visibly plugged such that nutrients required for growth could no longer reach the cell mass at levels sufficient to promote growth. At this point the medium was acidified slightly in hopes of resolving the intra- and extracellular components of the P_i resonance. The two components were not resolved, and the intensity of the gamma-ATP resonance decreased dramatically. At this point, the experiment was terminated.

Since preliminary experiments suggested that saturation-transfer experiments would not yield meaningful results within a reasonable period of time (determined for these purposes to be one hour *per* spectrum), the loop presented in figures 33b and 34b was inoculated at a much higher cell density. The cells within the reactor demonstrated a lag period of slightly less than one day. Once growth became apparent

(approximately 20 hours post-inoculation) the bioreactor feed was switched from RPMI + 2.5% Nu-serum to serum-free RPMI with a 20% conditioned medium supplement. The cell number appeared to increase dramatically over the first few hours following the switch to conditioned medium, but further increases were not observed following the 28th hour post-inocculation. The conditioned medium treatment was continued for another 20 hours, and the 2.5% Nu-serum supplement re-added. A small amount of growth was observed, but no further increases occured following the 70th hour in culture. Additional saturation-transfer data was acquired, although no further attempt was made to re-initiate growth. At this point, the perfusate was being oxygenated with 60% oxygen, and the medium flow rate through the reactor was approximately 100 ml/min. A further increase in this flow rate to 150 ml/min. may have been sufficient to permit further growth.

2. Magnetization transfer studies. Saturation of the P_i resonance was repeatedly observed to induce measurable changes in the gamma resonance af ATP, and vice versa. This conflicts with the observations of Neeman *et al* (1987), who did not observe this transfer, citing estimations of the first-order rate constant as being too small relative to the ATP relaxation rate to induce any measurable change in magnetization.

Overall, increases in the P_i to gamma-ATP rate constant were observed to correlate with increases in the rate of growth. This observation suggests a regulatory mechanism which ties the growth rate to the enzymatic rate constant for ATP synthesis. If the data presented in figure 38 is used to extrapolate a rate constant under conditions in

which no growth is occuring ((dATP/dt)/ATP = 0), one finds a specific rate constant (k/ATP) equal to approximately 0.03. This would correspond to the culture "maintenance energy," or the amount of energy required to sustain a cell population in the absence of division, as postulated by Pirt in 1965 (Pirt, 1965).

The γ-ATP to P_i rate constants were less informative. The rate constants determined did not seem to correlate with increases in the specific growth rate and were consistently lower than the P_i to ATP rate. The ratio of $kATP/kP_i$ (after both have been normalized to cell number by dividing by the gamma-ATP signal intensity) was equal to 3.9 ± 1.2. This suggests that the P_i to ATP transfer is approximatly four times that of the ATP to P_i transfer rate. This could occur if ATP were involved in reactions other than energy-generateing hydrolysis, such as substrate-level phosphorylation (M. Weiner, personal communication).

The γ-ATP to P_i transfer rate (as presented here, determined from the saturation ofγATP) is difficult to determine. The observed P_i peak represents the intracellular, as well as the extracellular pool of inorganic phosphate. Under physiological conditions, the pH gradient across the cell membrane is insufficient to resolve the resonances. In addition, the two components have different relaxation times, as demonstrated by the decreasing T_1s determined with increasing cell density. The ratio of $\Delta M/M_o$ must be used for the calculation of transfer rates. The intra- and extracellular P_i pools cannot, however, be separated out of this value. The rate of P_i disappearance, therefore, cannot be measured reliably under these conditions. The

removal or reduction of medium phosphate could potentially allow the determinations of the P_i transfer rate, although it is unknown whether cells could be maintained or grown under these conditions.

3. MAb yields. MAb production levels were significantly lower among bioreactor cultures than in suspension (figures 35 and 23). These low MAb yields may be related to the decreased growth rate of the bioreactor cultures compared to cells in suspension. Alternatively, low MAb yields may reflect limitations of the bioreactors themselves, such that the cell mass cannot obtain the nutrients or growth factors required for optimal MAb production.

Increased MAb production levels appeared to correlate well with increased periods of culture growth, indicating that, in the case of EPO8F7 cultures, MAb production in bioreactor culture was also optimal under conditions of cell growth.

V. Conclusions.

A. Proliferating *vs.* growth-limited EPO8F7 cultures.

Proliferating and growth-limited EPO8F7 cultures demonstrate differing rates of metabolism, as determined from measurements of glycolytic flux, oxygen consumption, and relative magnetization transfer rates determined using saturation transfer NMR. The energy distributions determined for these culture conditions could reasonably be expected of proliferating and non-proliferating cultures. Non-proliferating, leucine-limited cultures not only consume less glucose and oxygen to produce less total ATP, but they show proportionately less energy to be consumed in synthetic pathways essential to division. Non-proliferating cultures in 20% conditioned medium consume oxygen at approximately the same rate as proliferating cultures, although the glucose consumption and lactate production rates are much lower and of the magnitude of those rates determined for leucine-limited cultures.

A comparison of the reductions seen in glycolytic and oxidative energy production produced in response to various metabolic inhibitors (notably cycloheximide and ouabain) suggests that specific pathways may preferentially utilize energy derived from glycolysis. This hypothesis has been suggested by other investigators (Lynch and Balaban, 1987b), although it currently remains unsubstantiated.

Growth-limited cells in suspension, as well as in bioreactor culture, also produce dramatically lower MAb yields than their proliferating counterparts. This may be a characteristic specific to

EPO8F7 hybridoma cells and does not necessarily suggest that all proliferating hybridomas secrete higher levels of monoclonal antibodies than if they were in a non-proliferating state. Since each MAb-producing hybridoma is the result of a discrete fusion event, it is reasonable to assume that different fusion products may retain differential regulatory mechanisms for growth as well as protein synthesis.

B. Bioreactor cultures.

Bioreactor cultures demonstrated lower growth rates than observed in suspension. This decreased rate of growth may be indicative of the inavailability of essential nutrients and growth factors such that the cell mass in the reactor is unable to grow maximally. Such a problem could be overcome by increasing the fiber density of the capillary bed such that interfiber distances were smaller and the cells between the fibers would be more likely to be adequatley nourished. This would reduce the maximum number of cells that could potentially be housed within the reactor. This reduction, however, could be offset by the fact that any cells within the reactor would be healthier, and perhaps more representative of the true physiological state.

1. Magnetization transfer studies. Transfer of magnetization was observed to occur between P_i and the gamma resonance of ATP (and vice versa), and this transfer rate does appear to correlate with the growth rate of cells in bioreactor culture. The P_i to gamma-ATP transfer rate is substantially larger than the ATP to P_i transfer

rate, possibly indicating the existence of other pools to which the ATP can donate its terminal phoshpate, such as occurs in substrate-level phosphorylation reactions (Lehninger, 1965).

C. Future directions.

Magnetization-transfer NMR shows promise as a means of investigating cell metabolism in bioreactor cultures. The high cell densities produced in such systems allows the measurement of transfer repeatedly and reproducibly. In the study presented here, P_i to ATP transfer rates are clearly correlated with the rate of culture growth. The bioreactor systems used in this study appear to provide an excellent means of growing and maintaining cells for NMR study.

Future studies utilizing this sytem should include the investigation of how fiber densities affect cell growth, metabolism, and product yields.

The potential future uses for these systems are virtually limitless. Since phenotypically homogeneous populations of cells can be maintained for study, in contrast to the mixtures of cells encountered in tissue, it is conceivable, for example, that the effects of drugs or anti-tumor agents could be evaluated as the their differential metabolic effects of cancerous and normal cell types.

IV. List of References

Abragam, A. The Principles of Nuclear Magnetism. Clarendon Press, Oxford. 1960

Ackerman, J.J.H; Grove, T.H.; Wong, G.G.; Gadian, D.G.; Radda, G.K. Mapping of metoabolies in whole animals by ^{31}P NMR using surface coils. Nature. 283, 167-170 (1980).

Adamson, R. R. Metabolism of hybridoma cells in suspension culture: Evaluation of three commercially available media. In Commercial Production of Monoclonal Antibodies. Ed. Sally S. Seaver. Marcel Dekker, New York. 1987. pp. 17-34.

Alger, J.R.; Sillerud, L.O., Behar, K.L.; Gillies, R.J.; Shulman, R.G.; Gordon, R.E.; Shaw, D.; Hanley, P.E. In vivo carbon-13 nuclear magnetic resonance studies of mammals. Science. 241, 660-662 (1981).

Anderson, B.G.; Gruenberg, M.L. Optimization techniques for the production of monoclonal antibodies utilizing hollow fiber technology. In Commercial Production of Monoclonal Antibodies. Ed. Sally S. Seaver. Marcel Dekker, NY. 1987. pp 175-198.

Anzano, M.A.; Roberts, A.B.; Smith, J.M.; Sporn, M.B.; DeLarco, J.E.. Sarcoma growth factor from conditioned media of virally transformed cells is composed of both type alpha and type beta transforming growth factors. Proc. Natl. Acad. Sci., USA. 80, 6264-6268 (1983).

Arany, I.; Rady, P.; Kertai, P. Regulation of glycolysis and oxygen consumption in lymph-node cells of normal and leukemic mice. Br. J. Cancer. 43, 804-808 (1981).

Atkinson, D.E.. Cellular energy metabolism and its regulation. Adademic Press. New York, NY, 1977.

Bailey, I.A.; Gadian, D.G.; Matthew, P.M.; Radda, G.K. Seeley, P. J. Studies of metabolism in the isolated, perfused rat heart using ^{13}C NMR. FEBS Letters. 123, 315-318 (1981).

Balaban, R.S.; Kantor, H.L.; Katz, L.A.; Briggs, R.W. Relation between work and phosphate metabolite in the *in vivo* paced mammalian heart. Science. 232, 1121-1123 (1986).

Ballard, F.J. Regulation of protein accumulation in cultured cells. Fed. Proc. 29, 1248-1254 (1982).

Bax, A.; Lerner, L. Two-dimensional NMR spectroscopy. Science. 232, 960-967 (1986).

Berridge, M.J.; Irvine, R.F. Inositol trisphosphate, a novel second messenger in cellular signal transduction. Nature. 312, 315-320 (1984).

Bloch, F. Nuclear induction. Phys. Rev. 70, 460-474 (1946).

Bloom, M.; Holmes, K.T. Mountford, C.E.; Williams, P.G. Complete proton magnetic resonance in whole cells. J. Mag. Res. 69, 73-91 (1986).

Bodenhausen, G.; Freeman, R.; Morris, G.A. A simple pulse sequence for selective excitation in fourier transform NMR. J. Mag. Res. 23, 171-175 (1976).

Bottomly, P.A. Human *in vivo* NMR spectroscopy in diagnostic medicine. Radiology. 170, 1-15 (1990).

Bovey, F.A. Nuclear magnetic resonance spectroscopy, 2nd Ed. Bell Telephone Laboratories. Academic Press, San Diego. 1988.

Bowen-Pope, D.F.; Seifert, R.A.; Ross, R. The platelet-derived growth factor receptor. In Control of Animal Cell Proliferation. Eds. Alton L. Boynton and Hyam L. Leffert. Academic Press, 1985. pp 281-312.

Bresnick, E.; Thompson, U.B.; Morris, H.P. Liebelt, A.G. Inhibition of thymidine kinase activity in liver and hepatomas by TTP and d-CTP. Biochem. Biophys. Res. Commun. 16, 278-284 (1964).

Briasco, C.A.; Ross, D.A.; Robertson, C.R. A hollow fiber design for NMR studies of microbial cells. Biotechnol. Bioeng. 36, 879-886 (1990).

Brown, T.R.; Ogawa, S. ^{31}P nuclear magnetic resonance kinetic measurements on adenylate kinase. Proc. Natl. Acad. Sci., USA. 74, 3627-3631 (1977).

Brown, T.R.; Nelson, S.J.; Taylor, J.S. ^{31}P chemical shift images. Proc. Experimental NMR conference 31, 1990. p 49.

Buick, R.N., McCulloch, E.A.. The role of stem cells in normal and malignant tissue. In Control of Animal Cell Proliferation, Eds. Alton L. Boynton, Hyam L. Leffert. Academic Press, 1985. pp 25-57.

Burnett, M. The Clonal Selection Theory of Acquired Immunity. Vanderbilt University Press, Nashville. 1959.

Campisi, J. Pardee, A.B. Post-transcriptional control of the onset of DNA syntheses by an insulin-like growth factor. Mol. Cell. Biol. 4, 1807-1814 (1984).

Canioni, P.; Alger, J.R.; Shulman, R.G. Natural abundance carbon-13 nuclear magnetic resonance spectroscopy of liver and adipose tissue of the living rat. Biochemistry. 22, 4964-4980 (1983).

Carpenter, G. Epidermal growth factor. Ann. Rev. Biochem. 48, 193-216 (1979).

Carpenter, G.; Cohen, S. Human epidermal growth factor and the proliferation of human fibroblasts. J. Cell Physiol. 88, 227-238 (1975).

Carpenter, G.; Cohen, S. Epidermal growth factor. J. Biol. Chem. 265, 7709-7712 (1990).

Chambard, J.C.; Paris, S.; L'Allemain, G. Pouyssegur, J. Two growth factor signalling pathways in fibroblasts distinguished by pertussis toxin. Nature. 326, 800-803 (1987).

Chance, B. Quantitative aspects of the control of oxygen utilization. CIBA foundation symposium on the regulation of cell metabolism. Eds. G.E.W. Wolsthenholme and Cecilia M. O'Connor. Little, Brown and Co. Boston. (1959). pp. 91-121.

Chance, B. Electron transfer: pathways, mechanisms, and controls. Ann. Rev. Biochem. 46, 967-980 (1977).

Chance, B.; Williams, G.R. The respiratory chain and oxidative phosphorylation. Adv. Enzymol. 17, 65-134 (1956).

Chance, B.; Leigh, J.S. Jr.; Nioka, S.; Sinwell, T.; Younkin, D.; Smith, D.S. An approach to the problem of metabolic heterogenetity in brain. Ischemia and reflow after ischemia. Ann. NY Acad. Sci. 508, 309-320 (1987).

Chance, E.M.; Seeholzer, S.H., Kobayshi, K.; Williamson, J.R. Mathematical analysis of isotope labeling in the citric acid cycle with applications to ^{13}C studies in perfused rat hearts. J. Biol. Chem. 259, 13785-13794 (1983).

Chandler, J.P. Factors influencing monoclonal antibody production in mouse ascites fluid. In Commercial Production of Monoclonal Antibodies: A Guide for Scale-up. Ed. S. Seaver., Marcel Dekker, NY. 1987. pp. 75-92.

Civan, M.M.; Lin, L.; Peterson-Yantorno, K.; Taylor, J.; Deutsch, C. Intracellular pH of perfused single frog skin: Combined ^{19}F- and ^{31}P-NMR analysis. Am. J. Physiol. C506-C510 (1984).

Cohen, S.H.; Ogawa, S.; Shulman, R.G. ^{13}C NMR studies of gluconeogenesis in rat liver cells: Utilization of labelled

glycerol by cells from euthyroid and hyperthyroid rats. Proc. Natl. Acad. Sci., USA. 76, 1603-1607 (1979a).

Cohen, S.M; Shulman, R.G.; McLaughlin, A.C. Effects of ethanol on alanine metabolism in perfused mouse liver studied by 13C NMR. Proc. Natl. Acad. Sci., USA. 76, 4808-4812 (1979b).

Crabtree, H.G. Observations on the carbohydrate metabolism of tumors. Biochem. J. 23, 526-545 (1929).

Crueger, W. (Ed.) Physical Aspects of Bioreactor Performance. Eur. Fed. Biotechnol. Frankfurt. 1987.

DeLarco, Joseph E.; Todaro, George J.. Growth factors from murine sarcoma virus transformed cells. Proc. Natl. Acad. Sci., USA. 75, 4001-4005 (1978).

Den Hollander, J.A.; Brown, T.R.; Ugurbil, K.; Shulman, R. 13C nuclear magnetic resonance studies of anaerobic glycolysis in suspensions of yeast cells. Proc. Natl. Acad. Sci., USA. 76, 6096-6100 (1979).

Dikens, F.; Simer, F. The metabolism of normal and tumor tissue. The respiratory quotient, and the relationship of respiration to glycolysis. Biochem. J. 24, 1301-1326 (1930).

Dreyer, J.J.; Bennet, J. C. The molecular basis of antibody formation: A paradox. Proc. Natl. Acad. Sci., USA. 54, 864-869 (1965).

Dulbecco, R. Topoinihibition and serum requirements of transformed cells. Nature. 227, 802-806 (1970).

Eagle, H. Nutrition needs of mammalian cells in culture. Science. 122, 501-504 (1955).

Edelman, G.M. The structure and function of antibodies. Sci. Am. 223(2), 34-42 (1970).

Edelman, G.M.; Gally, J.A.. A model for the 7S antibody molecule. Proc. Natl. Acad. Sci., USA. 51, 846-853 (1964).

Eithier, S.P.; Cundiff, K.C.. Importance of extended growth potential and growth factor independence on in vivo neoplastic potential of primary rat carcinoma cells. Cancer Res. 47, 5316-5322 (1987).

Eldar, H.; Degani, H. ^{31}P NMR studies of the thermodynamics and kinetics of the creatine kinase reaction. Mag. Res. Med. 11, 121-126 (1989).

Ernst, R.R.; Bodenhausen, G., Wokaun, A. Principles of Nuclear Magnetic Resonance in One and Two Dimensions. Clarendon Press. Oxford. 1987.

Eshhar, Z. Monoclonal antibody strategy and techniques. In Hybridoma Technology in the Biosciences and Medicine. Plenum Press, New York. 1985. pp 3-41.

Feldman, M. Induction of humoral respnses in vitro. In Theoretical Immunology. Eds. George I. Bell, Alan S. Perelson, George H. Pimbley, Jr. Marcel Dekker, Inc., New York. 1978.

Fernandez, E.J.; Mancuso, A.; Clark, D. NMR spectroscopy studies of hybridoma metabolism in a simple membrane reactor. Biotech. Prog. 1988.

Findly, R.C.; Gillies, R.J.; Shulman, R.G. In vivo phosphorous-31 nuclear magnetic resonance reveals lowered ATP during heat shock of tetrahymena. Science. 219, 1223-1225 (1977).

Fisher, H.W.; Yeh, J. Contact inhibition of colony formation. Science. 155, 581-582 (1967).

Fix, J.A.; Moore, W.V. Growth hormone stimulation of glucose transport in isolated rat hepatocyte suspensions and primary cultures. Endocrinology. 108, 239-246 (1981).

Forsen, S.; Hoffman, R.A. Study of moderately rapid chemical exchange reactions by means of nuclear magnetic double resonance. J. Chem. Phys. 39, 2892-2901 (1963).

Freidrich, J.O; Freeman, R. A "straddle coil" for in vivo NMR. J. Mag. Res. 68, 582-587 (1986).

Freshney, R.I. Culture of Animal Cells: A Manual of Basic Technique. 2nd ed. Alan R. Liss, New York. 1987.

Fukishima, E.; Roeder, S.B.W. Experimental Pulse NMR, A Nuts and Bolts Approach. Addison-Wesley Publishing Co., Inc., Reading, Mass. 1981.

Gadian, D.G. Nuclear Magnetic Resonance and its Applications to Living Systems. Oxford University Press, New York. 1982.

Gadian, D.G.; Radda, G.K. NMR studies of tissue metabolism. Ann. Rev. Biochem. 50, 69-83 (1981).

Gadian, D.G.; Radda, G.K.; Brown, T.R.; Chance, Edwin M.; Dawson, M.J.; Wilkie, D.R. The activity of creatine kinase in frog muscle studied by saturation-transfer nuclear magnetic resonance. Biochem. J. 194, 215-228 (1981).

Gadian, D.G.; Radda, G.K.; Richards, R.E.; Seeley, P.J. 31P NMR in living tissue: the road from a promising to an important tool in biology. In Biological Applications of Magnetic Resonance. Ed. Robert G. Shulman. Academic Press, New York. 1979. pp 463-529.

Gillies, R.J.; Alger, J.R.; denHollander, J.A.; Shulman, R.G. Intracellular pH measured my NMR: Methods and results. In Intracellular pH: Its Measurement, Regulation, and Utilization in Cellular functions. Alan R. Liss, New York. 1982a. pp 79-104.

Gillies, R.J.; Chresand, T.J.; Drury, D.D.; Dale, B.E.. Design and application of bioreactors for analyses of mammalian cells by NMR. Rev. Mag. Res. Med. 1, 155-179 (1986).

Gillies, R.J.; MacKenzie, N.E.; Dale, B.E. Analyses of hollow fiber bioreactor performance by nuclear magnetic resonance spectroscopy. Bio/technology. 7 1989.

Gillies, R.J.; Ogino, T.; Shumlan, R.G.; Ward, D.C. 31P nuclear magnetic resonance evidence for the regulation of intracellular pH by Ehrlich ascites tumor cells. J. Cell Biol. 95, 24-28 (1982b).

Glacken, M.W.; Fleischaker, R.J.; Sinsky, A.J.. Large scale production of mammalian cells and their products: Engineering principles and barriers to scale up. Ann. NY. Acad. Sci., USA. 413, 355-372 (1983).

Gonzalez-Mendez, R.; Moseley, M.E; Murphy-Boesch, J.; Chew, W.M.; Lott, L.; James, T.L. Selective inversion with surface coils. Use of depth pulses for the inversion-transfer experiment in vivo. J. Mag. Res. 65, 516-512 (1985).

Gospodarowicz, D. Epidermal and fibroblastic growth factor. In Control of Animal Cell Proliferation, Eds. Alton L. Boynton, Hyam L. Leffert. Adademic Press, 1985. pp 61-90.

Graff, S.; Moser, H.; Kastner, O.; Graff, A; Tannenbaum, M. The significance of glycolysis. J. Natl. Cancer Inst. 34, 511-519 (1965).

Greaves, M.F.; Owen, J.J.; Raff, M.C.. T and B Lyphocytes: Origins, Properties, and Roles in Immune Responses. American Elsevier Publishing. New York. 1973.

Griffiths, J.R.; Stevens, A.N.; Iles, R.A.; Gordon, R.E.; Shaw, D. ^{31}P investigation of solid tumors in the living rat. Biosci. Rep. 1, 319-325 (1981).

Halliday, K.R.; Fenoglio-Preiser, C.; Sillerud, L.O. Differentiation of tumor from non-malignant human tissue by natural abundance 13C NMR in vitro. Ann. NY Acad. Sci. 508, 469-470 (1987).

Halper, J.; Moses, H.L.. Purification and characterization of a novel transforming growth factor. Cancer Res. 47, 4552-4559 (1987).

Ham, R.G. Cloning of mammalian cells. Methods in Cell Physiology. 5, 37-74. Ed. D. Prescott. Academic Press, 1972.

Handa-Corrigan, A. Large scale in vitro hybridoma culture: Current status. Bio/technology. 6, 784-786 (1988).

Hashman, H.R. The EGF receptor. In Control of Animal cell Proliferation. Eds. Alton L. Boynton, Hyam L. Leffert. Academic Press, New York. 1985. pp 169-199.

Hayflick, L.. The limited in vitro lifetime of human diploid cell strains. Exp. Cell Res. 37, 614-636 (1965).

Heath, C.; Dilwith, R.; Belfort, G.. Methods for increasing monoclonal antibody production in suspension and entrapped cell cultures: biochemical and flow cytometric analysis as a function of medium serum content. J. Biotechnol. 15, 71-90 (1990).

Heldin, C.; Westermark, B. Growth factors: Mechanism of action and relation to oncogenes. Cell. 37, 9-20 (1984).

Hey, R.J.; Strehler, B.L.. The limited growth span of cell strains isolated from the chick embryo. Exp. Gerontol. 2, 123-135 (1967).

Holley, R.W. Control of growth of mammalian cells in cell culture. Nature. 258. 1248-1254 (1975).

Holley, R.W., Kiernan, J.A.; "Contact inhibition" of division in 3T3 cells. Proc. Natl. Acad. Sci. USA. 60, 300-304 (1968).

Hopkins, C.R. Epidermal growth factor and mitogenesis. Nature. 286, 205-206 (1980).

Hopkinson, J. Hollow fiber cell culture systems for economical cell product manufacturing. Bio/technology. 3, 225-230 (1985).

Hoult, D.I. NMR imaging techniques. Brit. Med. Bull. 40, 132-138 (1984).

Hsieh, P.S.; Balaban, R.S. ^{31}P imaging of *in vivo* creatine kinase reaction rates. J. Mag. Res 74, 574-579 (1987).

Inman, W.H; Colowick, S.P. Growth factor stimulation of sugar uptake. Meth. Enzymol. 146, 399-302 (1987).

Jacobus, W.E.; Taylor, G,J.; Hollis, D.P.; Nunnally, R.L. Phosphorous nuclear magnetic resonance of perfused working rat hearts. Nature. 265, 756-758 (1977).

James, R. Polypeptide Growth factors. Ann. Rev. Biochem. 53, 259-292 (1984).

Jensen, M.D.. Production of anchorage-dependent cells. Problems and their possible solutions. Biotechnol. Bioeng. 23, 2703-2716 (1981).

Jerne, N.K. The immune system. Sci. Am. 229(1), 52-60 (1973).

Klein, B.; Jourdan, M.; Vazquez, A.; Dugas, B.; Brataille, R. Production of growth factors by hyman myeloma cells. Cancer Res. 47, 4856-4860 (1987).

Knazek, R.A.; Gullino, P.M.; Kohler, P.O.: Dedrick, R. L. Cell culture on artificial capillaries: An approach to tissue growth in vitro. Science. 178, 65-67 (1972)

Kohler, G.; Milstein, C.. Continuous cultures of fused cells secreting antibody of predefined specificity. Nature. 256, 495-497 (1975).

Kurhanewicz, J.; Thomas, M.A.; Jajodia, P.; Weiner, M.W.; James, T.L.; Narayan, P. Transrectal surface coils for localized (^{31}P, ^{1}H) spectroscopy of the human prostate. Proc. Exp. NMR Conference 31. 1990. p 203.

Lebherz, W.B. III. Batch production of monoclonal antibody by large scale suspension culture. In Commercial Production of Monoclonal Antibodies. Ed. Sally S. Seaver. Marcel Dekker, New York. 1983. pp 93-118.

Leblond, C.P.; Stevens, C.E. The constant renewal of the intestinal epithelium in the albino rat. Anat. Record. 100, 357-370 (1948).

Lehninger, A.L. *Bioenergetics*. W.A. Benjamin Inc., NY 1965.

Lehninger, A.L.; Smith, S.; Wagner, H. Efficiency of phosphorylation couples to electron transport between dihydrodiphosphopyridine nucleotide and oxygen. J. Biol. Chem. 181, 415-429 (1949).

Levintow, L.; Eagle, H. Biochemistry of cultured mammalian cells. Ann. Rev. Biochem. 30, 605-640 (1961).

Lewis, G.D.; Aggarwal, B.B.; Eessalu, T.E.; Sugarman, B.J.; Shepar, H.M. Modulation of the growth of transformed cells by human tumor necrosis factor-alpha and interferon-gamma. Cancer Res. 47, 5382-5385 (1987).

Lipton, A. Platelet growth factors: Presence and biological significance. In Control of Animal Cell Proliferation Eds. Alton L. Boynton and Hyam L. Leffert. Academic Press, 1985. pp 281-312.

Lynch, R.M.; Balaban, R.S. Coupling of aerobic glycolysis and Na^+-K^+-ATPase in renal cell line MDCK. Am. J. Physiol. 253, C269-C276 (1987a).

Lynch, R.M.; Balaban, R.S. Energy metabolism of renal cell lines, A6 and MKCK; regulation by Na^+-K^+-ATPase. Am. J. Physiol. 252, C224-C231 (1987b).

Marcipar, A.; Henno, P.; Lentwogt, E.; Roseto, A.. Ceramic-supported hybridomas for continuous production of monoclonal antibodies. Ann. NY Acad. Sci. 413, 416-420 (1983).

Marquardt, H.; Hunkapiller, M.W.; Hood, L.E.; Todaro, G.J. Rat transforming growth factor type 1: Structure and relation to epidermal growth factor. Science. 223, 1079-1082 (1984).

Martin, G.M.; Sprague, C.A.; Epstein, C.J.. Replicative life span of cultivated human cells. Effects of donor's age, tissue, and genotype. Lab. Invest. 23, 86-92 (1970).

Martin, L.F.; Fehr, D.M.; Peter, A.O.; Sanford, J.B.; Gorman, I.N.; Briggs, Richard W. ^{31}P NMR evaluation of *in vivo* renal ischemia and reperfusion injury in rabbits and dogs. Ann. NY Acad. Sci. 508, 417-419 (1987).

Massaque, J. Epidermal growth factor-like transforming growth factor. J. Biol. Chem. 258, 13606-13613 (1983).

Matthews, P.M.; Bland, J.L.; Gadian, D.G.; Radda, G.K. The steady state rate of ATP synthesis in the perfused rat heart measured by 31P saturation transfer. Biochem. Biophys. Res. Commun. 103, 1052-1059 (1981).

McKeehan, W.L. Glycolysis, glutaminolysis, and cell proliferation. Cell Biology Int. Rep. 6, 635-650 (1982).

McMaster, P.D.; Kruse, H.; Sturm, E.; Edwards, J. Persistence of bovine gamma-globulin injected as an antigen into rabbits. J. Exp. Med. 100, 341-361 (1954).

Metcalf, D.. The roles of stem cell self-renewal and autocrine growth factor production in the biology of myeloid leukemia. Cancer Res. 49, 2305-2311 (1989).

Miles, C.P.. Prolonged culture of diploid human cells. Cancer Res. 24, 1070-1076 (1964).

Miller, W.M; Wilke, C.R. Blanch, H.W. Transient responses of hybridoma cells to nutrient additions in continuous culture: I. Glucose pulse and step changes. Biotechnol. Bioeng. 33, 477-486 (1989a)

Miller, W.M; Wilke, C.R. Blanch, H.W. Transient responses of hybridoma cells to nutrient additions in continuous culture: I. Glutamine pulse and step changes. Biotechnol. Bioeng. 33, 487-489 (1989b).

Miller, W.; Wilke, C.; Blanch, H. Effects of dissolved oxygen concentration on hybridoma growth and metabolism in continuous culture. J. Cell Physiol. 132, 524-530 (1987).

Mitchell, P. Keilen's respiratory chain concept and its chemiosmotic consequences. Science. 206, 1148-1159 (1979).

Morris, G.A.; Freeman, R. Selective excitation in fourier transform nuclear magnetic resonance. J. Mag. Res. 29, 433-462 (1978).

Murakami, H. Serum free media used for cultivation of hybridomas. In. Monoclonal Antibodies: Production and Application. Alan R. Liss, Inc. 1989. pp. 107-141.

Neeman, M; Rushkin, E.; Kaye, A.M; Degani, H. ^{31}P-NMR studies of phosphate transfer rates in T47D human breast cancer cells. Biochim. Biophys. Acta. 930, 179-192 (1987)

Neurohr, K.J.; Barret, E.J.; Shulman, R.G. In vivo carbon-13 nuclear magnetic resonance studies of heart metabolism. Proc. Natl. Acad. Sci., USA. 1603-1607 (1983).

Nilausen, K.; Green, H.. Reversible arrest of growth in G1 of an established fibroblast line (3T3). Exp. Cell Res. 40, 166-168 (1965).

Ochoa, S. Enzymic mechanisms in the citric acid cycle. Adv. Enzymol. 15, 183-270 (1954).

Ollis, D.F. A simple batch fermentation model: Theme and variations. Ann. NY. Acad. Sci. 413, 144-156 (1983).

Pardee, A.B. A restriction point for control of normal animal cell proliferation. Proc. Natl. Acad. Sci., USA. 71, 1286-1290 (1974).

Pierce, G.B. Differentiation of normal and malignant cells. Fed. Procs. 29, 1248-1254 (1979).

Pirt, S.J. The maintenance energy of bacteria in growing culture. Proc. Roy. Soc. London B. 163, 224-231 (1965).

Pledger, W.J.; Stiles, C.D.; Antoniades, H.N.; Scher, C.D.. Induction of DNA synthesis in BALB/c-3T3 cells by serum components: Reevaluation of the commitment process. Proc. Natl. Acad. Sci., USA. 74, 4481-4485 (1977).

Porter, R.R. Structural studies of immunoglobulins. Science. 180, 713-716 (1973).

Prescott, D.M. Regulation of cell reproduction. Cancer Res. 28, 1815-1820 (1968).

Purcell, E.M.; Torrey, H.C.; Pound, R.V. Resonance absorption by nuclear magnetic moments in a solid. Phys. Rev. 69, 37-38 (1946).

Putnam, J.E.. Monoclonal antibody production in a ceramic matrix. In Commercial Production of Monoclonal Antibodies. Ed. Sally S. Seaver. Marcel Dekker, New York. 1983. pp. 119-138.

Rabi, I.I. On the process of space quantitation. Phys. Rev. 49, 324-328 (1936).

Racker, E. Alternative pathways of glucose and fructose metabolism. Adv. Enzymol. 15, 141-182 (1954).

Racker, E. A New Look at Mechanisms in Bioenergetics. Academic Press. New York, NY 1976.

Racker, E.; Wu, R.. Limiting factors in glycolysis of ascites tumor cells and the Pasteur effect. CIBA Foundation Symposium on the Regulation of Cell Metabolism. Eds. G.E.V. Wolsthenholme and Ceciliam M. O'Connor. Little, Brown and Co. Boston, 1959. pp 205-218.

Reuveny, S.; Mizrahi, A.; Kotler, M.; Freeman, A.. New microcarriers for culturing mammalian cells. Ann. NY Acad. Sci. 413, 413-415 (1983).

Rous, P,; Jones, F.S. A method for obtaining suspensions of living cells from fixed tissues, and for the plating out of individual cells. J. Exp. Med. 23, 549-555 (1916).

Rudland, P.S.; Seifert, W.; Gospodarowicz, D.. Growth control in cultured mouse fibroblasts: Induction of the pleotypic and mitogenic responses by a purified growth factor. Proc. Natl. Acad. Sci., USA. 71, 2600-2604 (1974).

Sakano, H.; Rogers, J.H.; Huppi, K.; Brack, C.; Traunecker, A.; Maki, R.; Wall, R.; Tonegawa, S. Domains and the hinge region of an immunoglogulin heavy chain are encoded in separate DNA segments. Nature. 227, 627-633 (1979).

Sanford, K.K.; Earle, W.R.; Likely, G.D. The growth in vitro of single isolated tissue cells. J. Natl. Cancer Inst. 9, 229-246 (1948).

Sappy-Marinier, D.; Hugg, J.; Calabrese, G.; Derken, R.; Ferin, G.; Weiner, M.W. Increased lactate in human visual cortex. Proc. 31st Ann. ENC (1990)

Sato, G.; Reid, L.; Replacement of serum in cell culture by hormones. Int. Rev. Biochem. 20, 219-251 (1978).

Schneider, W.C. Intracellular distribution of enzymes. J. Biol. Chem. 176, 259-266 (1948).

Schumpe, A; Adler, I.; Deckner, W.D. Solubility of oxygen in electrolyte solutions. Biotechnol. Bioeng. 10, 145-150 (1950).

Schutz, L.; Mora, P.T. The need for direct cell contact in "contact" inhibition of cell division in culture. J. Cell. Physiol. 71, 1-6 (1968).

Seaver, S.S. Culture method affects antibody secretion of hybridoma cells. In Commercial Production of Monoclonal Antibodies. Ed. Sally S. Seaver. Marcel Dekker, New York. 1983. pp. 49-71.

Sefton, B.M. The role of tyrosine protein kinases in the action of growth factors. In Control of Animal Cell Proliferation. Eds. Alton L. Boynton and Hyam L. Leffert. Academic Press, 1985. pp 315-330.

Shank, B.B.; Smith, N.E. Regulation of cellular growth by sodium pump activity. J. Cell Physiol. 87, 377-388 (1976).

Shoubridge, E.A.; Griggs, R.W.; Radda, G.K. ^{31}P-NMR saturation transfer measurements of the steady state rates of creatine kinase and ATP synthetase in the rat brain. FEBS Lett. 140, 288-292 (1982).

Shrivastava, G.C.; Quastel, J.H.. Malignancy and tissue metabolism. Nature. 196, 876-880 (1962).

Shulman, R.G.; Brown, T.R.; Ugurbil, K.; Ogawa, S.; Cohen, S.M.; denHollander, J.A. Cellular applications of 31P nuclear magnetic resonance. Science. 205, 160-166 (1979).

Sillerud, L.O.; Shulman, R.G. Stucture and metabolism of mammalian liver glycogen monitored by carbon-13 nuclear magnetic resonance. Biochemistry. 22, 1087-1094 (1983).

Slichter, C.P. Principles of Magnetic Resonance. 2nd ed. Springer Verlag. New York, 1978.

Slonczewski, J.L.; Rosen, B.P.; Alger, J.R.; Macnab, R,M. pH homeostasis in Escherichia coli: Measurements by ^{31}P nuclear magnetic resonacne of methyl phosphonate and phosphate. Proc. Natl. Acad. Sci., USA. 78, 6271-6275 (1981).

Stevens, A.N.; Iles, R.A.; Morris, P.G.; Griffiths, J.R. Detection of glycogen in a glycogen storage disease by ^{13}C nuclear magnetic resonance. FEBS letters. 150, 489-493 (1982).

Stoker, M.; O'Neill, C.; Berryman, S.; Waxman, V. Anchorage and growth regulation in normal and virus transformed cells. Int. J. Cancer. 3, 683-693 (1968).

Suzuki, S.; Karube, I.; Matsuoka, H.; Ueyama, S. Biochemical energy conversion by immobilized whole cells. Ann. NY Acad. Sci. 413, 133-143 (1983).

Swim, H. E.; Parker, R.F. Culture characteristics of human fibroblasts propagated serially. Am. J. Hyg. 66, 235-243 (1957).

Thoma, W.J.; Ugurbil, K. Saturation-transfer studies of ATP-Pi exchange in isolated perfused rat liver. Biochim. Biophys. Acta. 893, 225-231 (1987).

Thomas, M.A.; Kurhanewicz, J.; Jajodi, P.; James, T.L.; Weiner, M.W., Narayan, P. Multinuclear transrectal spin echo MRS of human prostate. Proc. Exp. NMR Conference 31. 1990. p 174.

Todaro, G.H.; Green, H. Quantitative studies of the growth of mouse embryo cells in culture and their development into established cell lines. J. Cell Biol. 17, 299-313 (1963).

Todaro, G.H.; Lazar, Gerald K.; Green, H. The initiation of cell division in a contact-inhibited mammalian cell line. J. Cell. Comp. Physiol. 66, 325-334 (1965).

Ugurbil, K.; Brown, T.R.; denHollander, J.A.; Blynn, P.; Shulman, R.G. High resolution 13C nuclear magnetic resonance studies of glucose metabolism in Escherichia coli. Proc. Natl. Acad. Sci. USA. 75, 3742-3746 (1979).

Ugurbil, K.; Petein, M.; Maidan, R.; Michurski, S.; From, A.H.L. Measurement of an individual rate constant in the presence of multiple exchanges. Application to myocardial creatine kinase reaction. Biochemistry. 25, 100-107 (1986).

Urso, P.; Makinodan, T. The roles of cellular division and maturation in the formation of precipitating antibody. J. Immunol. 90, 897-907 (1963).

Van Damme, J.; Opdenakker, G.; Simpson, R.J.; Rubira, M.R.; Cayphas, S.; Vink, A., Billiau, A.; VanSnick, J.. Identification of the human 26-kd protein, interferon beta2, as a b cell hybridoma/plasmacytoma growth factor induced by interleukin 1 and tumor necrosis factor. J. Exp. Med. 165, 914-919 (1987).

Vuk-Pavlivic, S.; Opara, E.C.; Levanat, S.; Vrbanic, D.; Pavelic, K.. Autocrine tumor growth regulation and tumor-associated hypoglycemia in murine melanoma B16 in vivo. Cancer Res. 46, 2208-2213 (1986).

Vogel, A.; Raines, E.; Kariya, B.; Rivest, M.; Ross, R. Coordinate control of 3T3 cell proliferation by platelet derived growth factor and plasma components. Proc. Natl. Acad. Sci., USA. 75, 2810-2814 (1978).

vonWedel, R.J. Mass culture of mouse and human hybridoma cells in hollow fiber culture. In Commercial Production of Monoclonal Antibodies. Ed. Sally S. Seaver. Marcel Dekker, New York. 1987. pp 159-174.

Waldmann, H.; Howard, J.. Cellular basis of the immune response. Int. Rev. Biochem. 22, 29-95 (1979).

Warburg, O. On the origin of cancer cells. Science. 123, 309-314 (1956).

Wenner, C.E. Regulation of energy metabolism in normal and tumor tissues. In Cancer: A comprehensive treatise, Vol. 3. pg 389-403. Plenum Press, NY. 1975.

Williams, S.R.; Gadian, D.G.; Proctor, E.; Sprague, D.B.; Talbot, D.F. Proton NMR studies of muscle metabolites in vivo. J. Mag. Res. 63, 406-412 (1985).

Yaffe, D. Retention of differentiation potentialities during prolonged cultivation of myogenic cells. Proc. Natl. Acad. Sci., USA. 61, 477-483 (1968).

Yoshizaki, K.; Sio, Y.; Nishikawa, H. High resolution proton magnetic resonance spectra of muscle. Biochim. Biophys. Acta. 678, 283-291 (1981).

Zielke, H.R.; Zielke, C.L.; Ozand, P.T. Glutamine: a major energy source for cultured mammalian cells. Fed. Proc. 43, 121-125 (1984).

Zimmer, S.D,; From, A.H.L.; Foker, J.E.; Michurski, S.P.; Ugurbil, K. Post-ischemic mechanical performance: Independence from ATP levels. Ann. NY Acad. Sci. 508, 501-503 (1987).